LBL-4109

1/f NOISE: DIFFUSIVE SYSTEMS AND MUSIC

Richard Frederick Voss
(Ph. D. thesis)

November 1975

Prepared for the U. S. Energy Research and
Development Administration under Contract W-7405-ENG-48

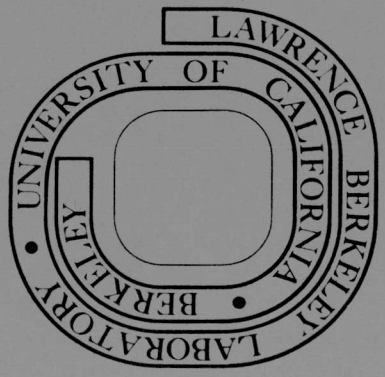

LBL-4109

1/f NOISE: DIFFUSIVE SYSTEMS AND MUSIC

Contents

1/f NOISE: DIFFUSIVE SYSTEMS AND MUSIC

Richard Frederick Voss

Inorganic Materials Research Division, Lawrence Berkeley Laboratory
and Department of Physics; University of California
Berkeley, California 94720

ABSTRACT

Measurements of the 1/f voltage noise in continuous metal films are reported. At room temperature, samples of pure metals and bismuth (with a carrier density smaller by 10^5) of similar volume had comparable noise. The power spectrum, $S_V(f) \propto \bar{V}^2/\Omega f^\gamma$, where $\bar{V}$ is the mean voltage across the sample, Ω is the sample volume, and $1.0 \lesssim \gamma \lesssim 1.4$. $S_V(f)/\bar{V}^2$ was reduced as the temperature was lowered. Manganin, with a temperature coefficient of resistance (β) close to zero, had no discernible noise. These results suggest that the noise arises from equilibrium temperature fluctuations modulating the resistance to give $S_V(f) \propto \bar{V}^2\beta^2 k_B T^2/C_V$, where C_V is the total heat capacity of the sample. The noise was spatially correlated over a length $\lambda(f) \approx (D/f)^{1/2}$, where D is the thermal diffusivity, implying that the fluctuations obey a diffusion equation. The usual theoretical treatment of spatially uncorrelated fluctuations gives a spectrum that flattens at low frequencies and has an $f^{-3/2}$ high frequency limit. These calculated spectra are verified experimentally for number fluctuations of independent particles undergoing Brownian motion but do not explain the 1/f spectrum. However, the empirical inclusion of an explicit 1/f region and appropriate normalization lead to $S_V(f)/\bar{V}^2 \propto \beta^2 k_B T^2/C_V[3+2 \ln (\ell/w)]f$, where ℓ is the length and w is the width of the film, in excellent agreement with the measured noise.

If the fluctuations are assumed to be spatially correlated, the diffusion equation can yield an extended 1/f region in the power spectrum. The temperature response of a sample to delta and step function power inputs is shown to have the same shape as the auto-correlation function for uncorrelated and correlated temperature fluctuations respectively. The spectrum obtained from the cosine transform of the measured step function response is in excellent agreement with the measured 1/f voltage noise spectrum. Spatially correlated equilibrium temperature fluctuations are not the dominant source of 1/f noise in semiconductors and metal films. However, the agreement between the low frequency spectrum of fluctuations in the mean square Johnson noise voltage and the resistance fluctuation spectrum measured in the presence of a current demonstrates that in these systems the 1/f noise is also due to equilibrium resistance fluctuations. The 1/f spectrum is not limited to "physical systems". Loudness fluctuations in music and speech and pitch fluctuations in music also show the 1/f behavior. 1/f noise sources, consequently, are demonstrated to be the natural choice for stochastic composition.

"How is't with me, when every noise appals me?"
William Shakespeare, Macbeth

"One man's noise is another man's signal."
Sir Edward Bullard

I. INTRODUCTION

1/f noise has been shown to be the dominant form of low frequency noise in most physical systems. Although numerous theories have been advanced to explain this ubiquitous phenomenon, they have generally proven unsatisfactory. We report here some of our research on the subject of 1/f noise, primarily in continuous metal films. Our choice of metal films as a system to study was dictated by our belief that the simplest system in which the physical processes were well understood offered the best opportunity for determining the physical origin of the 1/f noise.

Our initial experiments set the direction of our theoretical ideas, which in turn guided further experiments. In general we follow here this chronological progression, and provide below a summary of the logical development.

Hooge and Hoppenbrouwers[1] have measured the 1/f noise voltage generated in continuous gold films (with physical properties close to bulk values) in the presence of a steady current. They found that the noise power spectrum, $S_V(f)$, for samples at room temperature could be expressed by the empirical formula

$$\frac{S_V(f)}{\bar{V}^2} \approx \frac{2\times10^{-3}}{N_c f} \quad . \tag{1.1}$$

In Eq. (1), N_c is the number of charge carriers in the sample, f is the frequency, and $\bar{V}$ is the average voltage across the sample. This dependence on $\bar{V}$ is universally found in resistive systems. The 1/f noise is, consequently, often considered as arising from resistance fluctuations that generate a fluctuating voltage in the presence of a constant current.[2] Hooge and Hoppenbrouwers[1] pointed out that the inverse volume dependence for samples of the same material implied by Eq. (1.1) was strong evidence for believing that the 1/f noise is a bulk effect rather than a surface effect in metal films. They found that the noise was still present when the samples were immersed directly in liquid nitrogen or liquid helium, and concluded that $S_V(f)$ had a temperature dependence no stronger than $T^{1/2}$.

Williams and co-workers[3,4] studied very thin metal films which no longer have bulk properties, and in which electrical condition is probably partially via a hopping process. Such films exhibit much more noise than is predicted by Eq. (1.1).

Hooge[5] has examined measurements of 1/f noise in semiconductors, and has found that, with a few notable exceptions, $S_V(f)$ was again quite well expressed by Eq. (1.1). Agreement with this formula was also found in single-crystal III-V compounds by Vandamme.[6] Both results imply that 1/f noise in semiconductors is a bulk effect. Hooge, who studied noise in ionic cells,[7] and Kleinpennig,[8] who studied noise in the thermoelectric emf of intrinsic and extrinsic semiconductors, both concluded that the noise arises from fluctuations in carrier mobility. However, the view that 1/f noise in semiconductors is a bulk effect arising from mobility fluctuations is not universally

held. McWhorter's[9] theory suggests that 1/f noise arises from surface traps with an appropriate distribution of trapping times that generate noise by inducing fluctuations in the number of carriers. This theory has considerable experimental support.[10-12] However, it is possible that, in general, the 1/f noise in semiconductors arises from both bulk and surface effects.

In Section II, we report our own measurements on 1/f noise in thin films made of a variety of materials. Initial results were reported earlier.[13] We found general agreement with Eq. (1.1), with two important exceptions. First, Bi, a semimetal with a carrier density about 10^5 smaller than gold, exhibited about the same 1/f noise for similar sized samples. Second, manganin, an alloy with a temperature coefficient of resistance close to zero, showed no observable 1/f noise. The absence of 1/f noise in manganin indicated that the 1/f noise in metal films could be caused by temperature fluctuations that modulate the sample resistance, R, and generate voltage fluctuations in the presence of a steady current, I. Thus, we expect $S_V(f) \propto I^2(\partial R/\partial T)^2\langle(\Delta T)^2\rangle = \bar{V}^2\beta^2\langle(\Delta T)^2\rangle$, where $\beta = (1/R)\, dR/dT$, and $\langle(\Delta T)^2\rangle$ is the mean square temperature fluctuation. The similarity of the 1/f noise in Bi and other metals suggests that $S_V(f)/\bar{V}^2 \propto \Omega^{-1}$ (where Ω is the sample volume), not N_c^{-1}; and, consequently, that the temperature fluctuations may be those of an equilibrium system. In thermal equilibrium, $\langle(\Delta T)^2\rangle = k_B T^2/C_V$, where C_V is the heat capacity of the sample. At room temperature, $C_V \approx 3Nk_B$, where N is the number of <u>atoms</u> in the sample, and $S_V(f) \propto \bar{V}^2\beta^2T^2/3N$.

Energy fluctuations ($\Delta E = C_V \Delta T$) are expected to obey a diffusion equation, and in Section III we describe the spectrum of such fluctuations in a small subvolume of a uniform medium, assuming the fluctuations to be uncorrelated in space. This system has been extensively studied in the past.[14] The diffusion model was rejected as an explanation for 1/f noise because, in this system, it fails to predict a 1/f power spectrum over many decades of frequency,[15] and because it seriously underestimates the noise in semiconductors. However, the experimental configuration involving a metal film on a glass substrate is a poor approximation of the uniform medium for which the spectra are calculated. If an explicit 1/f region is empirically included in the spectrum, and the spectrum normalized by setting $\langle(\Delta T)^2\rangle = k_B T^2/C_V = \int_0^\infty S_T(f)\, df$, the calculated noise is in excellent agreement with the data.

The diffusion theory introduces a frequency-dependent correlation length $\lambda(f) \approx (D/f)^{1/2}$, where D is the thermal diffusivity. $\lambda(f)$ is roughly the length over which a fluctuation at frequency f is correlated. Frequency-dependent correlation is thus an identifying characteristic of fluctuations in a diffusive medium. In Section IV, we describe an experiment on Bi samples in which the noise across two sections becomes more correlated in the predicted manner as the frequency is lowered.

The absence of 1/f noise in manganin, the dependence of $S_V(f)$ on $\bar{V}^2\beta^2/N$, and the observation of frequency-dependent spatial correlation for the 1/f noise provide overwhelming experimental evidence that equilibrium temperature fluctuations are the physical origin of 1/f

noise in metal films. Moreover, the introduction of an explicit 1/f region in the spectrum enables us to make quantitative predictions of the 1/f noise in excellent agreement with experiment. The manner in which the temperature fluctuations produce the 1/f spectrum is, however, an open question. One possibility is that the non-uniform nature of the experimental system modifies the simple diffusion theory to produce a 1/f spectrum. Indeed, experiments[16] on the 1/f noise in Sn films at the superconducting transition have shown that a change in the thermal coupling between the film and the substrate can dramatically affect the spectrum. Another possibility is that the temperature fluctuations have some spatial correlation. In Section V, we show that spatial correlation of the temperature fluctuations can produce a spectrum with an extended 1/f region.

Fluctuation spectra are calculated on the assumption that the fluctuations are on the average governed by the same decay laws (in this case, the diffusion equation) as macroscopic perturbations.[17] In Section VI, we show that the temperature response of a subvolume of a diffusive system to a delta function power input uniform over the subvolume has the same shape as the autocorrelation function for uncorrelated temperature fluctuations. On the other hand, the response to a step function in power corresponds to the autocorrelation function for correlated temperature fluctuations. We then describe an experiment in which we measure the temperature response of a small Au film to delta function and step function power inputs. The cosine transforms of the responses yield power spectra that are compared with the measured noise power spectrum. The spectrum obtained

from the delta function is similar to that calculated for uncorrelated fluctuations, flattening at low frequencies, and is unlike the measured noise spectrum. The spectrum obtained from the step function, however, is not only 1/f over many decades, but, when appropriately normalized, has a magnitude and shape in excellent agreement with the measured noise power spectrum.

In Section VII, we briefly summarize measurements on superconducting films at the transition[16] and Josephson junctions[18] that strongly suggest that the 1/f noise in these systems is also due to equilibrium temperature fluctuations. However, although equilibrium temperature fluctuations should generate noise in all systems (except those for which $\beta = 0$), they may not be the dominant noise source. For example, the 1/f noise in semiconductors and discontinuous metal films is too large to be explained by temperature fluctuations, and lacks the spatial correlation characteristic of a diffusive process. However, we show in Section VIII that the 1/f noise in these systems is due to <u>equilibrium</u> resistance functions. The measured low frequency spectrum (appropriately normalized) of fluctuations in the mean square Johnson noise voltage across these samples is 1/f, and is in excellent agreement with the resistance fluctuation spectrum obtained in the presence of a current.

The disagreement between $S_V(f)/\bar{V}^2$ measured for metal films and the calculated $S_T(f)$ for uncorrelated temperature fluctuations suggests that we examine the spectra from other diffusive systems. In Section IX we describe a series of light scattering experiments which verify the calculations of Section III for independent particles undergoing Brownian motion.

In Section X we show that 1/f noise is not limited to "physical systems". Loudness fluctuations in music and speech and pitch fluctuations in music also have the 1/f spectrum. Moreover, we describe the use of a 1/f noise source in a stochastic algorithm to generate a very agreeable form of "1/f music".

Section XI contains our concluding discussion.

"It is a capital mistake to theorize before one has data."
Sir Arthur Conan Doyle,
The Adventures of Sherlock Holmes

II. MEASUREMENTS OF 1/f NOISE IN METAL FILMS

We have measured the spectrum of current-induced 1/f voltage noise in small samples of evaporated or sputtered metal films on glass substrates. Our films were 250Å to 2000Å thick, and had resistivities close to bulk values. Each film was cut with a diamond knife in a micromanipulator to produce a small bridge or necked down region of typical dimensions 10 μm×100 μm with large areas of metal at either end suitable for contacts. Two variations of the sample geometry are shown in Figs. 1(a) and 2(a). Four pressed indium contacts were placed on each sample and the contacts were checked for excessive resistance. A current source, consisting of a bank of batteries and a large wirewound resistor (which exhibited no 1/f noise) of resistance $R_0 \gg R$ (R is the sample resistance), was connected to two of the contacts. The other two contacts were used as voltage leads. The average voltage across the sample, $\bar{V}$, ranged from 0.2 to 2V. The high resistance current source and the four-terminal configuration were necessary to eliminate contact 1/f noise at the current carrying contacts. The current and voltage leads were often reversed to further assure the absence of contact noise. Moreover, the sample was replaced by a wirewound resistor of the same resistance to insure that no significant noise arose from the current source.

The sample, current supply, and battery-operated preamplifier were placed in an electrically screened room to reduce pickup of external

noise. In some cases, the samples were also placed in a vacuum with no change of the measured noise spectrum. For the high resistance Bi samples ($R \sim 1K\Omega$), the voltage leads were ac coupled directly to a PAR113 preamplifier. To improve the sample noise to preamplifier noise ratio for the low resistance samples ($R \lesssim 100\Omega$) it was necessary to provide a better impedance match. These samples were either transformer coupled to the PAR113 or ac coupled through a large capacitor to a Keithley 824 preamplifier. Correction to the spectrum was made for the transformer response or the low frequency amplifier roll-off. In some cases, the sample was used as one arm of a Wheatstone bridge to allow dc coupling to the preamplifier. Although such an arrangement is a three-terminal measurement and more susceptible to contact noise, by cutting two symmetric arms from the same continuous film, the bridge arrangement could be made insensitive to contact noise.

The voltage noise spectrum was measured by an interfaced PDP-11 computer. The preamplifier output was filtered to eliminate unwanted high frequencies and was fed to a 1 MHz voltage-to-frequency converter. The converter, in turn, drove an internal counter in the computer. An external oscillator of frequency f_o generated an interrupt in the computer every $\tau_o = 1/f_o$. On the first interrupt, the counter was cleared and started. On successive interrupts, the counter was read, cleared and restarted. This arrangement provided a highly accurate analog-to-digital converter (up to 24 bits) with automatic averaging over τ_o. Successive counts stored in the computer thus provided a digital record of the noise. Once 1024 points had been accumulated, a Fast Fourier Transform was used to calculate the 512 sine and 512

cosine transforms of the data. These values were squared and added to an accumulating array of 512 frequency points. The entire process was repeated at least 40 times to provide an average measure of the noise spectrum in the frequency range $f_o/1024$ to $f_o/2$. By changing f_o, the spectrum could be measured over any desired range, although the digitizing electronics and interrupt delays gave an upper frequency limit of about 10 kHz.

The spectrum, $S(f)$, was measured with an average voltage, $\bar{V}$, across the sample. The background spectrum, $S_o(f)$, was then measured with zero average voltage across the sample and included contributions from both external pickup and amplifier noise. The difference, $S_V(f)$, between $S(f)$ and $S_o(f)$ was thus the current induced voltage noise in the sample. These measured spectra for a typical Bi sample ($R \sim 400\Omega$) coupled directly to a PAR113 preamplifier are shown in Fig. 1. The increasing steepness of the spectrum below 1 Hz was found in most samples and was probably due to a gradual deterioration of the sample caused by the high current densities ($\sim 10^6$ Acm^{-2}). With the FFT method of measuring the spectrum a slow monotonic drift generates a $1/f^2$ spectrum. This effect can be eliminated if the cosine transforms alone are used.

Figure 2 shows the measured spectra for a Au sample coupled through a large capacitor to a Keithley 824 preamplifier. In this case, it was necessary to correct for the low frequency roll-off of the amplifier and capacitor as well as to subtract out the background to obtain $S_V(f)$. In Figs. 1 and 2, the corrected spectra show a behavior close to $1/f$.

Similar measurements were made on a wide variety of samples of different materials. We found $S_V(f) \propto \bar{V}^2/f^\gamma$, where $1.0 \lesssim \gamma \lesssim 1.4$. By varying sample size, it was possible to show that $S_V(f)$ was roughly proportional to Ω, the sample volume. Otherwise identical samples often showed noise spectra whose magnitude differed by up to a factor of 3. This irreproducibility between different samples and our inability to change Ω over a wide range while still observing the 1/f noise made a more accurate determination of the Ω dependence impossible. A summary of the measured noise spectra for various samples (typically, 10 μm×120 μm×1000Å) of different materials, including metals and a semimetal (Bi), is shown in Table I. The measured temperature coefficient of resistivity, β, is also shown for each of the metal films.

Hooge and Hoppenbrouwers[1] reported no consistent variation of the 1/f noise in their Au films when immersed directly in liquid N_2 or liquid He. These measurements, however, may not be indicative of the temperature dependence of $S_V(f)/\bar{V}^2$. We found that placing the samples directly in the liquids caused the spectrum to become steeper than 1/f and to be dominated by bubbling in the liquid. Moreover, at all temperatures, the high current densities (up to 10^6 Acm^{-2}) and high levels of power dissipation (up to 1 $kWcm^{-2}$) necessary to observe the 1/f noise caused the film to operate much above ambient temperature. In the case of some "room temperature" metal films, the departure of the I-V characteristics from linearity together with the known value of β showed that the sample was as much as 40°C above room temperature. The non-linearity of the I-V characteristic

Table I. The measured temperature coefficient of resistance for several materials and the measured and calculated noise power at 10 Hz (measured $S_V(f)/\bar{V}^2$ differs by $2/\pi$ from previous table in Ref. 13 because of recalibration).

Material	Measured β (K^{-1})	$S_V(f)/\bar{V}^2$ Measured at 10 Hz (10^{-16} Hz^{-1})	$S_V(f)/\bar{V}^2$ Calculated at 10 Hz (10^{-16} Hz^{-1})
Cu	0.0038	6.4	16.00
Ag	0.0035	6.4	2.00
Au	0.0012	0.6	0.76
Sn	0.0036	7.7	7.7
Bi	-0.0029	13.0	9.3
Manganin	$\lvert\beta\rvert<10^{-4}$	$<7\times10^{-3}$	$<3.5\times10^{-3}$

at high currents due to heating is shown in Fig. 3 for the Au film whose noise spectrum is shown in Fig. 2. The heating causes an increase in resistance at high currents. The somewhat amorphous nature of our Bi films caused a negative temperature coefficient of resistivity. The Bi films, consequently, exhibited I-V characteristics which curved toward lower resistance at high currents.

In order to get some indication of the temperature dependence of $S_V(f)/\bar{V}^2$ it was necessary to place the samples in a vacuum can and to isolate them from temperature fluctuations in the liquid bath by a long thermal time constant. We found that $S_V(f)/\bar{V}^2$ for both Au and Bi samples decreased by about an order of magnitude in going from room temperature to a liquid N_2 bath, but that $S_V(f)/\bar{V}^2$ did not change further in going to a liquid He bath. In all cases, however, the presence of heating non-linearities indicated that the samples were much above the bath temperature. In liquid N_2 and liquid He baths, we were unable to make an accurate measurement of β and determine the actual temperature of the samples. Although we can say that with careful measurement $S_V(f)/\bar{V}^2$ is found to decrease as the temperature is lowered we can make no quantitative statement about the temperature dependence.

The dependence of $S_V(f)$ of $\bar{V}^2$ suggests that the 1/f noise may be caused by resistance fluctuations. The measurements summarized in Table I provide important clues as to the nature of 1/f noise in continuous metal films. The absence of detectable 1/f noise in manganin with $\beta \approx 0$ indicates that temperature fluctuations generate the 1/f noise. The similarity of the spectra from Bi ($\beta < 0$) and the metals ($\beta > 0$) indicates that thermal feedback, in which a resistance fluctuation

changes the power dissipated in its neighborhood thereby raising or lowering the local temperature, do not play a role. The observation that Bi, with a carrier density 10^5 smaller than metals, has roughly the same relative noise spectrum suggests that the size effect is not N_c^{-1}, as suggested by Hooge and Hoppenbrouwers.[1] However, both our measurements and those of Hooge and Hoppenbrouwers[1] on Au are consistent with $S_V(f)/\bar{V}^2 \propto \Omega^{-1}$. In thermal equilibrium a body of total heat capacity $C_V = c_V\Omega$ has a mean square temperature fluctuation $\langle(\Delta T)^2\rangle = k_B T^2/C_V$. Thus, the absence of the 1/f noise in manganin, the scaling of $S_V(f)/\bar{V}^2$ as $1/\Omega$, and the fact that $S_V(f)/\bar{V}^2$ decreases with decreasing temperature are all consistent with the idea that the 1/f noise voltage in continuous metal films supplied with a steady current is due to equilibrium temperature fluctuations modulating the resistance.

"Facts are stubborn things; whatever may be our wishes, our inclinations, or the dictates of our passions, they cannot alter the state of facts and evidence."

John Adams, Defense of the British soldiers on trial for the Boston Massacre

III. FLUCTUATION SPECTRA FOR DIFFUSIVE SYSTEMS

A temperature fluctuation, ΔT, in a resistor of resistance, R, and temperature coefficient of resistivity, $\beta = (1/R)\,\partial R/\partial T$, will be observed as a voltage fluctuation, $\Delta V = IR\beta\Delta T$, in the presence of a constant current, I. The voltage fluctuation spectrum, $S_V(f)$, is then related to the temperature fluctuation spectrum, $S_T(f)$, by

$$S_V(f) = \bar{V}^2\beta^2 S_T(f) \quad , \tag{3.1}$$

where $\bar{V} = IR$ is the average voltage across the resistor. If the temperature fluctuations are due to equilibrium exchange of energy between the resistor and its environment, $S_T(f) \propto k_B T^2/C_V$, where C_V is the total heat capacity of the resistor. In this case $S_V(f) \propto \bar{V}^2\beta^2 k_B T^2/C_V$, which predicts the observed behavior of the 1/f noise in metal films. It is necessary, however, to determine whether or not the idea of equilibrium temperature fluctuations can account for both the observed magnitude of the 1/f noise and the 1/f spectrum. In this section, we shall use a Langevin-type approach to calculate $S_T(f)$ for a system characterized by a single correlation time, and for uniform diffusive systems. Although many of the results have been previously derived,[14,15,19-24] neither the generalized three-dimensional spectra nor the frequency-dependent spatial correlation length, $\lambda(\omega) \propto (D/\omega)^{1/2}$, have been emphasized. Our simple physical

derivation, which stresses the importance of $\lambda(\omega)$ in determining the shape of the spectra, not only provides the basis for our latter experiments, but also introduces methods that can easily be extended to the case of correlated fluctuations discussed in Section V.

We begin by considering the system shown in Fig. 4(a). A mass of total heat capacity, C, is coupled via a thermal conductance, G, to a heat reservoir at temperature T_o. Macroscopic deviations in T will obey the decay equation

$$C \frac{dT}{dt} = -G(T - T_o) \quad . \tag{3.2}$$

In the Langevin approach[25] equilibrium fluctuations are also assumed to obey Eq. (3.2). The stochastic nature of the fluctuations is introduced by adding a "random driving term", F(t), to the right-hand side of Eq. (3.2). F(t) is assumed to have zero average and to be uncorrelated in time ($\langle F(t)\, F(t+\tau)\rangle = F_o^2 \delta(\tau)$) for the time scales in which we are interested. Physically, F(t) represents the random exchange of energy between the mass and the reservoid through the thermal conductance. The equilibrium temperature fluctuations thus obey the equation:

$$dT/dt = -(T - T_o)/\tau_o + F(t)/C \tag{3.3}$$

where $\tau_o = C/G$ is the time constant for decay of a given fluctuation. We wish to calculate the spectrum for temperature fluctuations, $S_T(\omega) = \langle |T(\omega)|^2 \rangle$, where

$$T(\omega) = (2\pi)^{-1/2} \int (T(t) - T_o)\, e^{i\omega t}\, dt \quad .$$

From Eq. (3.3), $T(\omega) = F(\omega)/C[1/\tau_o + i\omega]$ and $S_T(\omega) = S_F(\omega)/C^2[1/\tau_o^2 + \omega^2]$. The Wiener-Khintchine relations

$$c_x(\tau) = \langle x(t)\, x(t+\tau)\rangle = \int_{-\infty}^{\infty} S_x(\omega)\cos\omega\tau\, d\omega \qquad (3.4a)$$

and

$$S_x(\omega) = \frac{1}{2\pi}\int_{-\infty}^{\infty} c_x(\tau)\cos\omega\tau\, d\tau \qquad (3.4b)$$

that connect the autocorrelation function, $c_x(\tau)$, of a fluctuating quantity, x, with its spectrum, $S_x(f)$, may be used to calculate $S_F(\omega)$ from $\langle F(t)\, F(t+\tau)\rangle = F_o^2\delta(\tau)$. Since F(t) is uncorrelated in time, $S_F(\omega) = F_o^2/2\pi$ is "white" (independent of frequency). Thus, $S_T(\omega) = F_o^2/2\pi C^2(\tau_o^{-2} + \omega^2)$. F_o^2 may be determined from the normalization condition (Eq. (3.4a)) that

$$c_T(0) = \langle(\Delta T)^2\rangle = k_B T^2/C = \int_{-\infty}^{\infty} S_T(\omega)\, d\omega \quad .$$

We find that $F_o^2 = 2k_B T^2 G$ and

$$S_T(\omega) = k_B T^2/\pi G\left[1 + \omega^2\tau_o^2\right] \quad . \qquad (3.5)$$

$S_T(\omega)$ is the usual Lorentzian spectrum characteristic of processes with a single correlation time, τ_o.[25] This spectrum is obviously not 1/f. In fact, the 1/f spectrum can only arise from physical processes characterized by the appropriate distribution of correlation times.[26] One process with a distribution of correlation times is diffusion, which, moreover, represents a better approximation to the heat flow in the metal samples.

With a simple extension of this single correlation time system, one may approach a 1-dimensional diffusion system. Figure 4(b) shows a string of equal masses of heat capacity C connected by thermal conductances, G. The temperature of the n^{th} mass obeys the Langevin equation:

$$CdT_n/dt = G(T_{n+1} + T_{n-1} - 2T_n) + F_{n+1/2} - F_{n-1/2} \quad . \tag{3.6}$$

Each of the random driving terms $F_{n+1/2}$ is independent of the others. If we assume that each of the masses is separated by a distance ℓ_o, we may define $c = C/\ell_o$ as the heat capacity per unit length and $g = G\ell_o$ as the thermal conductivity. In the limit $\ell_o \to 0$, T becomes a continuous function of position and time, $T = T(x,t)$, and obeys the diffusion equation:

$$\partial T/\partial t = D\partial^2 T/\partial x^2 + c^{-1}\partial F/\partial x \quad , \tag{3.7}$$

where $D = g/c$ is the thermal diffusivity and $F(x,t)$ obeys the relation $\langle F(x,t)\ F(x + s,t + \tau)\rangle = 2\pi F_o^2 \delta(s)\delta(\tau)$. The quantity of interest is now the spatial average of the temperature, $\bar{T}(t)$, over the length 2ℓ from $x = -\ell$ to $x = \ell$:

$$\bar{T}(t) = \frac{1}{2\ell}\int_{-\ell}^{\ell} T(x,t)\, dx \quad . \tag{3.8}$$

$T(x,t)$ may be defined in terms of its space and time Fourier transform:

$$T(x,t) = \frac{1}{2\pi}\int_{-\infty}^{\infty} dk \int_{-\infty}^{\infty} d\omega e^{ikx} e^{-i\omega t} T(k,\omega). \tag{3.9}$$

From Eq. (3.7) we find

$$T(k,\omega) = ikF(k,\omega)/c[Dk^2 - i\omega] \quad . \tag{3.10}$$

Since from Eq. (3.8),

$$\bar{T}(\omega) = \frac{1}{2\ell}\int_{-\ell}^{\ell} T(x,\omega)\, dx \quad ,$$

using Eq. (3.9) we have

$$\bar{T}(\omega) = (2\pi)^{-1/2}\int_{-\infty}^{\infty} \frac{\sin k\ell}{k\ell}\; T(k,\omega)\, dk \quad . \tag{3.11}$$

The frequency spectrum is defined by $S_T(\omega) = \langle \bar{T}(\omega)\, \bar{T}^*(\omega)\rangle$. The uncorrelated nature of F in space and time implies that it has a white spectrum in ω space and k space. We thus set $\langle F(k,\omega)\, F^*(k',\omega)\rangle = F_o^2\delta(k - k')/2\pi$ so that $S_T(\omega)$ reduces to

$$S_T(\omega) = \frac{F_o^2}{(2\pi)^2c^2}\int_{-\infty}^{\infty} \frac{\sin^2 k\ell}{k^2\ell^2}\; \frac{k^2 dk}{D^2k^4 + \omega^2} \tag{3.12}$$

Once again F_o^2 may be determined from the normalization condition

$$\langle(\Delta T)^2\rangle = k_B T^2/2\ell c = \int_{-\infty}^{\infty} S_T(\omega)\, d\omega \quad .$$

We find $F_o^2 = 2k_BT^2g$. $S_T(\omega)$ may now be explicitly integrated to give

$$S_T(\omega) = \frac{k_BT^2D^{1/2}}{4\sqrt{2}\ell^2c\pi\omega^{3/2}}\; [1 - e^{-\theta}(\sin\theta + \cos\theta)] \quad , \tag{3.13}$$

where $\theta \equiv (\omega/\omega_o)^{1/2}$, and $\omega_o = D/2\ell^2$ is the natural frequency defined by the problem. $S_T(\omega) \to k_BT^2/2\sqrt{2\pi}D^{1/2}\omega^{1/2}c$ for $\omega \ll \omega_o$ and

$S_T(\omega) \to k_B T^2 D^{1/2}/4\sqrt{2}\pi \ell^2 c\omega^{3/2}$ for $\omega \gg \omega_0$.[20,21]

As a check on the formalism one may obtain from Eq. (3.10) the space-time correlation function, $c_T(s,\tau) \equiv \langle \Delta T(x + s, t + \tau)\, \Delta T(x,t) \rangle$,

$$c_T(s,\tau) = [k_B T^2/c(4\pi D\tau)^{1/2}] \exp(-s^2/4D\tau) \quad , \tag{3.14}$$

which is the familiar result for 1-dimensional diffusion processes.[27] The physical insight into the connection between diffusion and the 1/f-like spectrum, however, comes from a calculation of the frequency-dependent correlation function, $c_T(s,\omega) \equiv \langle T(x + s,\omega)\, T^*(x,\omega) \rangle$. For the 1-dimensional case we obtain from Eq. (3.10)

$$c_T(s,\omega) = \frac{k_B T^2 \cos[(\pi/4) + |s|/\lambda]}{2\pi c D^{1/2} \omega^{1/2}}\, e^{-|s|/\lambda} \quad , \tag{3.15}$$

where $\lambda(\omega) \equiv (2D/\omega)^{1/2}$ is the ω-dependent correlation length and is a measure of the average spatial extent of a fluctuation at frequency ω. A low ω fluctuation effectively samples $F(x,t)$ over a large coherent volume giving a large amplitude.

When $\omega \ll \omega_0$, $\lambda(\omega) \gg 2\ell$ and the fluctuations become correlated across the entire length. In this case $S_T(\omega)$ can also be expressed as

$$S_T(\omega) = \int_{-\ell}^{\ell} \frac{dx_1}{2\ell} \int_{-\ell}^{\ell} \frac{dx_2}{2\ell}\, c_T(x_1 - x_2,\omega) \quad . \tag{3.16}$$

Since $c_T(s,\omega)$ is independent of s as $\omega \to 0$, $S_T(\omega) \to c_T(0,\omega)$ as $\omega \to 0$ leading to the same low ω limit as that obtained from Eq. (3.13).

In the high ω region ($\omega \gg \omega_o$) $\lambda(\omega) \ll 2\ell$. Although 2ℓ may be divided into many correlated regions each of length λ only the two end regions can fluctuate independently of the others. Energy exchange between any of the internal lengths cannot change $\bar{T}(t)$. The behavior is then best understood in terms of 1-dimensional energy flow across the boundaries. The energy flow, $j(x,t)$, obeys the equation, $J = -g\partial T/\partial x - F(x,t)$. From Eq. (3.10), $j(k,\omega) = i\omega F(k,\omega)/[Dk^2 - i\omega]$. If $E(t)$ represents the total energy on one side of the boundary at $x = \ell$ and we consider only flow across this signal boundary, then $dE(t)/dt = j(\ell,t)$, and

$$E(\omega) = -i(2\pi)^{-1/2}\omega^{-1}\int_{-\infty}^{\infty} \exp(ik\ell)\, j(k,\omega)\, dk \quad .$$

Thus,

$$\langle|E(\omega)|^2\rangle = \frac{F_o^2}{(2\pi)^2}\int_{-\infty}^{\infty} \frac{dk}{D^2k^4 + \omega^2} = \frac{k_B T^2 g}{2^{3/2}D^{1/2}\pi\omega^{3/2}} \qquad (3.17)$$

for energy fluctuations due to flow across a single boundary. For $\omega \gg \omega_o$ the flows across the two ends are independent; and, since $\Delta T = \Delta E/2\ell c$, $S_T(\omega) = 2\langle|E(\omega)|^2\rangle/4\ell^2c^2 = k_B T^2/4\sqrt{2}\pi\ell^2 c\omega^{3/2}$ as before.

This formalism may readily be extended to m dimensions. $T(x,t)$ obeys the Langevin diffusion equation

$$\frac{\partial T}{\partial t} = D\nabla^2 T + \underset{\sim}{\nabla}\cdot\underset{\sim}{F}/c \quad , \qquad (3.18)$$

where $\langle\underset{\sim}{F}(\underset{\sim}{x} + \underset{\sim}{s}, t + \tau)\cdot\underset{\sim}{F}(\underset{\sim}{x},t)\rangle = (2\pi)^m F_o^2 \delta(\underset{\sim}{x})\,\delta(\tau)$. If $\bar{T}(t)$ is the spatially averaged temperature of a box of volume $\Omega = 2^m \ell_1 \ldots \ell_m$ in m-dimensions, then

$$S_T(\omega) = \frac{F_o^2}{(2\pi)^{m+1}c^2}\int \frac{d^m k k^2}{D^2k^4 + \omega^2}\prod_{i=1}^{m}\frac{\sin^2 k_i\ell_i}{k_i^2\ell_i^2} \quad . \qquad (3.19)$$

The requirement that $\langle(\Delta T)^2\rangle = \int S_T(\omega)\, d\omega$ gives $F_o^2 = 2k_B T^2 g$. Although we have been unable to determine a general analytic expression for $S_T(\omega)$, we can determine its limiting forms from the behavior of the appropriate ω-dependent correlation function, which retains its dependence on $\exp(-|s|/\lambda)$ in all dimensions. Thus, in 2 dimensions

$$c_T(\underset{\sim}{s},\omega) = (k_B T^2/2\pi Dc)\, \ker(\sqrt{2}|\underset{\sim}{s}|/\lambda) \quad , \tag{3.20}$$

where $c_T(\underset{\sim}{s},\omega) \to (k_B T^2/2\pi^2 Dc)\, \ln(\sqrt{2}\lambda/|s|)$ for $|s| \ll \lambda$ and $c_T(\underset{\sim}{s},\omega) \to |\underset{\sim}{s}|^{-1/2} \exp(-\sqrt{2}|\underset{\sim}{s}|/\lambda)$ for $|\underset{\sim}{s}| \gg \lambda$. In 3 dimensions

$$c_T(\underset{\sim}{s},\omega) = \frac{k_B T^2}{4\pi^2 Dc|\underset{\sim}{s}|}\, \cos(|\underset{\sim}{s}|/\lambda)\, e^{-|\underset{\sim}{s}|/\lambda} \quad . \tag{3.21}$$

For a regular 3 dimensional volume of lengths $\ell_1 \gg \ell_2 \gg \ell_3$ the three natural frequencies, $\omega_i = D/2\ell_i^2$, separate the spectrum into four regions. In the frequency region $\omega \gg \omega_1, \omega_2$ the lengths ℓ_1 and ℓ_2 may be considered infinite and the spectrum becomes 1-dimensional with temperature fluctuations only due to energy flow in the x_3 direction. Thus as calculated above $S_T(\omega) \propto \omega^{-3/2}$ for $\omega \gg \omega_3$ and $S_T(\omega) \propto \omega^{-1/2}$ for $\omega_2 \ll \omega \ll \omega_3$. If $\omega \gg \omega_1$, the spectrum looks 2-dimensional with temperature fluctuations only due to energy flow in the x_2 and x_3 directions. The low frequency limit of the 2-dimensional spectrum may be calculated from Eq. (3.20) and the observation that

$$S_T(\omega) = \Omega^{-2} \int_\Omega d\underset{\sim}{x} \int_\Omega d\underset{\sim}{x}'\, c_T(\underset{\sim}{x} - \underset{\sim}{x}',\omega) \quad . \tag{3.22}$$

From the limiting form of Eq. (3.20) as $\omega \to 0$ it can be seen that $S_T(\omega) \propto [\text{const} + \ln(1/\omega)]$ for $\omega_1 \ll \omega \ll \omega_2$.[24] For $\omega \ll \omega_1$ $S_T(\omega)$ is determined from the low frequency limit of the 3-dimensional $c_T(s,\omega)$ (Eq. (3.21)) and Eq. (3.22). Thus, for $\omega \ll \omega_1$, $S_T(\omega) \propto$ const.[14] The behavior of $S_T(\omega)$ for the four regions of the spectrum of a regular 3-dimensional volume are shown in Fig. 5(a). The $\omega^{-3/2}$ behavior at high ω for all dimensionalities is characteristic of diffusive flow across a sharp boundary.[23] When λ is $\ll$ any length 2ℓ; only the outer shell of an arbitrary volume, Ω, can fluctuate independently of the remainder and then only by local 1-dimensional flow across the boundary. A generalization of Eq. (3.17) gives

$$S_T(\omega) \to k_B T^2 A / 2^{3/2} \pi \Omega^2 c \omega^{3/2} \quad \text{as} \quad \omega \to \infty \tag{3.23}$$

where A is the total surface area of Ω. If, on the other hand, the boundary is not sharp but has a finite width, w, $S_T(\omega)$ varies as ω^{-2} for $\omega \gg D/w^2$.

As discussed in Section IX these calculated spectra for diffusive systems have been verified experimentally by a direct measurement of the spectra. However, unlike the measured $S_V(f)$ for metal films shown in Figs. 1 and 2, Fig. 5(a) does not show an extended region of 1/f behavior. Figure 5(a) was calculated for temperature fluctuations in a regular subvolume of a uniform medium. On the other hand, the experimental system of metal film on glass substrate does not present a uniform medium for heat conduction. We expect diffusive flow along the film to dominate the heat conduction creating primarily a 2-dimensional system; but with some effects due to coupling

to the substrate. The importance of coupling to the substrate on the spectrum has, in fact, been demonstrated for superconducting films at T_c.[16] It is also possible that path switching effects, in which a temperature configuration that does not change $\bar{T}(t)$ does change R, ($\Delta V \neq \bar{V}\beta\Delta\bar{T}$) may play a role. However, at the frequencies measured λ is large enough that temperature fluctuations are expected to be correlated across the cross section of the strip, hence $\Delta V = \bar{V}\beta\Delta\bar{T}$.

If we assume that the temperature fluctuations in the metal films obey a diffusion equation, but that the complex nature of the system introduces an explicit 1/f region into the spectrum at intermediate frequencies, we may form a model spectrum that will allow quantitative comparison of the measured noise with that predicted from temperature fluctuations. Since the thermal conductivity of the film is so much higher than the substrate, we expect the high frequency behavior to be 2-dimensional while at low enough frequencies the spectrum must become 3-dimensional and independent of frequency. This simple model spectrum is illustrated in Fig. 5(b). The limits of the 1/f region are defined by the natural frequencies of the film, $D/\pi\ell^2$ and $D/\pi w^2$ where ℓ and w are the length and width of the film. The high and low frequency limits are taken to be diffusion-like: $S_T(f) \propto f^{-3/2}$ for $f > D/\pi w^2$ and $S_T(f) \propto$ const for $f < D/\pi\ell^2$. The normalization condition

$$\langle(\Delta T)^2\rangle = k_B T^2/C_V = \int_0^\infty S_T(f)\, df$$

then determines the magnitude of the spectrum. In the 1/f region

$$S_V(f)/\bar{V}^2 = \beta^2 k_B T^2 / C_V [3 + 2 \ln(\ell/w)] f \quad , \tag{3.24}$$

independent of D. The term $\ln(\ell/w)$ makes Eq. (3.24) extremely insensitive to changes in the limits of the 1/f region. For metals at room temperature $C_V \approx 3Nk_B$ where N is the total number of atoms in the sample, and

$$S_V(f) = \bar{V}^2 \beta^2 T^2 / 3N[3 + 2 \ln(\ell/w)] f \quad . \tag{3.25}$$

For the samples of Hooge and Hoppenbrouwers,[1] Eq. (3.25) predicts $S_V(f)/\bar{V}^2 \approx 3.6\times10^{-3}/Nf$ which is within a factor of two of their experimental results (Eq. (1.1)) if we replace N_c by N. The last column of Table I shows the calculated values of $S_T(f)$ from Eq. (3.25) for our samples. The agreement is excellent.

Although the calculated $S_T(\omega)$ for simple uniform diffusive media do not have an explicit 1/f region, the assumption of such a 1/f region in $S_T(f)$ for the complex experimental systems allows a quantitave prediction of the 1/f noise in excellent agreement with experiment.

"But the main thing is, does it hold good measure?"
Robert Browning

IV. MEASUREMENT OF SPATIAL CORRELATION OF 1/f NOISE

The usual diffusion theory does not provide an explanation for the 1/f spectrum, it does, however, suggest an important experimental test of the correctness of a diffusion mechanism. Fluctuations in a diffusive medium are characterized by the frequency-dependent correlation length, $\lambda(f) = (D/\pi f)^{1/2}$. Thus, the temperature fluctuations of two regions separated by a length ℓ should be independent if $\ell \gg \lambda(f)$, and correlated if $\ell \ll \lambda(f)$. The extent of the correlation depends on the dimensionality of the diffusion process and the exact geometry of the two regions.

Figure 6(a) shows the experimental configuration for an experiment designed to measure the frequency dependence of the correlation of the 1/f noise from two regions of a single Bi film. A Bi film of thickness 1000Å was cut to form two strips each of length ℓ and width 12 μm. Separate batteries and large resistances R_o were used to supply a constant current to each strip and prevent any correlation via a common power supply. The two noise voltages $V_1(t)$ and $V_2(t)$ were separately amplified with PAR113 preamplifiers and the spectrum of their sum or difference measured with the PDP-11 as described in Section II. If $S_+(f)$ is the spectrum of $[V_1(t) + V_2(t)]$ and $S_-(f)$ is the spectrum of $[V_1(t) - V_2(t)]$, the fractional correlation between the strips, $C(f)$, is given by

$$C(f) = [S_+(f) - S_-(f)]/[S_+(f) + S_-(f)] . \quad (4.1)$$

When $V_1(t)$ and $V_2(t)$ are independent, $S_+(f) = S_-(f)$ and $C(f) = 0$. When the two strips are completely correlated $V_1(t) = V_2(t)$, $S_-(f) = 0$, and $C(f) = 1$. For temperature fluctuations at high f, $\lambda(f) \ll \ell$ and $C(f) \to 0$, while at low f, $\lambda(f) \gg \ell$ and $C(f) \to$ const. The change from correlated to uncorrelated behavior occurs when $\lambda(f) \approx \ell$. Experimental results for two different values of ℓ are shown in Fig. 6(b). The condition $\lambda(f) = 1$ corresponds to f = 0.13 Hz for ℓ = 7.5 mm, and f = 1.2 Hz for ℓ = 2.5 mm (with $D \approx 0.2$ $cm^2 sec^{-1}$), in good agreement with the frequencies at which C(f) changes rapidly. As ℓ is increased, the low frequency limit of C(f) decreases because a fluctuation in one strip has an increasing probability of decaying without influencing the other strip. For ℓ much greater than 7.5 mm, it became increasingly difficult to observe any correlation. Since we could not measure $S_+(f)$ and $S_-(f)$ simultaneously, we often observed errors due to slow changes with time of S(f). Depending upon whether we measured $S_+(f)$ or $S_-(f)$ first, a slow change would appear either as a positive or negative offset to C(f), as in the ℓ = 2.5 mm case in Fig. 6(b).

These measurements of the frequency-dependent spatial correlation of the 1/f noise in metal films and the observation that the change from uncorrelated to correlated behavior occurs at a frequency predicted by the thermal diffusivity provide strong experimental evidence that the 1/f noise arises from a thermal diffusion mechanism.

"A thing may look evil in theory, and yet be in practice excellent."
Edmund Burke

V. SPATIALLY CORRELATED FLUCTUATIONS

The absence of 1/f noise in manganin, the scaling of $S_V(f)/\bar{V}^2$ as $1/\Omega$, the general decrease of $S_V(f)$ with temperature, the observed frequency-dependent spatial correlation, and the ability of temperature fluctuations to correctly predict the absolute magnitude of $S_V(f)$ (with an assumed 1/f spectrum for $S_T(f)$) provide overwhelming evidence that the 1/f noise in metal films is due to equilibrium temperature fluctuations modulating the film resistance. Yet, the inability of the usual diffusion theory as outlined above to yield a 1/f spectrum suggests a reexamination of the theory.

In Section III we presented a physically simple derivation of the spectrum of temperature fluctuations in infinite, uniform, diffusive media. The results have been verified experimentally for independent particles undergoing Brownian motion. As mentioned in Section III, it is possible that the non-uniform nature of a metal film on a glass substrate is responsible for the 1/f spectrum. However, more sophisticated models of the experimental configuration (for example, a diffusive medium coupled to a constant temperature substrate, or two coupled diffusive media) were unsuccessful in generating a 1/f spectrum. In most cases the increasing complexity of the models only brought in more low-frequency flattening. The measured spectra correspond to the frequency range $f < f_3$ in Fig. 5(a) and, consequently, would be expected to vary as $\lesssim f^{-1/2}$. Any coupling to a substrate could only be expected to cause a temperature fluctuation to decay more

rapidly and further flatten the spectrum. The measured spectra, on the other hand, have a 1/f behavior down to frequencies as low as $f_1/1000$.

The calculated diffusion spectra of Section III assume that the fluctuations are spatially uncorrelated: $\langle \Delta T(\underset{\sim}{x} + \underset{\sim}{s},t)\ \Delta T(\underset{\sim}{x},t) \rangle \equiv c_0(\underset{\sim}{s}) \propto \delta(\underset{\sim}{s})$. A spatial correlation of the temperature fluctuations, $c_0(\underset{\sim}{s}) \neq \delta(\underset{\sim}{s})$, could drastically alter the shape of $S_T(f)$; and, as suggested by Lundstrom, McQueen and Klason,[28] in certain cases give an explicit 1/f region. Such spatial correlation would occur if the free energy of a given temperature configuration is non-local and contains higher order terms such as $(\nabla T)^2$. A familiar example of this effect is the large correlation length of density fluctuations at a critical point.[29] The presence of a term such as $(\nabla T)^2$ implies that configurations with slow spatial variations require a smaller free energy and, consequently, have a greater probability of occurring than configurations with rapid spatial variations.

More explicitly, if $\bar{T}(t)$ is the spatially averaged temperature over some arbitrary volume Ω, then

$$T(t) = \int_{\Omega} T(\underset{\sim}{x},t)\ d^3x = \int B^*(\underset{\sim}{k})\ T(\underset{\sim}{k},t)\ d^3k \quad , \tag{5.1}$$

where

$$B(\underset{\sim}{q}) \equiv (2\pi)^{-1/2} \int_{\Omega} e^{-i\underset{\sim}{q}\cdot\underset{\sim}{x}}\ d^3x \quad . \tag{5.2}$$

Thus, the autocorrelation function $c_T(\tau) = \langle \bar{T}(t)\ \bar{T}(t+\tau) \rangle$ has the form

$$c_T(\tau) = \int |B(\underset{\sim}{k})|^2\ \langle T(\underset{\sim}{k},t)\ T^*(\underset{\sim}{k},t+\tau) \rangle\ d^3k \quad . \tag{5.3}$$

Because the temperature fluctuations obey a diffusion equation,

$$\langle T(\underset{\sim}{k},t)\, T^{*}(\underset{\sim}{k},t+\tau)\rangle = \langle |T(\underset{\sim}{k})|^{2}\rangle\, e^{-Dk^{2}\tau}$$

where $\langle |T(\underset{\sim}{k})|^{2}\rangle$ is the mean square amplitude of temperature fluctuations of wavevector $\underset{\sim}{k}$. By Eq. (3.4b) the spectrum then has the form

$$S_{T}(\omega) \propto \int \frac{|B(\underset{\sim}{k})|^{2}\, Dk^{2}\, \langle |T(\underset{\sim}{k})|^{2}\rangle\, d^{3}\underset{\sim}{k}}{D^{2}k^{4} + \omega^{2}} \quad . \tag{5.4}$$

$\langle |T(\underset{\sim}{k})|^{2}\rangle$ is related to $c_{o}(\underset{\sim}{s})$ by the spatial Wiener-Khintchine relation

$$\langle |T(\underset{\sim}{k})|^{2}\rangle = (2\pi)^{-3} \int c_{o}(\underset{\sim}{s})\, e^{i\underset{\sim}{k}\cdot\underset{\sim}{s}}\, d^{3}s \quad .$$

For uncorrelated temperature fluctuations, $c_{o}(\underset{\sim}{s}) \propto \delta(\underset{\sim}{s})$ and $\langle |T(\underset{\sim}{k})|^{2}\rangle$ = cost. Moreover, for a regular volume of sides $2\ell_{i}$,

$$B(\underset{\sim}{k}) \propto \prod_{i=1}^{3} \sin(k\ell_{i})/k_{i} \quad ;$$

and Eq. (5.4) reproduces Eq. (3.19) for $S_{T}(\omega)$.

If, however, the $(\nabla T)^{2}$ term dominates the free energy we find $\langle |T(\underset{\sim}{k})|^{2}\rangle \propto 1/k^{2}$, $c_{o}(\underset{\sim}{s}) \propto 1/|\underset{\sim}{s}|$, and

$$S_{T}(\omega) \propto \int \frac{|B(\underset{\sim}{k})|^{2}\, d^{3}k}{D^{2}k^{4} + \omega^{2}} \quad . \tag{5.5}$$

We now show that it is possible to treat these spatially correlated fluctuations in the Langevin formalism by replacing the $\underset{\sim}{\nabla}\cdot\underset{\sim}{F}$ term in Eq. (3.18) by a random source, $F(\underset{\sim}{x},t)$, to give

$$\partial T/\partial t = D\nabla^{2}T + F(\underset{\sim}{x},t)/c \quad . \tag{5.6}$$

$F(\underset{\sim}{x},t)$ is assumed to be uncorrelated in space and time, $\langle F(\underset{\sim}{x}+\underset{\sim}{s},t+\tau)\,F(\underset{\sim}{x},t)\rangle = (2\pi)^m F_o^2 \delta(\underset{\sim}{s})\delta(\tau)$. $F(\underset{\sim}{x},t)$ is a random source which adds or substracts energy from the diffusive system. The $\underset{\sim}{\nabla}\cdot\underset{\sim}{F}$ term (Eq. (3.18)), on the other hand, represents a random flow of energy within the diffusive system.

As with Eq. (3.18) we may determine the spectrum of the spatially averaged temperature of a box of volume $\Omega = 2^m \ell_1 \ldots \ell_m$ in m-dimensions. Thus:

$$T(\underset{\sim}{k},\omega) = F(\underset{\sim}{k},\omega)/c[Dk^2 - i\omega] \quad , \tag{5.7}$$

and

$$S_T(\omega) = \frac{F_o^2}{(2\pi)^{m+1} c^2} \int \frac{d^m k}{D^2 k^4 + \omega^2} \prod_{i=i}^{m} \frac{\sin^2 k_i \ell_i}{k_i^2 \ell_i^2} \quad . \tag{5.8}$$

A comparison of Eqs. (5.4) and (5.8) shows that the introduction of $F(\underset{\sim}{x},t)$ is equivalent to $\langle |T(\underset{\sim}{k})|^2 \rangle \propto k^{-2}$. The normalization condition,

$$\langle (\Delta T)^2 \rangle = \int_{-\infty}^{\infty} S_T(\omega)\, d\omega \quad ,$$

cannot be applied unless $m \geq 3$ since for one and two dimensions $\int S_T(\omega)\, d\omega$ diverges.

The general behavior of the spectrum can be determined from the three dimensional frequency dependent correlation function,

$$c_T(\underset{\sim}{s},\omega) = \frac{F_o^2 \cos[(\pi/4) + |\underset{\sim}{s}|/\lambda]}{16\pi^2 D^{3/2} \omega^{1/2}} \underset{\sim}{e}^{-|s|/\lambda} \quad , \tag{5.9}$$

where, as before, $\lambda(\omega) = (2D/\omega)^{1/2}$. In the limit $\omega \to 0$ ($\lambda(\omega) \gg |\underset{\sim}{s}|$), $c_T(\underset{\sim}{s},\omega) \propto \omega^{-1/2}$. Because $F(\underset{\sim}{x},t)$ is an external source, each correlated region may be considered as fluctuating independently of the other correlated volumes with a spectrum $S_c(\omega) \propto \omega^{-1/2}$ from Eq. (5.9).

If Ω, the volume of interest, consists of N independent correlated volumes, $S_T(\omega) \propto S_c(\omega)/N$. Thus, when $\omega \gg \omega_3$, $\lambda(\omega) \ll \ell_3$ and Ω is composed of $N = \Omega/\lambda^3(\omega)$ independent volumes:

$$S_T(\omega) \propto S_c(\omega)\ \lambda^3(\omega)/\Omega \propto \omega^{-2} \quad . \quad (\omega \gg \omega_3) \tag{5.10a}$$

When $\omega_2 \ll \omega \ll \omega_3$, $\ell_2 \gg \lambda(\omega) \gg \ell_3$, and Ω is composed of $N = \ell_1\ell_2/\lambda^2$ independent volumes:

$$S_T(\omega) \propto S_c(\omega)\ \lambda^2(\omega)/\ell_1\ell_2 \propto \omega^{-3/2} \quad . \quad (\omega_2 \ll \omega \ll \omega_3) \tag{5.10b}$$

when $\omega_1 \ll \omega \ll \omega_2$, $\ell_1 \gg \lambda(\omega) \gg \ell_2$, and Ω is composed of $N = \ell_1/\lambda(\omega)$ independent volumes:

$$S_T(\omega) \propto S_c(\omega)\ \lambda(\omega)/\ell_1 \propto \omega^{-1} \quad . \quad (\omega_1 \ll \omega \ll \omega_2) \tag{5.10c}$$

and, for $\omega \ll \omega_1$ all of Ω is correlated:

$$S_T(\omega) \propto S_c(\omega) \propto \omega^{-1/2} \quad . \quad (\omega \ll \omega_1) \tag{5.10d}$$

The shape of $S_T(f)$ for this type of spatially correlated temperature fluctuation is shown in Fig. 7. Not only does $S_T(f)$ contain an explicit 1/f region, but this region corresponds to the low frequency limit of a two dimensional system and matches the frequency range over which the metal films are observed to have the 1/f spectrum. In fact, if we assume that $\langle(\Delta T)^2\rangle = \bar{T}^2/3N$, we find

$$\frac{S_V(f)}{\bar{V}^2} = \frac{\beta^2 T^2}{3N[4 - d/w + 2\ \ln(l/w)]\ f} \quad , \tag{5.11}$$

where d is the film thickness. This result differs from our earlier model spectrum, Eq. (3.25), only by a factor close to unity.

Although the introduction of spatially correlated fluctuations provides a means of achieving the 1/f spectrum for simple diffusive systems, the theoretical justification of the spatial correlation in the case of equilibrium temperature fluctuations poses new problems: notably the physical origin of the correlations, and the proper normalization of the spectrum. Moreover, it remains to be demonstrated that the correlated temperature fluctuations can produce the 1/f spectrum for the thermally inhomogeneous experimental systems.

It is interesting to note that when treated by the Langevin method (the association of an uncorrelated random source, F(t), with each thermal conductance), a diffusive system coupled to a substrate at constant temperature, T_o, via a thermal conductance, G, may be treated by an $F_1(\underset{\sim}{x},t)$ term representing exchange of energy with the substrate. In this case,

$$c\partial T/dt = g\nabla^2 T + \underset{\sim}{\nabla}\cdot\underset{\sim}{F} - G(T - T_o) + F_1(\underset{\sim}{x},t) \quad . \tag{5.12}$$

It can be shown, however, that the frequency region in which $F_1(\underset{\sim}{x},t)$ dominates $\underset{\sim}{\nabla}\cdot\underset{\sim}{F}$ corresponds to the region in which the -GT decay term dominates $g\nabla^2 T$ and the spectrum never achieves a 1/f behavior.

"The energies of our system will decay, ..."

Arthur James Balfour,
The Foundations of Belief

"... by a gentle decay."

Walter Pope, The Old Man's Wish

VI. AUTOCORRELATION FUNCTIONS FROM DECAY MEASUREMENTS

The theoretical calculations of Sections III and V, as all such theoretical calculations, are based on the assumption that the spontaneously occurring fluctuations in equilibrium on the average obey the same decay law as small non-equilibrium macroscopic perturbations of the system.[17] The autocorrelation function for temperature fluctuations, $c_T(\tau)$, thus reflects the average manner in which a temperature fluctuation decays in time. By perturbing the temperature of the experimental system and measuring its response, we are able to measure $c_T(\tau)$. The cosine transform (Eq. (3.4b)) of $c_T(\tau)$ gives $S_T(\omega)$.

This procedure will be illustrated for the simple system shown in Fig. 4(a), and described by Eq. (3.2). If the temperature at $t = 0$ is raised ΔT above T_o the decay for $t > 0$ will proceed according to

$$T(t) = T_o + \Delta T e^{-t/\tau_o} \qquad (t > 0) \quad . \tag{6.1}$$

Thus, $c_T(\tau) \propto e^{-\tau/\tau_o}$ for $\tau > 0$. Since $c_T(\tau)$ is symmetric about $\tau = 0$, the normalization condition $c_T(0) = \langle(\Delta T)^2\rangle = k_B T^2/C$ implies

$$c_T(\tau) = (k_B T^2/C) \exp(-|\tau|/\tau_o) \quad , \tag{6.2}$$

which gives the same $S_T(\omega)$ as Eq. (3.5). Thus, the response of the system to a temperature perturbation determines the shape of the spectrum while the normalization condition, $c_T(0) = \langle(\Delta T)^2\rangle$, determines the magnitude.

This procedure is not so straightforward for extended media described by a diffusion equation. In this case, we are interested in the spatially averaged temperature of some volume Ω,

$$\bar{T}(t) \equiv \int_{\Omega} T(\underset{\sim}{x},t)\, d^3x/\Omega \quad . \tag{6.3}$$

It is obvious that a given perturbation ΔT in $\bar{T}(t)$ could occur for an infinite variety of perturbation distributions, $\Delta T(\underset{\sim}{x},t)$, each of which might have a different decay in time. We must determine which perturbation distribution corresponds to the desired spectrum. In the simplest distribution, the temperature of Ω is uniformly raised a height ΔT above the surroundings at $t = 0$. This is accomplished by dissipating the power, $P(t) = c\Delta T\delta(t)$, uniformly throughout Ω. The decay equation then becomes

$$\partial T/\partial t = D\nabla^2 T + \Delta T\delta(t)\, B(\underset{\sim}{x}) \quad , \tag{6.4}$$

where $B(\underset{\sim}{x}) = 1$ if $\underset{\sim}{x}$ is in Ω and $B(\underset{\sim}{x}) = 0$ otherwise. Introducing

$$T(\underset{\sim}{k},t) \equiv (2\pi)^{-1/2} \int T(\underset{\sim}{x},t)\, e^{-i\underset{\sim}{k}\cdot\underset{\sim}{x}}\, d^3x \quad ,$$

we find

$$T(\underset{\sim}{k},t) = \Delta T B(\underset{\sim}{k})\, e^{-Dk^2 t} \quad (t > 0) \quad , \tag{6.5}$$

where

$$B(\underset{\sim}{k}) = (2\pi)^{-1/2} \int B(\underset{\sim}{x})\ e^{-i\underset{\sim}{k}\cdot\underset{\sim}{x}}\ d^3x \quad .$$

Now, since

$$\bar{T}(t) = \int B(\underset{\sim}{x})\ T(\underset{\sim}{x},t)\ d^3x = \int B^*(\underset{\sim}{k})\ T(\underset{\sim}{k},t)\ d^3k \qquad (6.6)$$

we find from Eq. (6.5) that

$$\bar{T}(t) = \Delta T \int |B(\underset{\sim}{k})|^2\ e^{-Dk^2t}\ d^3k \qquad (t > 0) \quad . \qquad (6.7)$$

The cosine transform of Eq. (6.7) determines the shape of the spectrum:

$$S_T(\omega) \propto \int_0^\infty \bar{T}(t)\ \cos\omega t dt \propto \Delta T \int \frac{Dk^2 |B(\underset{\sim}{k})|^2\ d^3k}{D^2k^4 + \omega^2} \qquad (6.8)$$

For a regular Ω of sides $2\ell_1$, $2\ell_2$, $2\ell_3$,

$$|B(k)|^2 \propto \prod_{i=1}^{3} \sin^2(k_i\ell_i)/k_i^2 \quad ,$$

and we see that Eq. (6.8) predicts the same shape for the spectrum as Eq. (3.19) for uncorrelated fluctuations. This is not surprising. For uncorrelated fluctuations the average manner in which a fluctuation ΔT in $\bar{T}(t)$ occurs is by a uniform distribution of temperature over Ω. The importance of this result, however, is that it gives an experimental method of determining the shape of $S_T(\omega)$ for uncorrelated temperature fluctuations in an arbitrary volume with arbitrary coupling.

Another important result comes from a consideration of the temperature response of Ω to a step function input of dissipated power,

$P(t) = p_0\theta(t)\ B(\underset{\sim}{x})$, where $\theta(t) = 0$ for $t < 0$ and $\theta(t) = 1$ for $t > 0$. In this case

$$\partial T/\partial t = D\nabla^2 T + p_0\theta(t)\ B(\underset{\sim}{x})/c \quad , \tag{6.9}$$

and

$$T(\underset{\sim}{k},t) = (1 - e^{-Dk^2t})\ p_0 B(\underset{\sim}{k})/Dk^2c \quad . \tag{6.10}$$

Thus, we find that

$$\bar{T}(t) = \frac{p_0}{c}\int |B(\underset{\sim}{k})|^2\ (1 - e^{-Dk^2t})d^3k/Dk^2 \quad . \tag{6.11}$$

The cosine transform of Eq. (6.11) shows that

$$S_T(\omega) \propto \frac{p_0}{c}\int \frac{|B(\underset{\sim}{k})|^2\ d^3k}{D^2k^4 + \omega^2} \quad , \tag{6.12}$$

which has the same shape as $S_T(f)$ for correlated temperature fluctuations given by Eq. (5.5). The response of an arbitrary volume to a step function input of power thus determines the shape of the spectrum for correlated temperature fluctuations.

Figures 8 and 9 show the response of the same Au sample used in Figs. 2 and 3 to delta function and step function power inputs. The sample was one arm of a Wheatstone bridge. The other three arms consisted of wirewound resistors with a zero temperature coefficient of resistivity. At $t = 0$, a 1 kHz ac current was applied to the bridge. As the Au film became hot, the bridge became unbalanced. The PDP-11 was used as a digital lockin detector to measure the voltage response of the bridge as a function of time. In this way, the decay of the sample temperature was determined. Each decay was averaged

over many repetitions. The ac current provided the heating as well as the bias for measuring the temperature response. This method had the advantage that the necked-down areas of the film, which contributed the most noise, also were weighted the most heavily in the temperature response. The delta function response was determined from the derivative of the step function response. Direct delta function (very narrow pulse) response measurements gave similar results.

Figure 8 shows the temperature response $\bar{T}(t)$ to a delta function power input on three different time scales. The decay is essentially complete by a few hundredths of a second. Figure 9, on the other hand, shows $\bar{T}(t)$ for a step function input of power. The decay is much slower and appears to have appreciable contributions on all time scales. Figure 10 shows the cosine transform of these decays over many decades of frequency. The decay was assumed to give the shape of $c_T(\tau)$ and was normalized to $\bar{T}(0) = \langle(\Delta T)^2\rangle = \beta^2 T^2/3N$ to allow comparison with $S(f) = S_V(f)/\bar{V}^2$. The dotted line shows the expected S(f) for uncorrelated temperature fluctuations. As predicted theoretically, S(f) is 1/f-like for higher frequencies, but flattens rapidly for low frequencies. In this case, the low frequench cutoff, $f_1 = D/\pi\ell^2 \approx 80$ Hz, also corresponds to the measured change in behavior. The solid line, however, shows the expected S(f) for correlated fluctuations. This spectrum shows the 1/f behavior down to the lowest frequencies measured. The squares in Fig. 10 show the measured relative noise spectrum for the same sample. The normalized cosine transform of the measured step function response, which contains no fitted parameters, provides an excellent reproduction of the measured

noise spectrum both in shape and magnitude. The observation that the cosine transform of the step function response retains its 1/f behavior down to 10^{-2} Hz implies that even on these long time scales the heat conduction is preferentially two dimensional. Similar experiments on Bi films ($\beta < 0$) also show that the cosine transform of the step function response matches the measured noise spectrum, indicating, in addition, that feedback effects are not important in measuring the decay.

We have shown experimentally that correlated temperature fluctuations in the complex experimental systems of metal films on glass substrates can, in fact, produce the measured 1/f spectrum. Moreover, we have shown that the usual assumption of uncorrelated fluctuations does not produce the measured 1/f spectrum for these samples. The assumption of correlated equilibrium temperature fluctuations in a diffusive medium together with the normalization $\langle|\Delta T|^2\rangle = k_B T^2/C_V$ are, thus, sufficient to predict all the measured characteristics of 1/f noise in continuous metal films.

"Then, farewell, heat and welcome, frost!"

William Shakespeare, The Merchant of Venice

VII. THERMAL FLUCTUATIONS IN OTHER SYSTEMS

It was not possible to test in detail the dependence of $S_V/\bar{V}^2$ (Eq. (3.24)) on Ω, β, and T using the metal films. However, Clark and Hsiang[16] measured the 1/f noise in Sn films at the superconducting transition, where β is larger than at room temperature by a factor of about 10^5. In the first series of experiments, the Sn was evaporated directly onto a glass substrate. The main conclusions were:

(i) $S_V/\bar{V}^2 \propto 1/\Omega$ (for a factor of 30 variation in Ω);

(ii) $S_V \propto \beta^2$ (for a factor of 30 variation in β^2);

(iii) $S_V \propto \bar{V}^2$ (for a factor of 500 variation in $\bar{V}^2$);

(iv) the noise showed the expected spatial correlation;

(v) the magnitude of the noise was well represented by Eq. (3.24), thus verifying the dependence of S_V on T.

Equation (3.24) thus correctly predicts the measured 1/f noise in Sn both at 4K and 300K. In the subsequent experiments the Sn evaporation was preceded by a thin underlay of Al, that greatly enhanced the thermal coupling of the film to the substrate. Not only did the observed spectrum flatten at low frequencies to become white, but the degree of spatial correlation of the 1/f noise was appreciably reduced. As the coupling to the substrate increased a given temperature fluctuation in one section of the film could decay more rapidly by heat flow into the substrate and, consequently, was less likely to influence the neighboring sections. These results add strong support to the diffusion theory.

Clarke and Hawkins[18] measured the 1/f noise in Josephson tunnel junctions that were resistively shunted to eliminate hysteresis in the current-voltage characteristic. The noise was measured by passing a constant current, I, greater than the critical current, I_c, through the junction and measuring the voltage fluctuations with a superconducting voltmeter. If the noise is assumed to be due to equilibrium temperature fluctuations modulating I_c, a suitable modification of Eq. (3.24) leads to the following result for the noise power spectrum:

$$S_V(f) \approx \frac{(\partial V/\partial I_c)_I^2 (\partial I_c/\partial T)^2 k_B T^2}{3 C_V f} \quad . \tag{7.1}$$

C_V is the heat capacity of a volume given by the product of the junction area and a superconducting coherence length. The dependence of $S_V(f)$ on $(\partial V/\partial I_c)_I$ and $(\partial I_c/\partial T)$ was experimentally verified. In addition, the magnitude of the noise was accurately predicted by Eq. (7.1).

Weissman and Feher[30] have studied the low frequency noise in electrolytes in the presence of a current. Their system consisted of a capilliary tube connecting two large reservoirs. $S_V/\bar{V}^2$ was proportional to β^2 and was quantitatively predicted by the 3-dimensional diffusion model (Eq. (3.19)). Presumably the thermal conductivities of the solution and the glass capilliary were comparable and the boundary resistance between them not too large, so that the system was reasonably thermally homogeneous.

Thus, there are several different systems in which strong evidence exists for a thermal diffusion model of 1/f noise. However, in a series of experiments on semiconductors, we found no evidence for this model. In evaporated films of InSb we found that the noise was typically three orders of magnitude larger than that predicted by Eq. (3.25), and that there was no spatial correlation of the noise on a scale of a few mm at frequencies down to 10^{-3} Hz. We also found that the 1/f noise in very thin (~100Å) discontinuous metal films[3,4] was much larger than predicted by Eq. (3.25). In these systems, the noise due to thermal diffusion presumably exists, but is completely dominated by another mechanism. The lack of spatial correlation indicates that, if diffusive in nature, this additional mechanism must be characterized by $D < 10^{-5}$ $cm^2 sec^{-1}$. However, we were able to show that the 1/f noise in semiconductors and very thin metal films is also an equilibrium process.

"This humour of passive resistance ..."
Sir Walter Scott, Ivanhoe

VIII. EQUILIBRIUM MEASUREMENTS OF 1/f NOISE FROM RESISTANCE FLUCTUATIONS

We have observed a 1/f-like power spectrum for low frequency fluctuations of the mean square Johnson noise voltage across a very small sample of semiconductor or discontinuous metal film in thermal equilibrium. The 1/f spectrum is shown to be due to resistance fluctuations in the sample, and closely matches the resistance fluctuation spectrum obtained by passing a current through the sample.

Consider a resistance, R, of total heat capacity, C_V, shunted by a capacitance, C, and in thermal contact with reservoir at temperature T_o. The voltage across the capacitor, V(t), represents a single degree of freedom that can exchange energy with the resistor via the charge carriers in the resistor. The exchange takes place on time scales of order $\tau = RC$. In thermal equilibrium the average energy of the capacitor, $\langle E_c \rangle = \frac{1}{2} C\langle V^2 \rangle = \frac{1}{2} k_B T_o$. These voltage fluctuations (Johnson noise) are limited to a bandwidth of $1/4\tau$, and consequently have a spectrum of the form $S_V(f) = 4k_B T_o R/[1 + 4\pi^2 f^2 \tau^2]$. If the resistor is assumed to exchange energy with the reservoir on a time scale of order τ_R that is much greater than τ, the capacitor is able to reach equilibrium with the internal degrees of freedom of the resistor before the internal energy of the resistor can change. The temperature of the capacitor is then the same as the temperature of the resistor. $V^2(t)$, like V(t), is a rapidly fluctuating quantity in time due to this exchange of energy between the resistor and capacitor. However, the average of $V^2(t)$ over a time, θ, such that

$\tau \ll \theta \ll \tau_R$, $\langle V^2(t)\rangle_\theta = k_B T/C$ (T is now the instantaneous temperature of the resistor), is sensitive to slow energy or temperature fluctuations in the resistor on time scales τ_R or longer.

Experimentally, the Johnson noise voltage, V(t), is passed through a filter with a bandpass from f_o to f_1, squared, and averaged over a time $\theta > 1/f_o$ to give P(t), a slowly varying signal proportional to the Johnson noise power in the bandwidth f_o to f_1. Thus,

$$P(t) \approx 4k_B TR \int_{f_o}^{f_1} df/(1 + 4\pi^2 f^2 \tau^2) + P_o(t) \quad , \qquad (8.1)$$

where $P_o(t)$ represents the fluctuations in P(t) due to the rapid exchange of energy between capacitor and resistor. Because this exchange is so rapid, $P_o(t)$ has a spectrum, $S_{P_o}(f)$, that is independent of f for the low frequencies in which we are interested. S_{P_o} may be reduced by increasing the bandwidth or by moving the bandwidth to higher frequencies, but in practice $P_o(t)$ severely limits the accuracy of measurements of P(t).

If the bandwidth in Eq. (8.1) is either totally above or totally below the knee at $1/2\pi\tau$, P(t) is sensitive to slow resistance as well as temperature fluctuations. These resistance fluctuations, ΔR, may be driven by temperature fluctuations with a spectrum $S_T(f)$ so that $\Delta R = \bar{R}\beta\Delta T$; or be temperature independent fluctuations, ΔR_o, with a spectrum $S_{R_o}(f)$ (such as number or mobility fluctuations of the charge carriers). Thus, from Eq. (8.1), $\Delta P(t)/\bar{P} = (1 \pm \beta T_o)\Delta T/T_o + \Delta R_o/\bar{R} + P_o(t)/\bar{P}$, and the relative power spectrum for fluctuations in P(t) is of the form

$$\frac{S_P(f)}{\bar{P}^2} = (1 \pm \beta T_o)^2 \frac{S_T(f)}{T_o^2} + \frac{S_{R_o}(f)}{\bar{R}^2} + \frac{S_{P_o}}{\bar{P}^2} \quad , \tag{8.2}$$

where the plus sign corresponds to $f_o < f_1 \ll 1/2\pi\tau$, and the minus sign corresponds to $f_1 > f_o \gg 1/2\pi\tau$. If, however, most of the noise power and the knee frequency, $1/2\pi\tau$, are included in the bandwidth (i.e., $f_o \ll 1/2\pi\tau \ll f_1$), from Eq. (8.1) we find $P(t) \approx k_B T/C + P_o(t)$ and $S_P(f)/\bar{P}^2 = S_T(f)/T_o^2 + S_{P_o}/\bar{P}^2$. In this limit, P(t) is not sensitive to resistance fluctuations. Thus, with an appropriate choice of bandwidth, the low frequency spectrum of P(t) is an equilibrium measurement of $S_T(f)$ or $S_{R_o}(f)$ provided the temperature or resistance fluctuations are large enough to dominate S_{P_o}.

Our initial measurements were on evaporated InSb films with a thickness of 1000Å and a resistivity of about 1 Ωcm. As indicated in section VII, we expected to observe only the resistance fluctuations $\Delta R_o(t)$. In order to make the relative resistance fluctuation spectrum, $S_{R_o}(f)/\bar{R}^2$, large enough to dominate $S_{P_o}/\bar{P}^2$, the samples were made as small as possible. The resistance of a strip of InSb was monitored while the strip was cut transversely with a diamond knife until only a small bridge containing typically about 10^6 atoms remained. In the presence of a direct current, I, the relative power spectrum of the voltage fluctuations is $S(f) = S_V(f)/\bar{V}^2 = S_{R_o}(f)/\bar{R}^2$. The solid line in Fig. 11 shows S(f) for a 20 MΩ bridge of InSb measured with a direct current. The spectrum was remeasured using an ac technique in which a square wave current was applied to the sample,

and the PDP-11 was used as a digital lock-in detector to measure the spectrum of the amplitude fluctuations of the induced voltage. The relative spectrum is plotted with open circles in Fig. 11. In a third technique the current was supplied as a series of pulses to reduce the power dissipated in the sample. The relative spectrum is shown in Fig. 11 as open triangles. All three techniques measure the resistance spectrum, $S_{R_o}(f)/\bar{R}^2$. The agreement of the three spectra demonstrates that neither a direct current nor a constant dissipation of power is the cause of the 1/f spectrum.

For the measurement of P(t), the sample was capacitively coupled to a preamplifier to prevent any leakage current flowing through the sample. The input capacitance produced a knee frequency, $1/2\pi RC \approx 500$ Hz, in the Johnson noise spectrum. After amplification the noise was filtered with a 10 kHz to 300 kHz bandpass filter, squared with an analog multiplier, and filtered to remove frequencies above the digitizing frequency. Since the bandpass is above the knee frequency the calculated relative spectrum of this signal is given by Eq. (8.2) (with the minus sign), while the measured relative spectrum is shown as the open squares in Fig. 11. The white spectrum above 1 Hz represents $S_{P_o}/\bar{P}^2$. The 1/f spectrum below 1 Hz closely matches the current-biased measurements. To insure that the 1/f spectrum was generated by fluctuations in the sample rather than by spurious effects from our electronics, the InSb was replaced by a metal film resistor (which did not exhibit 1/f noise) of the same resistance. This relative spectrum is shown dotted in Fig. 11. The spectrum is white down to the lowest frequency measured, and represents only the term $S_{P_o}/\bar{P}^2$.

We have made similar measurements on metal films. The three current-biased techniques gave identical relative spectra for continuous metal films in which the resistance fluctuations are temperature induced, confirming that the current serves only as a probe of the equilibrium fluctuations. However, we were unable to make these films small enough for $S_R(f)/\bar{R}^2$ to dominate $S_{P_o}/\bar{P}^2$ at frequencies down to 10^{-3} Hz. We therefore used very thin (<100Å) films in which temperature induced fluctuations are not dominant. In Fig. 12, the continuous curve is the relative spectrum of a very thin Nb film ($R \approx 200$ kΩ) measured with an ac current bias. The open squares are a Johnson noise measurement with a bandwidth of 100 kHz to 200 kHz, above the knee frequency of 40 kHz. The agreement below 10^{-2} Hz is excellent. The dotted spectrum was obtained from the same sample using a bandwidth of 5 kHz to 200 kHz, which includes the knee frequency and most of the Johnson noise power. Although the low frequency spectrum is substantially reduced (as expected when P(t) is no longer sensitive to resistance fluctuations), it is still above the background spectrum of a large metal film resistor. This residual noise is possibly due to the temperature fluctuation term $S_T(f)/T_o^2$. Indeed, the assumption of a 1/f spectrum for $S_T(f)$ (Fig. 5(b)) for a sample of 10^6 atoms yields.

$$S_T(f)/T_o^2 \sim 3\times10^{-7}/f \text{ Hz}^{-1} \quad ,$$

a value that is consistent with the observed spectrum.

It was sometimes necessary to use the digital lockin technique to eliminate drifts in the analog multiplier zero offset. The amplifier output was grated on and off to provide a multiplier output consisting

of equal periods of offset and offset plus squared signal. These periods were digitized and the offset subtracted within the computer before analyzing the spectrum

Our results strongly suggest that 1/f noise in semiconductors and discontinuous metal films arises from equilibrium resistance fluctuations. Current-biased measurements probe these resistance fluctuations, but in no way generate them. This idea is consistent with several current theories of 1/f noise that propose various mechanisms for the resistance fluctuations, for example: the McWhorter[9] theory for semiconductors, carrier mobility fluctuations in semiconductions and ionic solutions,[7,8] and the temperature fluctuation model. Our results are obviously inconsistent with theories that involve non-equilibrium processes. For example: turbulence theories,[31] theories that require a long term steady current or power,[33] and theories involving thermal feedback via the heat generated by an external current.

"The thing to do is to supply light and not heat."
Woodrow Wilson,
Speech in Pittsburg 1/29/1916

IX. NUMBER FLUCTUATION SPECTRA FROM LIGHT SCATTERING

The calculated spectra of Sections III and V apply to any quantity governed by a diffusion equation. The disagreement, however, between the measured $S_V(f)/\bar{V}^2$ for metal films and the expected $S_T(f)$ for uncorrelated temperature fluctuations (Fig. 5(a)) suggests that we examine a different diffusive system. Perhaps the simplest and most extensively studied diffusive system is that of independent particles undergoing Brownian motion. The intensity of light scattered from a solution of these particles is sensitive to the number of particles in the illuminated region. To our knowledge, however, light scattering (or any other technique) has not been previously used to verify the theoretical spectrum (Fig. 5(a)) by a direct spectral measurement. Although light scattering is a common technique, number fluctuations are generally dominated by interference effects.

The intensity fluctuations of monochromatic coherent light scattered by a suspension of independent particles undergoing Brownian motion have been used to measure the diffusion constant, D, of the particles.[33] Similar methods have also been used to gain information about the motion of motile organisms.[34] Two closely related experimental techniques have been developed, namely heterodyne and homodyne detection. In the heterodyne experiment, first performed by Cummins et al.,[35] light scattered by the particles is mixed with light of constant phase from the same source, which acts as a local oscillator.

Interference between the constant phase component and the light scattered by each independent particle gives rise to intensity fluctuations. The heterodyne spectrum is, therefore, proportional to $\langle N \rangle$, the average number of illuminated particles. In the homodyne experiment, first performed by Ford and Benedek,[36] only light scattered from the particles is detected. The intensity fluctuations arise from interference between the light scattered by pairs of particles: as one particle moves relative to another, the phase difference of their electric fields at the detector varies. The fluctuation spectrum is thus proportional to the number of pairs of illuminated particles, $\langle N \rangle^2$. Both of these interference effects depend on the coherent nature of the incident light. The heterodyne and homodyne experiments may be considered as an elastic scattering of light from wavevector $\underset{\sim}{k}$ to $\underset{\sim}{k}'$ by $n_{\underset{\sim}{K}}$, a density fluctuation of wavevector $\underset{\sim}{K} = \underset{\sim}{k}' - \underset{\sim}{k}$. The autocorrelation function for the intensity then depends on the average manner in which $n_{\underset{\sim}{K}}$ decays in time. For independent particles undergoing Brownian motion $\langle n_{\underset{\sim}{K}}(t) \rangle = \langle n_{\underset{\sim}{K}}(0) \rangle e^{-DK^2 t}$. The fluctuations thus are correlated over a time $\tau_c \approx 1/DK^2$. By measuring τ_c or the shape of the spectrum, $S_I(f) \propto \tau_c/[1 + (2\pi\tau_c f)^2]$, one is able to determine D.

More recently, Schaefer and Berne[37] studied suspensions of polystyrene spheres in water when the average number of particles, $\langle N \rangle$, in the illuminated volume, Ω_i, was very small. In this limit, the relative fluctuations in the number of particles become significant, and introduce additional intensity fluctuations in the scattered light. These additional fluctuations are not an interference effect but arise because the intensity of the scattered light is sensitive

to the number of particles in Ω_i. Number fluctuations have also been observed by the fluorescence of individual particles.[38] The correlation time for the number fluctuations is of order ℓ^2/D, where ℓ is the smallest dimension of Ω_i, and is usually much greater than $1/DK^2$. Schaefer and Berne showed that the number fluctuations may be observed as a slowly varying excess background in the homodyne autocorrelation function. They were able to subtract out the contribution of the number fluctuations, and thus recover the usual homodyne autocorrelation function. The number fluctuations had a detectable effect for $\langle N \rangle \lesssim 10^2$.

We describe here a series of homodyne experiments in which laser light was scattered by a suspension of polystyrene spheres in water. The spectra of the intensity fluctuations of the scattered light were measured from 5×10^{-4} Hz to 5×10^{3} Hz. The spectra show clearly both the homodyne Lorentzian and the $f^{-3/2}$ behavior of $S_N(f)$. Provided $\langle N \rangle$ is not too small, the two spectra can easily be separated. Spectra were also obtained with a white light source; in this case, the interference Lorentzian was absent, and only $S_N(f)$ was observed. The observed spectra are in excellent quantitative agreement with the theoretical predictions.

Light of wavevector $\underset{\sim}{k}$ illuminates a small subvolume, Ω_i, of a cell of total volume Ω containing a suspension of M particles. Each of the illuminated particles scatters the light elastically with a phase that varies in time due to the particle motion. We wish to calculate the intensity fluctuation spectrum for light scattered with wavevector $\underset{\sim}{k}'$ into the detector. We assume initially that the

light is coherent over the area of the detector and that the electric field is of the form

$$\underset{\sim}{E}(t) = \underset{\sim}{E}_o e^{-i\omega_o t} + \underset{\sim}{\beta} \sum_{j=1}^{M} B(\underset{\sim}{r}_j)\, e^{-i\omega_o t}\, e^{i\underset{\sim}{K}\cdot\underset{\sim}{r}_j} \quad . \tag{9.1}$$

$\underset{\sim}{E}_o$ is the constant phase heterodyne component, and $\underset{\sim}{K} = \underset{\sim}{k}' - \underset{\sim}{k}$ is the scattering wavevector. $B(\underset{\sim}{r}_j) = 1$ if $\underset{\sim}{r}_j$ is in Ω_i, while $B(\underset{\sim}{r}_j) = 0$ otherwise. The intensity of the light, $I(t) = \underset{\sim}{E}(t)\cdot\underset{\sim}{E}^*(t)$, is given by

$$I(t) = E_o^2 + 2\underset{\sim}{\beta}\cdot\underset{\sim}{E}_o \sum_j B(\underset{\sim}{r}_j) \cos\underset{\sim}{K}\cdot\underset{\sim}{r}_j + \beta^2 \sum_{jk} B(\underset{\sim}{r}_j)\, B(\underset{\sim}{r}_k)\, e^{i\underset{\sim}{K}\cdot(\underset{\sim}{r}_j - \underset{\sim}{r}_k)} . \tag{9.2}$$

The positive frequency spectrum of the intensity fluctuations is given by the cosine transform of the autocorrelation function (Eq. 3.4b),

$$S_I(f) = 4\int_0^\infty \langle I(0)\, I(\tau)\rangle \cos(2\pi f\tau)\, d\tau \quad . \tag{9.3}$$

We assume that the motion of each of the particles is independent, that Ω is large enough that we may neglect any effects due to its boundaries, and that $|\underset{\sim}{K}| \gg \ell^{-1}$ where ℓ is the smallest dimensions of Ω_i. This last assumption is equivalent to setting $B(\underset{\sim}{K}) = 0$, where $B(\underset{\sim}{q})$ is the spatial Fourier transform of $B(\underset{\sim}{r})$. In other words,

$$B(\underset{\sim}{q}) \equiv (2\pi)^{-1/2} \int_\Omega B(\underset{\sim}{r})\, e^{i\underset{\sim}{q}\cdot\underset{\sim}{r}}\, d^3r = 0 \quad \text{for} \quad |\underset{\sim}{q}| \gg \ell^{-1} \quad .$$

$\langle I(0)\, I(\tau)\rangle$ involves the average of the product of two terms similar to Eq. (9.2), one at $t = 0$ and one at $t = \tau$. Because of our assumption that $B(\underset{\sim}{K}) = 0$, cross terms of the form $\langle B(\underset{\sim}{r}) \cos\underset{\sim}{K}\cdot\underset{\sim}{r}\rangle$ vanish. Since each particle is independent, terms containing more than one index factor into the product of averages for each index. Thus, for example,

$\langle B(\underset{\sim}{r}_j)\, B(\underset{\sim}{r}_k)\, e^{i\underset{\sim}{K}\cdot(\underset{\sim}{r}_j-\underset{\sim}{r}_k)}\rangle = \langle B(\underset{\sim}{r}_j)\, e^{i\underset{\sim}{K}\cdot\underset{\sim}{r}_j}\rangle\langle B(\underset{\sim}{r}_k)\, e^{-i\underset{\sim}{K}\cdot\underset{\sim}{r}_k}\rangle = 0$ for $j \neq k$, and $\langle B\rangle = \Omega_i/\Omega$ for $j = k$. $\langle I(0)\, I(\tau)\rangle$ thus simplifies to

$$\langle I(0)\, I(\tau)\rangle = E_o^4 + 2\beta^2 E_o^2 \langle N\rangle + 4(\underset{\sim}{\beta}\cdot\underset{\sim}{E}_o)^2 \sum_{j\ell} \langle B(\underset{\sim}{r}_j)\, B(\underset{\sim}{r}_\ell)\, \cos\underset{\sim}{K}\cdot\underset{\sim}{r}_j \cos\underset{\sim}{K}\cdot\underset{\sim}{r}_\ell\rangle$$

$$+ \beta^4 \sum_{jk\ell m} \langle B(\underset{\sim}{r}_j)\, B(\underset{\sim}{r}_k)\, B(\underset{\sim}{r}_\ell)\, B(\underset{\sim}{r}_m)\, e^{i\underset{\sim}{K}\cdot(\underset{\sim}{r}_j-\underset{\sim}{r}_k)}\, e^{i\underset{\sim}{K}\cdot(\underset{\sim}{r}_\ell-\underset{\sim}{r}_m)}\rangle \quad , \tag{9.4}$$

where $\langle N\rangle = M\Omega_i/\Omega$. The indices j and k refer to t = 0, while ℓ and m refer to $t = \tau$. The third term in Eq. (9.4) is zero for $j \neq \ell$. There are M terms for which $j = \ell$ so that the third term becomes

$$4(\underset{\sim}{\beta}\cdot\underset{\sim}{E}_o)^2\, M\, \langle B[\underset{\sim}{r}(0)]\, B[\underset{\sim}{r}(\tau)]\, \cos\underset{\sim}{K}\cdot\underset{\sim}{r}(0)\, \cos\underset{\sim}{K}\cdot\underset{\sim}{r}(\tau)\rangle$$

$$= 2(\underset{\sim}{\beta}\cdot\underset{\sim}{E}_o)^2\, M[F_+(\underset{\sim}{K},\tau) + F_-(\underset{\sim}{K},\tau)] \quad ,$$

where

$$F_\pm(\underset{\sim}{K},\tau) = \frac{1}{\Omega}\int_\Omega d^3r \int_\Omega d^3r'\, B(\underset{\sim}{r})\, B(\underset{\sim}{r}')\, e^{i\underset{\sim}{K}\cdot(\underset{\sim}{r}\pm\underset{\sim}{r}')}\, P(\underset{\sim}{r},0|\underset{\sim}{r}',\tau) \quad . \tag{9.5}$$

$P(\underset{\sim}{r},0\,\underset{\sim}{r}',\tau)\, d^3r'$ is the probability that a particle at $\underset{\sim}{r}$ at t = 0 will be in d^3r' about $\underset{\sim}{r}'$ at $t = \tau$. The last term in Eq. (9.4) reduces in a similar manner. In one index is different from the other three the average will be zero. There are thus only four possibilities for nonzero averages: the M terms where $j = k = \ell = m$ for which the last term reduces to

$$\beta^4 M\, \langle B[\underset{\sim}{r}(0)]\, B[(\underset{\sim}{r}(\tau)]\rangle = \beta^4 M F_-(0,\tau) \quad ;$$

the $M^2 - M$ terms where J = k and $\ell = m$, but $j \neq \ell$ for which

$$\beta^4(M^2 - M)\ \langle B[r_j(0)\, B[r_\ell(\tau)]\rangle = \beta^4(M^2 - M)\langle B\rangle^2 \quad ;$$

the M^2 - M terms where j = ℓ and k = m but j ≠ k for which

$$\beta^4(M^2 - M)\ \langle B[\underset{\sim}{r}(0)]\ B[\underset{\sim}{r}(\tau)]\ e^{i\underset{\sim}{K}\cdot[\underset{\sim}{r}(0)+\underset{\sim}{r}(\tau)]}\rangle^2 = \beta^4(M^2 - M)\ F_+^2(\underset{\sim}{K},\tau)$$

and the M^2 - M terms where j = m and k = ℓ, but j ≠ k for which

$$\beta^4(M^2 - M)\ \langle B[\underset{\sim}{r}(0)]\ B[\underset{\sim}{r}(\tau)]\ e^{i\underset{\sim}{K}\cdot[\underset{\sim}{r}(0)-\underset{\sim}{r}(\tau)]}\rangle^2 = \beta^4(M^2 - M)\ F_-^2(\underset{\sim}{K},\tau) \quad .$$

Thus, for $M \gg 1$

$$\langle I(0)\ I(\tau)\rangle = E_0^4 + 2\beta^2 E_0^2\langle N\rangle + 2(\underset{\sim}{\beta}\cdot\underset{\sim}{E}_0)^2\ M[F_+(\underset{\sim}{K},\tau) \tag{9.6}$$

$$+ F_-(\underset{\sim}{K},\tau)] + \beta^4 M F_-(0,\tau) + \beta^4\langle N\rangle^2 + \beta^4 M^2[F_+^2(\underset{\sim}{K},\tau) + F_-^2(\underset{\sim}{K},\tau)] \quad .$$

It remains to evaluate $F_\pm(\underset{\sim}{K},\tau)$. In the usual diffusion approximation[27]

$$P(\underset{\sim}{r},0|\underset{\sim}{r}',\tau) = (4\pi D\tau)^{-3/2}\ e^{-(\underset{\sim}{r}'-\underset{\sim}{r})^2/4D\tau} \quad . \tag{9.7}$$

By introducing the relative coordinate $\underset{\sim}{s} = \underset{\sim}{r}' - \underset{\sim}{r}$ in Eq. (9.5), we have

(9.8)

$$F_\pm(\underset{\sim}{K},\tau) = \Omega^{-1}(4\pi D\tau)^{-3/2}\int_\Omega d^3r \int_\Omega d^3s B(\underset{\sim}{r})\ B(\underset{\sim}{r}+\underset{\sim}{s})\ e^{\pm i\underset{\sim}{K}\cdot\underset{\sim}{s}}\ e^{i(\underset{\sim}{K}\pm\underset{\sim}{K})\cdot\underset{\sim}{r}}\ e^{-s^2/4D\tau} \quad .$$

In terms of the spatial transform, $B(\underset{\sim}{q})$,

$$F_\pm(\underset{\sim}{K},\tau) = \Omega^{-1}\int d^3q B(-\underset{\sim}{q})\ B(\underset{\sim}{q}+\underset{\sim}{K})\ e^{-D(\underset{\sim}{K}+\underset{\sim}{q})^2\tau} \quad . \tag{9.9}$$

Since $B(\underset{\sim}{q}) = 0$, for $|\underset{\sim}{q}| \gtrsim K$, we have

$$F_+(\underset{\sim}{K},\tau) = 0 \quad ,$$

$$F_-(\underset{\sim}{K},\tau) \approx \Omega^{-1}e^{-DK^2\tau}\int d^3q|B(\underset{\sim}{q})|^2 = e^{-DK^2\tau}\Omega_i/\Omega \quad ,$$

and

$$F_{-}(0,\tau) = \Omega^{-1} \int d^3q |B(\underset{\sim}{q})|^2 \, e^{-Dq^2\tau} \quad .$$

$\langle I(0)\ I(\tau)\rangle$ then takes the form

$$\langle I(0)\ I(\tau)\rangle = \text{const} + 2(\beta\cdot E_o)^2 \langle N\rangle e^{-DK^2\tau} + \tag{9.10}$$
$$+ \beta^4 \langle N\rangle^2 \, e^{-2DK^2\tau} + \beta^4 \langle \delta N(0)\ \delta N(\tau)\rangle \quad ,$$

where $\langle \delta N(0)\ \delta N(\tau)\rangle = MF_{-}(0,\tau)$ is the autocorrelation function for number fluctuations in Ω_i due to diffusion of the particles. $F_{-}(0,\tau)$ is the probability that a particle in Ω_i at $t = 0$ will also be in Ω_i at $t = \tau$. $1 - F_{-}(0,\tau)$ is the probability after-effect factor of Chandrasekhar.[27]

Substitution of Eq. (9.10) in Eq. (9.3) gives the frequency spectrum. Apart from zero-frequency components, we find

$$S_I(f) = \frac{8(\beta\cdot E_o)^2 \langle N\rangle DK^2}{D^2K^4 + (2\pi f)^2} + \frac{8\beta^2 \langle N\rangle^2 DK^2}{4D^2K^4 + (2\pi f)^2} + \beta^4 S_N(f) \quad , \tag{9.11}$$

where

$$S_N(f) = \frac{4M}{\Omega} \int \frac{|B(\underset{\sim}{q})|^2 Dq^2 d^3q}{D^2q^4 + (2\pi f)^2} \tag{9.12}$$

is the spectrum for number fluctuations which has the same shape as $S_T(f)$ for uncorrelated temperature fluctuations (Eq. (3.19)). The first term in Eq. (9.11), the heterodyne Lorentzian, and the second term, the homodyne Lorentzian, depend on the coherent nature of the light in producing interference fluctuations. $S_N(f)$, on the other hand, which is independent of K, does not depend on coherence, but

rather on the shape of Ω_i. The general behavior of $S_N(f)$ is the same as $S_T(f)$ shown in Fig. 5(a) for uncorrelated temperature fluctuations. Renormalizing Eq. (3.23) for number fluctuations, we find the high frequency limit of $S_N(f)$:

$$S_N(f) \to \frac{MAD^{1/2}}{2\Omega\pi^{3/2}f^{3/2}} \quad . \qquad (f >> f_3) \tag{9.13}$$

Although we initially assumed that the scattered light was coherent over the area of the detector, A_{det}, this assumption is usually not valid experimentally. In most cases, the coherence area at the detector, A_{coh}, is less than A_{det}. A_{coh} depends on the experimental configuration. Cummins and Swinney[1] show that $A_{coh} \approx \lambda^2 R^2/A'$ where λ is the wavelength of the light, R is the distance from Ω_i to the detector, and A' is the apparent area of Ω_i as seen by the detector. For the interference effects each A_{coh} fluctuates independently and the spectrum is proportional to $A_{det}A_{coh}$. As shown in Eq. (9.12), however, the number fluctuations do not depend on K and the spectrum is, therefore, proportional to A_{det}^2.

Interference and number fluctuations are best observed together in a homodyne experiment, for which $E_o \to 0$. In this case, from Eqs. (9.11) and (9.12), the relative spectrum for a finite area detector

$$\frac{S_I(f)}{\bar{I}^2} = \frac{8DK^2A_{coh}/A_{det}}{4D^2K^4 + (2\pi f)^2} + \frac{4}{M\Omega_i^2}\int \frac{|B(q)|^2 Dq^2 d^3q}{D^2q^4 + (2\pi f)^2} \tag{9.14}$$

where $\bar{I} = \langle N \rangle \beta^2 A_{det}$ is the average intensity. The position of the half-width of the Lorentzian, $f_{1/2} = DK^2/\pi$, allows one to determine the diffusion constant, D. The low frequency limit of the Lorentzian, $2A_{coh}/A_{det}DK^2 = 2A_{coh}/\pi f_{1/2} A_{det}$, then allows one to determine A_{coh} if A_{det} is known. The Lorentzian is expected to be on top of a "background" spectrum due to number fluctuations. For small enough Ω_i or low enough densities, $n_o = M/\Omega$, the number fluctuations may dominate the Lorentzian. The high frequency limit of the relative number fluctuations from Eq. (9.13)

$$S_I(f)/\bar{I}^2 \to D^{1/2} A/2 n_o \Omega_i^2 \pi^{3/2} f^{3/2} \quad , \tag{9.15}$$

allows one to determine n_o if D and Ω_i are known.

In our experiment, light from a helium-neon laser (λ = 6328Å) with a beam diameter of 1.7 mm passed through a small aperture of diameter 0.45 mm, and was focused by a microscope objective lens onto a thin closed cell containing a suspension of polystyrene spheres in distilled water. Light scattered through an angle θ passed through an aperture of area A_{det} at a distance R from the cell and was incident on a photomultiplier 3 cm behind the aperture. Stray light was minimized to make the heterodyne components negligible. The spectrum of the photomultiplier output was measured with the PDP-11 as described in Section II.

Our arrangement of passing the laser light through an aperture and focusing it onto the sample cell produced an illuminant cylindrical volume, Ω_i, of length ℓ_o = 1.5 mm with sharp boundaries and illumination uniform to within 10%. The diameter of the cylinder, d, could be

varied by changing the beam focus. The minimum beam diameter was 10 ± 2 μm. Since the particles could neither enter nor leave Ω_i via the ends of the cylinder, we expect the shape of the number fluctuations spectrum, $S_N(f)$, to be as shown in Fig. 5(a) with $f_1 \to 0$, and $f_2 = f_3 \approx D/\pi d^2$. In other words, we expect $S_N(f) \propto f^{-3/2}$ for $f \gtrsim D/\pi d^2$ with a gradual flattening of the spectrum as f is lowered below $D/\pi d^2$. From Eq. (9.15) for a cylindrical Ω_i the high frequency limit of the number fluctuation contribution is

$$S_I(f)/\bar{I}^2 \to 8D^{1/2}/\pi^{5/2} n_o d^3 \ell_o f^{3/2} \quad , \tag{9.16}$$

where $n_o = M/\Omega$ is the particle concentration. Since the knee for the number fluctuations $D/\pi d^2$, is at a much lower frequency than the knee for the interference Lorentzian, DK^2/π, the number fluctuations will have an $f^{-3/2}$ behavior in the region in which the Lorentzian is usually observed.

Figure 13 shows $S_I(f)/\bar{I}^2$ for a homodyne experiment on spheres of radius $r_o = 630\text{Å}$ with $\theta = 50°$, $d = 10$ μm, $R = 4$ cm, and $n_o \approx 5\times10^{11}$ cm^{-3}. The value of n_o was estimated from information supplied by the manufacturer (Dow Chemical Company) of the polystyrene spheres and our known dilution. Because of settling of the particles and evaporation of solvent we believe the value to be accurate only to within a factor of 2. In Fig. 13(a) $A_{det} = 0.009$ cm^2, and the spectrum is the usual homodyne Lorentzian. From the position of the half-width, $f_{1/2} = DK^2/\pi$, we may measure D. Here $K = 4\pi n \sin \frac{1}{2}\theta'/\lambda$, where n is the index of refraction of the solvent, λ is the vacuum wavelength of the light, and θ' is the angle through which the light is scattered in the

suspension. Using Snell's law to correct for refraction at the water-glass-air interface, we find that $\theta = 50°$ corresponds to $\theta' = 37.2°$ inside the cell. Using the value of $f_{1/2} = 85$ Hz from Fig. 13(a), we find $D = 4.2\times10^{-8}$ cm^2/sec. This is in good agreement with the value of $D = 3.73\times10^{-8}$ cm^2/sec calculated from the Einstein-Stokes relation, $D = k_B T/6\pi\eta r_o$, at room temperature.

In Fig. 13(b) A_{det} was increased by a factor of 77 to 0.7 cm^2 and the low frequency limit of the Lorentzian was reduced by a factor of 65 demonstrating the effect of A_{coh}/A_{det} in determining the absolute magnitude of the homodyne spectrum. From the low frequency limit, we find $2A_{coh}/A_{det}DK^2 = 2A_{coh}/A_{det}\pi f_{1/2} = 1.7\times10^{-6}$ Hz^{-1}, and estimate $A_{coh} = 1.6\times10^{-4}$ cm^2 at the aperture. This compares with a value of $A_{coh} = 4.0\times10^{-4}$ cm^2 calculated from the empirical formula, $A_{coh} = \lambda^2R^2/A'$, where A' is the apparent area of Ω_i as seen from the aperture. λ is taken as the wavelength in the solvent, and correction was made to A' for the water-glass-air interface. The number fluctuation contribution is unaffected by the change in A_{det} and, therefore, becomes more apparent at the low frequency end of the spectrum in Fig. 13(b).

Figure 14 shows the effect of changing particle concentration for a given experimental configuration with $r_o = 630$Å, $\theta = 50°$, $d = 10$ μm, and $A_{det} = 0.7$ cm^2. R was reduced to 3 cm in order to make the number fluctuations more apparent by decreasing A_{coh} and further suppressing the Lorentzian below that in Fig. 13(b). For a given value of Ω_i, we see from Eq. (9.14) that the relative interference fluctuations are independent of n_o while the number fluctuations

are proportional to n_o^{-1}. In Fig. 14(b) n_o is estimated to be 5×10^{11} cm^{-3}. At the lower frequencies, the number fluctuation spectrum varying as $f^{-3/2}$ becomes apparent. In Fig. 14(a) the suspension was diluted by a factor of 500 to give an estimated n_o of 10^9 cm^{-3}. The number fluctuations are observed to increase by a factor of about 750 to dominate the Lorentzian. A shoulder due to the Lorentzian is, however, still visible above 1 Hz. As in Fig. 5(a), as the frequency is lowered, there is an evventual flattening of the spectrum. The frequency below which this is expected, $D/\pi d^2 = 1.3\times10^{-2}$ Hz, is in excellent agreement with experiment. As noted above, if D is known (say from the Lorentzian half-width) the absolute magnitude of the high frequency behavior of the number fluctuations can be used to measure n_o. Using our measured value of $D = 4.2\times10^{-8}$ cm^2/sec and Eq. (19), we find that for Fig. 14(a) $S_I(f)/\bar{I}^2 = 1.0\times10^{-3}$ Hz^{-1} at 1.0 Hz, and thus $n_m = 6.6\times10^8$ cm^{-3}, where n_m is the measured concentration from $S_I(f)$. In Fig. 14(b) $S_I(f)/\bar{I}^2 = 1.3\times10^{-6}$ Hz^{-1} at 1.0 Hz, and we find $n_m = 4.7\times10^{11}$ cm^{-3}. Both of these values are within the limits of our estimated n_o. The flattening of the spectra in Fig. 14(a) and (b) above 1 kHz is due to shot noise in the photomultiplier. Using our values of n_m, we find that in Fig. 14(a) $\langle N \rangle = 77$, while in Fig. 14(b) $\langle N \rangle = 5.5\times10^4$.

For comparison, Fig. 14(c) shows the relative intensity spectrum for the laser used, measured by replacing the sample cell by ground glass. The laser was not stabilized and the fluctuations were due primarily to a drift in the output intensity, which gives a f^{-2} spectrum with our measurement technique. The laser intensity fluctuations were

orders of magnitude below the number and interference fluctuations. With an intensity stabilized laser it should be possible to see number fluctuations with $\langle N \rangle$ much greater than 10^5.

Figure 15 shows the effect of changing Ω_i, with $r_o = 630\text{Å}$, $\theta = 50°$, $A_{det} = 0.7\ cm^2$, $R = 3$ cm, and n_o estimated to be $10^9\ cm^{-3}$. Figure 15(a) reproduces Fig. 14(a) with $d = 10\ \mu m$. In Fig. 15(b) the beam was defocused to give a larger Ω_i. In addition to decreasing the relative number fluctuations and moving the knee to a lower frequency, the increase in Ω_i reduces A_{coh} and suppresses the Lorentzian. In Fig. 15(b) the spectrum is close to $f^{-3/2}$ over five decades while no definite knee or Lorentzian is apparent. Again, the high frequency flattening is due to photomultiplier shot noise. Although we could not make a direct measurement, the value of d in Fig. 15(b) can be determined from Eq. (9.16) and the ratio of the $f^{-3/2}$ regions in Fig. 15(a) and Fig. 15(b). We find $d = 120\ \mu m$ and predict that the knee should occur at $D/\pi d^2 = 9\times10^{-5}$ Hz, which is below the lowest frequency measured. In Fig. 15(b) $\langle N \rangle = 1.1\times10^4$.

Figure 16 shows a similar set of experiments on larger spheres, with $r_o = 6500\text{Å}$, $\theta = 30°$, $A_{det} = 0.7\ cm^2$, and $R = 6$ cm. In Fig. 16(c) we estimate $n_o = 5\times10^8\ cm^{-3}$. A large Ω_i was used and only the interference Lorentzian was observed. As with Fig. 13(a) we use the half-width of the Lorentzian, $f_{1/2} = 2$ Hz, to determine $D = 2.5\times10^{-9}\ cm^2/sec$. This compares with a value of $D = 3.62\times10^{-9}\ cm^2/sec$ from the Einstein-Stokes relation. In Fig. 16(b) d was reduced to 10 μm and the number fluctuation spectrum became visible at the low frequency end of the Lorentzian. From Eq. (9.16) and $S_I(f)/\bar{I}^2 = 0.10\ Hz^{-1}$ at

10^{-2} Hz we find $n_m = 1.5\times10^{9}$ cm^{-3}. In Fig. 16(a) the suspension was diluted by a factor of 50 to give an estimated $n_o = 10^{7}$ cm^{-3}, and the number fluctuations increased relative to the Lorentzian. Using $S_I(f)/\bar{I}^2 = 3.2$ Hz^{-1} at 10^{-2} Hz and Eq. (9.16) we find $n_m = 4.7\times10^{-7}$ cm^{-3}. In Fig. 16(a) and Fig. 16(b) a knee is expected at a frequency of $D/\pi d^2 = 8\times10^{-4}$ Hz. Although the lowest few points of Fig. 16(a) show some decrease which may be the start of the knee, the lowest points are unreliable due to a noticeable settling of the larger spheres over the time span of the experiment.

In the forward direction the approximation $|\underset{\sim}{K}| \gg 1/\ell$ breaks down. As the main beam is detected by the photomultiplier the heterodyne fluctuations dominate the spectrum. Figure 17(a) shows the spectrum from an experiment in the forward direction in which the main beam is detected, with $r_o = 630$Å, $\theta = 0°$, $A_{det} = 0.7$ cm^2, R = 10 cm and n_o estimated to be 5×10^{11} cm^{-3}. If one assumes that $\underset{\sim}{K}$ is exactly zero in the forward direction, there is no first order phase change when a particle moves, and we see from Eq. (9.12) that the interference terms have no finite frequency contribution. One would then expect to observe only number fluctuations and a spectrum like Fig. 14(a). Although the spectrum of Fig. 17(a), has a knee at 10^{-2} Hz, it is much sharper than the knee in Fig. 14(a), and the behavior between 10^{-2} Hz and 10 Hz is steeper than $f^{-3/2}$. We conclude that the fluctuations are due to heterodyne interference with a distribution of small $\underset{\sim}{K}$ values. From the position of the knee at 10^{-2} Hz we estimate that $|\underset{\sim}{K}| < 10^{3}$ cm^{-1}. A rough estimate of the range of θ's included due to the finite A_{det} gives $|\underset{\sim}{K}| < 4\times10^{3}$ cm^{-1}.

The number fluctuations are not an interference effect. It should, therefore, be possible to observe the number fluctuation spectrum with white or incoherent light. Figures 17(b), 17(c) and 17(d) show the spectra obtained from several experiments in which the light source was a dc powered incandescent bulb. In Fig. 17(b), $r_o = 6500\text{Å}$, $\theta = 45°$, $A_{det} = 0.7\ cm^2$, n_o is estimated to be $5\times10^8\ cm^{-3}$ and $R \approx 1$ cm. Ω_i was determined by a slit 130 μm×10 μm immediately in front of the sample cell rather than by a focused beam. Although the photomultiplier shot noise is more apparent, there is no interference Lorentzian and the $f^{-3/2}$ number fluctuation spectrum is quite clear. Using Eq. (9.15) and our measured $D = 2.5\times10^{-9}\ cm^2/sec$, we determine $n_m = 2.3\times10^9\ cm^{-3}$ from the magnitude of the $f^{-3/2}$ region. In Fig. 17(c), $r_o = 630\text{Å}$, $\theta = 50°$, $A_{det} = 0.7\ cm^2$, $n_o \approx 2\times10^{11}\ cm^{-3}$, and $R = 6$ cm. The microscope objective lens was used to focus an image of the bulk filament in the cell, and so produce an Ω_i of irregular shape for which no numerical calculations could be made. However, as expected, the spectrum is still proportional to $f^{-3/2}$ since the dimensions of Ω_i were greater than $(D/f)^{1/2}$. In Fig. 17(d), $r_o = 630\text{Å}$, $\theta = 0°$, $A_{det} = 0.7\ cm^2$, $n_o \approx 2\times10^{11}\ cm^{-3}$, and $R \approx 1$ cm. Ω_i was again determined by a slit of dimensions 2 mm×20 μm immediately in front of the cell. Although the $f^{-3/2}$ behavior is apparent its magnitude cannot in general be used to determine n_m from Eq. (9.15) as it was in Fig. 17(b). Since we are observing the main beam, $\bar{I} \neq \langle N\rangle\beta^2 A_{det}$. It is, however, sufficient to adopt a simple model in which $I = I_o e^{-N\sigma/A}$, where I is the transmitted intensity, I_o is the incident

intensity, N is the number of particles in the beam, σ is the cross section for scattering out of the beam, and A is the beam area. In this case $S_I(f)/\bar{I}^2 = [\ln(I_o/I)]^2$. Here, $I_o/I \approx 2$, and we find $n_m = 1.2\times10^{11}$ cm^{-3}. In Fig. 17(d), $\langle N\rangle = 8\times10^6$. The increased intensity stability of the bulb over the laser and the absence of interference fluctuations allow one to easily observe the number fluctuations even when $\langle N\rangle > 10^6$.

We have shown that for monochromatic light scattered by a suspension of independent particles the intensity fluctuation spectrum contains $S_N(f)$ in addition to the usual homodyne and heterodyne Lorentzian. All three terms arise in a unified manner from $P(\underset{\sim}{r},0|\underset{\sim}{r}',\tau)$. By measuring the homodyne fluctuation spectrum for light scattered from a suspension of polystyrene spheres down to frequencies as low as 5×10^{-4} Hz, we have been able to verify the calculated $S_N(f)$ for independent particles undergoing Brownian motion. We have experimentally demonstrated that the effects of varying A_{det}, A_{coh}, n_o, Ω_i, and D on the relative magnitudes of the interference and number fluctuation spectra are in excellent agreement with theory. The position of the half-width of the Lorentzian allows us to determine D. The theory predicts a gradual flattening of $S_N(f)$ as f is lowered below $D/\pi d^2$. The knee is observed experimentally at the predicted frequency. Knowing D and Ω_i we are also able to determine n_m from the $f^{-3/2}$ limit of $S_N(f)$. This value of n_m is in good agreement with our estimate based on the manufacturer's data. With an unstabilized laser $S_N(f)$ was easily discernible, and, consequently, a measurement of n_o was possible, even for $\langle N\rangle$ as high as 5.5×10^4.

$S_N(f)$ was also apparent with an incandescent bulb as the light source. In this case, the interference fluctuations were absent and the increased stability of the bulb over the laser allowed a measurement of n_m, even when $\langle N \rangle = 8 \times 10^6$.

"There is no music in Nature, neither melody nor harmony.
Music is the creation of man."

Rev. Hugh Reginald, Music and Morals

"There's music in the sighing of a reed;
There's music in the gushing of a rill;
There's music in all things, if men had ears;
Their earth is but an echo of the spheres."

Lord Byron, Don Juan

X. 1/f NOISE IN MUSIC: MUSIC FROM 1/f NOISE

Much of the interest in 1/f noise is due to the presence of the 1/f behavior as the low frequency limit to the power spectrum of most measured quantities coupled with its absence from most theoretical calculations. Even the voltage fluctuations across nerve membranes[39] and long term geological or hydrological records[40] exhibit the 1/f spectrum. For example, Fig. 18 shows the power spectrum of the flood levels of the river Nile. The 1/f behavior extends to frequencies as low as 3×10^{-11} Hz. In this section we present measurements on quantities associated with music and speech and show that these, too, have the 1/f spectrum. To conclude, we describe how a "1/f noise" may be used to make "1/f music".

Many fluctuating quantities, V(t), may be characterized by a single correlation time, τ_c. In such a case, V(t) is correlated with $V(t + \tau)$ for $|\tau| < \tau_c$, and is independent of $V(t + \tau)$ for $|\tau| > \tau_c$. For this case, $S_V(f)$ is "white" (independent of frequency) in the frequency range corresponding to time scales over which V(t) is uncorrelated ($f \ll 1/2\pi\tau_c$); and is a rapidly decreasing function of frequency, usually $1/f^2$, in the frequency range over which V(t) is correlated ($f \gg 1/2\pi\tau_c$). A quantity with a 1/f power spectrum cannot, therefore, be characterized by a single correlation time. In fact,

the 1/f power spectrum implies some correlation in V(t) over all time scales corresponding to the frequency range for which $S_V(f)$ is 1/f. In general, a negative slope for $S_V(f)$ implies some degree of correlation in V(t) over time scales of roughly $1/2\pi f$. A steep slope implies a higher degree of correlation than a shallow slope. Thus, a quantity with a $1/f^2$ power spectrum is highly correlated.

Figure 19 shows samples of white, 1/f, and $1/f^2$ noise. Each fluctuating quantity was scaled to cover the same vertical range. The white noise has the most random appearance and shows rapid uncorrelated changes. The $1/f^2$ noise is the most correlated showing only slow changes. The 1/f noise is intermediate, showing structure on all time scales. It is interesting to note that, although simple computer algorithms exist for a white or $1/f^2$ noise source over arbitrarily long time scales, no such algorithm exists to produce 1/f noise. This inability to produce a generating algorithm is related to our incomplete theoretical understanding of 1/f noise. Nature, however, has no such problem: any semiconductor, for example, provides a convenient source of 1/f noise.

In our measurements on music and speech, the fluctuating quantity of interest was converted to a voltage whose power spectrum was measured by the PDP-11 computer. The most familiar fluctuating quantity associated with music is the audio signal, V(t), such as the voltage used to drive a speaker system. Figure 20(a) shows a linear-linear plot of the power spectrum, $S_V(f)$, of the audio signal from J. S. Bach's 1st Brandenburg Concerto (Angel SB-3787) averaged over the entire concerto. The spectrum consists of a series of sharp

peaks in the frequency range 100 Hz to 2 kHz corresponding to the individual notes in the concerto and, of course, is far from 1/f. Although this spectrum contains much useful information, our primary interest is in more slowly varying quantities.

One such quantity is the loudness of the music. The audio signal, V(t), was amplified and passed through a bandpass filter in the range 100 Hz to 10 kHz. The filter output was squared and the audio frequencies filtered off to give a slowly varying signal, $V^2(t)$, proportional to the instantaneous loudness of the music. The power spectrum of the loudness fluctuations of the 1st Brandenburg Concerto, $S_{V^2}(f)$, averaged over the entire concerto is shown in Fig. 20(b). On this linear-linear plot, the loudness fluctuations appear as a peak close to zero frequency.

Figure 21 is the log-log plot of the same spectra as in Fig. 20. In Fig. 21(a), the power spectrum of the audio signal, $S_V(f)$, is distributed over the audio range. In Fig. 21(b), however, the loudness fluctuation spectrum, $S_{V^2}(f)$, shows the 1/f behavior below 1 Hz. The peaks between 1 Hz and 10 Hz are due to the rhythmic structure of the music.

Figure 22(a) shows the power spectrum of loudness fluctuations for a recording of Scott Joplin piano rags (Nonsuch H-71248) averaged over the entire recording. Although this music has a more pronounced metric structure than the Brandenburg Concerto, and, consequently, has more structure in the spectrum between 1 Hz and 10 Hz, the spectrum below 1 Hz is still 1/f-like.

In order to measure $S_{V^2}(f)$ down to even lower frequencies an audio signal of greater duration than a single record is needed, for example, that from a radio station. The audio signal from an AM radio was filtered and squared. $S_{V^2}(f)$ was averaged over approximately 12 hr, and thus included many musical selections as well as announcements and commercials. Figures 22(b) through (d) show the loudness fluctuation spectra for three radio stations characterized by different motifs. Figure 4(b) shows $S_{V^2}(f)$ for a classical station. The spectrum exhibits a smooth 1/f dependence. Figure 22(c) shows $S_{V^2}(f)$ for a rock station. The spectrum is 1/f-like above 2×10^{-3} Hz, and flattens for lower frequencies, indicating that the correlation of the loudness fluctuations does not extend over time scales longer than a single selection, roughly 100 sec. Figure 22(d) shows $S_{V^2}(f)$ for a news and talk station, and is representative of $S_{V^2}(f)$ for speech. Once again the spectrum is 1/f-like. In Fig. 22(b) and Fig. 22(d), $S_{V^2}(f)$ remains 1/f-like down to the lowest frequency measured, 5×10^{-4} Hz, implying correlations over time scales of at least 5 min. In the case of classical music this time is less than the average length of each composition.

Another slowly varying quantity in speech and music is the instantaneous pitch. A convenient means of measuring the pitch is by the rate, Z, of zero crossings of the audio signal, V(t). Thus an audio signal of low pitch will have few zero crossings per second and a small Z, while a high pitched signal will have a high Z. For the case of music, Z(t) roughly follows the pitch content. Figure 23 shows the power spectra of the rate of zero crossings,

$S_Z(f)$, for four radio stations averaged over approximately 12 hr. Figure 23(a) shows $S_Z(f)$ for a classical station. The power spectrum is closely 1/f above 4×10^{-4} Hz. Figures 23(b) and (c) show $S_Z(f)$ for a jazz and blues station and a rock station. Here the spectrum is 1/f-like down to frequencies corresponding to the average selection length, and is flat at lower frequencies. Figure 23(d), however, which shows $S_Z(f)$ for a news and talk station, exhibits a quite different spectrum. The spectrum is that of a quantity characterized by two correlation times: The average length of an individual speech sound, roughly 0.1 sec, and the average length of time for which a given announcer talks, about 100 sec. For most musical selections the pitch content has correlations that extend over a large range of time scales, and has a 1/f power spectrum. For normal English speech, on the other hand, the pitches of the individual speech sounds are unrelated. As a result, the power spectrum is "white" for frequencies less than about 3 Hz, and falls as $1/f^2$ for $f \gtrsim 3$ Hz. In fact, in Figs. 23(a) through (c), one observes shoulders at about 3 Hz corresponding to speech averaged in with the music. The prominence of this shoulder increases as the vocal content of the music increases, or as the commercial interruptions become more frequent.

The 1/f spectrum for quantities associated with music and speech is, perhaps, not so surprising. We speculate that measures of "intelligent" behavior should show a 1/f-like power spectrum. Whereas a quantity with a white power spectrum is uncorrelated with its past, and a quantity with a $1/f^2$ power spectrum depends very strongly on its past, a quantity with a 1/f power spectrum has an

intermediate behavior, with some correlation on all time scales, yet not depending too strongly on its past. Human communication is one example where correlations extend over various time scales. In music much of the communication is directly by the pitch content which exhibits a 1/f spectrum. In English speech, on the other hand, The communication is not directly related to the pitch of the individual sounds. The ideas communicated may have long time correlations even though the pitches of successive sounds are unrelated.

The observation of 1/f power spectra for the loudness and pitch fluctuations in music has implications for stochastic music composition. In the past, stochastic compositions have been based on a random number generator (white noise source) which is uncorrelated in time. In the simplest case the white noise source can be used to determine the pitch and duration (quantized in some standard manner) of successive notes. The resulting music is and sounds structureless. (Figure 24 shows an example of this "white music" which we have produced using a white noise source.) Most work on stochastic composition has been concerned with ways of adding the time structure that the random number generator could not provide. Low level Markov processes (in which the probability of a given note depends on its immediate predecessors) were able to impose some local structure but lacked long time correlations. Attempts at increasing the number of preceeding notes on which the given note depended gave increasingly repetitious results rather than interesting long term structure.[41] By adding rejection rules for the random choices

(a trial note is rejected if it violates one of the rules), Hiller and Isaacson were also able to obtain local structure but no long term correlations.[42] J. C. Tenney has developed an algorithm that introduces long term structure by slowly varying the distribution of random numbers from which the notes were selected.[43] Thus, although it has been possibly to impose some structure on a specific time scale, the stochastic music has been unable to match the correlations and structure found in music over a wide range of time scales.

The natural means of adding this structure is with the use of a 1/f noise source rather than by imposing constraints upon a white noise source. The 1/f noise source itself has the same time correlations as we have measured in various types of music. To illustrate this process at an elementary level, we present short typical selections composed by white, 1/f, and $1/f^2$ noise.

In each case a physical noise source was used to produce a fluctuating voltage of the desired spectrum. The voltage was sampled and digitized by the PDP-11 computer to produce a series of random numbers stored in the computer whose power spectrum was the same as that of the noise source. The series was then scaled so that successive numbers determined the pitch of successive notes over a two octave range. A high number specified a high pitch and vice versa. This process was then repeated to produce an independent series of stored random numbers whose value corresponded to the duration of successive notes.

The PDP-11 was then used to "perform" the stochastic composition by controlling a single amplitude modulated voltage controlled oscillator. The computer was also used to put the stochastic compositions in more conventional form. Samples of these computer "scores" are shown in Figs. 24 through 26. Accidentals apply only to the notes they precede. In Fig. 24 a white noise source was used to determine pitch and duration. In Fig. 25 a 1/f noise source was used, while in Fig. 26 a $1/f^2$ noise source was used. Although Figs. 24 through 26 are not intended as complete formal compositions, they are representative of the types of correlation that can be achieved when the three types of noise sources of Fig. 1 are used to control various musical parameters. In each case the noise sources were "Gaussian" implying that values near the mean were more likely than extreme values.

Our 1/f music was judged by most listeners to be far more pleasing than either the white music (which was "too random") or the scale-like $1/f^2$ music (which was "too correlated"). Indeed the surprising sophistication of the 1/f music (which was close to being "just right") suggests that the 1/f noise source is an excellent method of adding time correlations.

There is, however, more to music than 1/f noise. Although our simple algorithms were sufficient to demonstrate the superiority of a 1/f noise source over a white noise source in stochastic composition, the variation of only two parameters (pitch and duration of the notes of a single voice) can, at best, produce only a very simple form of music. More structure is needed, not all of which can be provided by

1/f noise sources. We improved on this elementary composition by using two voices that were either independent or partially correlated (notes having the same duration but independent pitches or vice versa), and by varying the overall loudness with an additional 1/f noise source. We added more structure to the music by introducing either a simple, constant rhythm, or a variable rhythm determined by another 1/f noise source. The use of 1/f noise sources on various structural levels (from the characterization of individual notes to that of entire movements) coupled with external constraints (for example, rhythm or the rejection rules of Hiller) offers promising possibilities for stochastic composition.

"What is that noise?"

William Shakespeare, Macbeth

"He who loves noise must buy a pig."

Spanish Proverb

XI. CONCLUSIONS

We have shown that 1/f noise in metal and semiconductor films is an equilibrium process. For continuous metal films the absence of 1/f noise in manganin; the scaling of $S_V(f)$ as $\bar{V}^2/\Omega$ for different materials; the general decrease of $S_V(f)/\bar{V}^2$ with decreasing temperature; the observation of frequency-dependent spatial correlation for the 1/f noise; the agreement of ac, dc and pulsed current resistance fluctuation spectra; and the ability of equilibrium temperature fluctuations to accurately predict the magnitude of the 1/f noise (with an assumed 1/f spectrum for $S_T(f)$) indicate that equilibrium temperature fluctuations modulating the resistance are the physical origin of the 1/f noise. The same mechanism also accounts for the 1/f noise in metal films at the superconducting transition and in Josephson junctions.

Although temperature fluctuations are expected to obey a diffusion equation, the usual calculated spectra for uniform diffusive systems, in which the fluctuations are spatially uncorrelated, do not give a 1/f spectrum. These theoretical spectra have, however, been verified experimentally for number fluctuations of independent particles undergoing Brownian motion. Attempts at more accurate models of the complex experimental configuration (in which the diffusive medium is coupled to a substrate) only flatten the spectrum further at low frequencies.

Moreover, we have demonstrated experimentally for the metal films (by a measurement for the shape of the autocorrelation function from the temperature response to a delta function power input) that uncorrelated temperature fluctuations do not produce the 1/f spectrum.

On the other hand, we have shown both theoretically and experimentally (by the temperature response to a step function of power) that spatially correlated temperature fluctuations can, in fact, account for the 1/f spectrum in the frequency range in which it is observed. The physical origin of the spatially correlated temperature fluctuations remains an unsolved problem. Another possible difficulty is the proper normalization of the spectrum for correlated fluctuations. However, the use of $\langle(\Delta T)^2\rangle = k_B T^2/C_V$ to normalize the spectrum for correlated fluctuations does lead to a result in excellent agreement with the experimental measurements.

A different physical mechanism for the 1/f noise dominates in semiconductors and discontinuous metal films: the observed noise is much larger than predicted by the theory, and is not spatially correlated. The agreement of the low frequency resistance fluctuation spectrum obtained from Johnson noise measurements with that obtained from current biased measurements shows, however, that even in these systems the 1/f noise is due to equilibrium resistance fluctuations.

The 1/f spectrum is not limited to physical systems. The same correlations on all time scales that yield the 1/f spectrum for many physical quantities are also found in various measures of human behavior. The loudness fluctuations of music and speech and the pitch fluctuations in music also have the 1/f behavior. Perhaps this accounts for some of the fascination of the 1/f noise problem.

ACKNOWLEDGEMENTS

I would like to thank Professor F. Reif for helpful discussions on physics; Dr. A. Moorer, Dr. M. V. Mathews, and Professor E. Dugger for their comments and encouragement on my work on music; my immediate colleagues for their creation of a stimulating atmosphere. And most of all I want to thank Professor John Clarke, who sparked my initial interest in "noise", and provided a restoring term that often turned a negative fluctuation in progress into a generally positive drift.

This work was done under the auspices of the U. S. Energy Research and Development Administration.

REFERENCES

1. F. N. Hooge and A. M. H. Hoppenbrouwers, Physica 45, 386 (1969).
2. Aldert van der Ziel, Noise (Prentice-Hall, Inc., Englewood Cliffs, NJ, 1954).
3. J. L. Williams and R. K. Burdett, J. Phys. C2, 298 (1969).
4. J. L. Williams and I. L. Stone, J. Phys. C5, 2105 (1972).
5. F. N. Hooge, Phys. Lett. 29A, 139 (1969).
6. L. K. J. Vandamme, Phys. Lett. 49A, 233 (1974).
7. F. N. Hooge, Physica 60, 130 (1972).
8. Th. G. M. Kleinpennig, Physica 77, 78 (1974).
9. A. L. McWhorter, Semiconductor Surface Physics, R. H. Kingston, ed. (University of Penn. Press, Philadelphia, PA, 1957), p. 207.
10. For a review see, Aldert van der Ziel, Noise: Sources, Characterization, Measurement (Prentice-Hall, Inc., Englewood Cliffs, NJ, 1970), p. 106.
11. S. T. Hsu, D. J. Fitzgerald and A. S. Grove, Appl. Phys. Lett. 12, 287 (1968).
12. F. M. Klaassen, IEEE Trans. Electron Devices ED18, 887 (1971).
13. John Clarke and Richard F. Voss, Phys. Rev. Lett. 33, 24 (1974).
14. For a review see, K. M. van Vliet and J. R. Fassett, in Fluctuation Phenomena in Solids, R. E. Burgess, ed. (Adacemic, NY, 1965), pp. 267-354.
15. K. M. van Vliet and A. van der Ziel, Physica 24, 415 (1958).
16. John Clarke and Thomas Y. Hsiang, Phys. Rev. Lett. 34, 1217 (1975).
17. L. Onsager, Phys. Rev. 37, 405 (1931).

18. John Clarke and Gilbert Hawkins, IEEE Trans. on Magnetics MAG11, 841 (1975).

19. J. M. Richardson, Bell Syst. Tech. J. 29, 117 (1950).

20. G. G. MacFarlane, Proc. Phys. Soc. B63, 807 (1950).

21. R. E. Burgess, Proc. Phys. Soc. B66, 334 (1953).

22. R. L. Petritz, Phys. Rev. 87, 535 (1952).

23. M. Lax and P. Mengert, Phys. Chem. Sol. 14, 248 (1960).

24. K. M. van Vliet and E. R. Chenette, Physica 31, 985 (1965).

25. For a general discussion of the Langevin approach for a single correlation time see F. Reif, Fundamentals of Statistical and Thermal Physics (McGraw-Hill, NY, 1965), p. 560.

26. A. van der Ziel, Physica 16, 359 (1950); R. F. Voss, Phys. Lett. 53A, 277 (1975).

27. S. Chandrasekhar, Rev. Mod. Phys. 15, 1 (1943).

28. I. Lundström, D. McQueen and D. Klason, Solid State Communications 13, 1941 (1973).

29. L. D. Landau and E. M. Lifshitz, Statistical Mechanics (Addison-Wesley Publishing Co., Reading, Mass., 1958), pp. 362-365.

30. To be published.

31. For example, P. H. Handel, Phys. Stat. Sol. 29, 299 (1968); Phys. Rev. A3, 2066 (1971).

32. For example, S. Teitler and M. F. M. Osbourne, J. Appl. Phys. 41, 3274 (1970); Phys. Rev. Lett. 27, 912 (1971).

33. For a Review, see H. Z. Cummins and H. L. Swinney, in Progress in Optics, E. Wolf, ed. (North-Holland, Amsterdam-London, 1970), Vol. VIII, p. 133.

34. See, for example, D. W. Schaefer, G. Banks and S. S. Alpert, Nature 248, 162 (1974).

35. H. Z. Cummins, N. Knahle, and Y. Yehn, Phys. Rev. Lett. 12, 150 (1964).

36. N. C. Ford and G. B. Benedek, Phys. Rev. Lett. 15, 649 (1965).

37. D. W. Schaefer and B. J. Berne, Phys. Rev. Lett. 28, 475 (1972).

38. E. L. Elson and D. Magde, Biopolymers 13, 1 (1974); D. Magde, E. L. Elson and W. W. Webb, ibid. 13, 29 (1974).

39. A. A. Verveen and H. E. Derkson, Proc. IEEE 56, 906 (1968).

40. B. B. Mandelbrot and J. R. Wallis, Water Resources Research 5, 321 (1969).

41. See, for example, R. C. Pinkerton, Sci. American 194, 77 (1956) or H. F. Olson and H. Belar, JASA 33, 1163 (1961).

42. L. A. Hiller, Jr. and L. M. Isaacson, Experimental Music (McGraw-Hill Book Co., NY, 1959).

43. Discussed by J. R. Pierce, M. V. Mathews and J. C. Risset, Gravesaner Blätter, 27/28, 92 (1965).

FIGURE CAPTIONS

Fig. 1. (a) Sample configuration for Bi film noise measurement. (b) Measured spectrum, $\bar{V}$ = 0.9V (•); background spectrum, $\bar{V}$ = 0.0V (o); and $S_V(f)$, noise-background (———).

Fig. 2. (a) Sample configuration for Au noise measurement. (b) Measured spectrum, $\bar{V}$ = 0.81V (•); background spectrum $\bar{V}$ = 0.0V (o); and $S_V(f)$ corrected for amplifier and capacitor frequency response.

Fig. 3. Nonlinearity of I-V characteristic caused by heating of Au sample of Fig. 2.

Fig. 4. (a) Simple system of heat capacity, C, coupled to reservoir at temperature T_o by thermal conductance, G. (b) String of these simple systems which approximate a 1-dimensional diffusive system.

Fig. 5. (a) $S_T(f)$ for spatially uncorrelated temperature fluctuations of a box $2\ell_1 \times 2\ell_2 \times 2\ell_3$. $f_i = \omega_i/2\pi = D/4\pi\ell_i^2$. (b) Model $S_T(f)$ for a metal film on glass substrate. $f_1 = D/\pi\ell^2$, where ℓ is the length of the film, and $f_2 = D/\pi w^2$, where w is the width of the film.

Fig. 6. (a) Experimental configuration for correlation measurement. (b) Fractional correlation for two samples.

Fig. 7. $S_T(f)$ for spatially correlated temperature fluctuations of a box $2\ell_1 \times 2\ell_2 \times 2\ell_3$. $f_i = D/4\pi\ell_i^2$

Fig. 8. Temperature response of Au sample of Fig. 2 to delta function of applied power.

Fig. 9. Temperature response of Au sample of Fig. 2 to step function of applied power.

Fig. 10. S(t) from cosine transform of temperature response to delta function (···) and step function (——) of applied power from Figs. 7 and 8 normalized to $\bar{T}(o) = \beta^2 T^2/3N$; and measured noise spectrum $S(f) = S_V(f)/\bar{V}^2$ (□).

Fig. 11. InSb bridge: $S_V(f)/\bar{V}^2$ using dc bias (——), ac bias (o), pulsed current bias (Δ); Johnson noise measurement, $S_p(f)/\bar{P}^2$ (□). Background $S_p(f)/\bar{P}^2$ from metal film resistor (···).

Fig. 12. Nb bridge: $S_V(f)/\bar{V}^2$ using ac bias (——); $S_p(f)/\bar{P}^2$ (□). $S_p(f)/\bar{P}$ including knee frequency (···).

Fig. 13. Effect of changing A_{det} on $S_I(f)/\bar{I}^2$ for light scattered from a suspension of polystyrene spheres with $r_o = 630\text{Å}$, $\theta = 50°$, $d = 10$ μm, $R = 4$ cm and $n_o \approx 5\times10^{11}$ cm^{-3}. (a) $A_{det} = 0.009$ cm^2; (b) $A_{det} = 0.7$ cm^2.

Fig. 14. Effect of changing n_o on $S_I(f)/\bar{I}^2$ with $r_o = 630\text{Å}$, $\theta = 50°$, $d = 10$ μm, $A_{det} = 0.7$ cm^2, and $r = 3$ cm. (a) $n_o \approx 10^9$ cm^{-3} and $\langle N\rangle = 77$; (b) $n_o \approx 5\times10^{11}$ cm^{-3} and $\langle N\rangle = 5.5\times10^4$. (c) Laser intensity fluctuation spectrum.

Fig. 15. Effect of changing Ω_i on $S_I(f)/\bar{I}^2$ with $r_o = 630\text{Å}$, $\theta = 50°$, $A_{det} = 0.7$ cm^2, $R = 3$ cm, $n_o \approx 10^9$ cm^{-3}. (a) $d = 10$ μm (reproduces Fig. 2(a)); (b) $d \approx 120$ μm.

Fig. 16. Measured $S_I(f)/\bar{I}^2$ for larger spheres with $r_o = 6500\text{Å}$, $\theta = 30°$ $A_{det} = 0.7$ cm^2, $R = 6$ cm. (a) $n_o \approx 10^7$ cm^{-3} and $d = 10$ μm; (b) $n_o \approx 5\times10^8$ cm^{-3} and $d = 10$ μm; (c) $n_o \approx 5\times10^8$ cm^{-3}, and d greatly enlarged.

Fig. 17. (a) (Right-hand scale) Measured $S_I(f)/\bar{I}^2$ for laser light scattered in the forward direction with $r_o = 630\text{Å}$, $\theta = 0°$, $A_{det} = 0.7\ cm^2$, R = 10 cm, and $n_o \approx 5\times10^{11}$. (b), (c), and (d). (left-hand scale) $S_I(f)/\bar{I}^2$ observed with a white light source. (b) $r_o = 6500\text{Å}$, $\theta = 45°$, $A_{det} = 0.7\ cm^2$, $n_o \approx 5\times10^{8}\ cm^{-3}$, $R \approx 1$ cm, Ω_i determined by a slit 130 μm×10 μm and $\langle N\rangle = 5\times10^{3}$; (c) $r_o = 630\text{Å}$, $\theta = 50°$, $A_{det} = 0.7\ cm^2$, r = 6 cm, and $n_o \approx 2\times10^{11}\ cm^{-1}$, and Ω_i determined by a focused image of the filament; (d) $r_o = 630\text{Å}$, $\theta = 0°$, $A_{det} = 0.7\ cm^2$, $r \approx 1$ cm, $n_o \approx 2\times10^{11}\ cm^{-3}$, Ω_i determined by a slit 20 μm×2 mm, and $\langle N\rangle = 8\times10^{6}$.

Fig. 18. Power spectrum of flood levels of the river Nile. (Data from Omar Toussoun, Mémoires l'Institut Egypte 8-10, (1925)).

Fig. 19. Samples of white, 1/f, and $1/f^2$ noise.

Fig. 20. Bach's 1st Brandenburg Concerto (linear scales): (a) power spectrum of audio signal, $S_V(f)$ vs f; (b) power spectrum of loudness fluctuations, $S_{V^2}(f)$ vs f.

Fig. 21. Bach's 1st Brandenburg Concerto (log scales): (a) $S_V(f)$ vs f; (b) $S_{V^2}(f)$ vs f.

Fig. 22. Loudness fluctuation spectra, $S_{V^2}(f)$ vs f for: (a) Scott Joplin piano rags; (b) classical radio station; (c) rock station; (d) news and talk station.

Fig. 23. Power spectra of pitch fluctuations, $S_Z(f)$ vs f, for four radio stations: (a) classical; (b) jazz and blues; (c) rock; (d) news and talk.

Fig. 24. Pitch and duration determined by a white noise source.

Fig. 25. Pitch and duration determined by a 1/f noise source.

Fig. 26. Pitch and duration determined by a $1/f^2$ noise source.

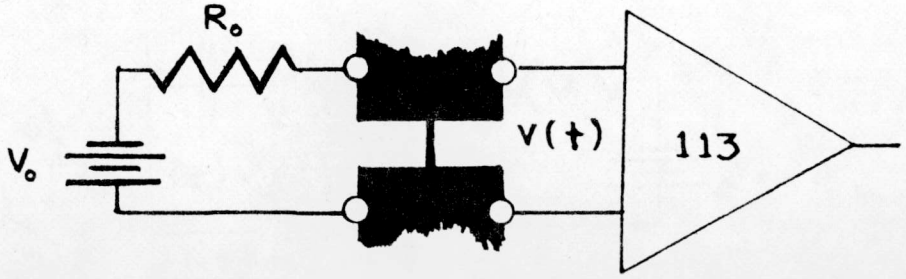

(a)

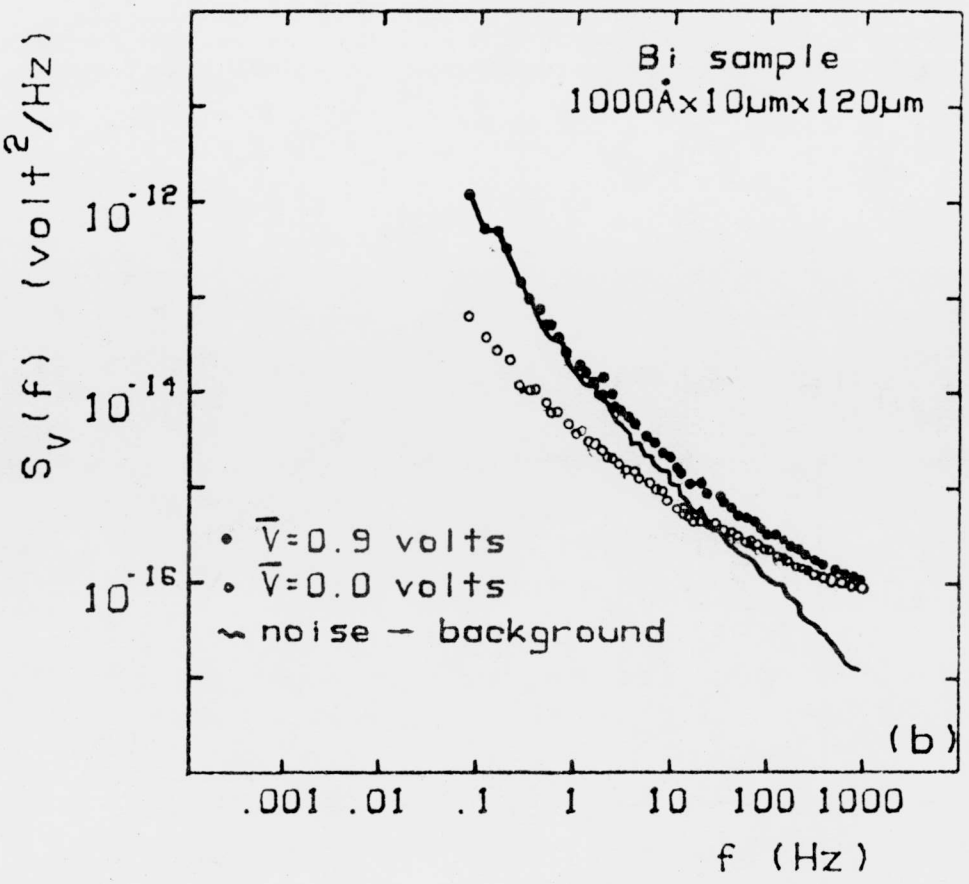

XBL758-6835

Fig. 1

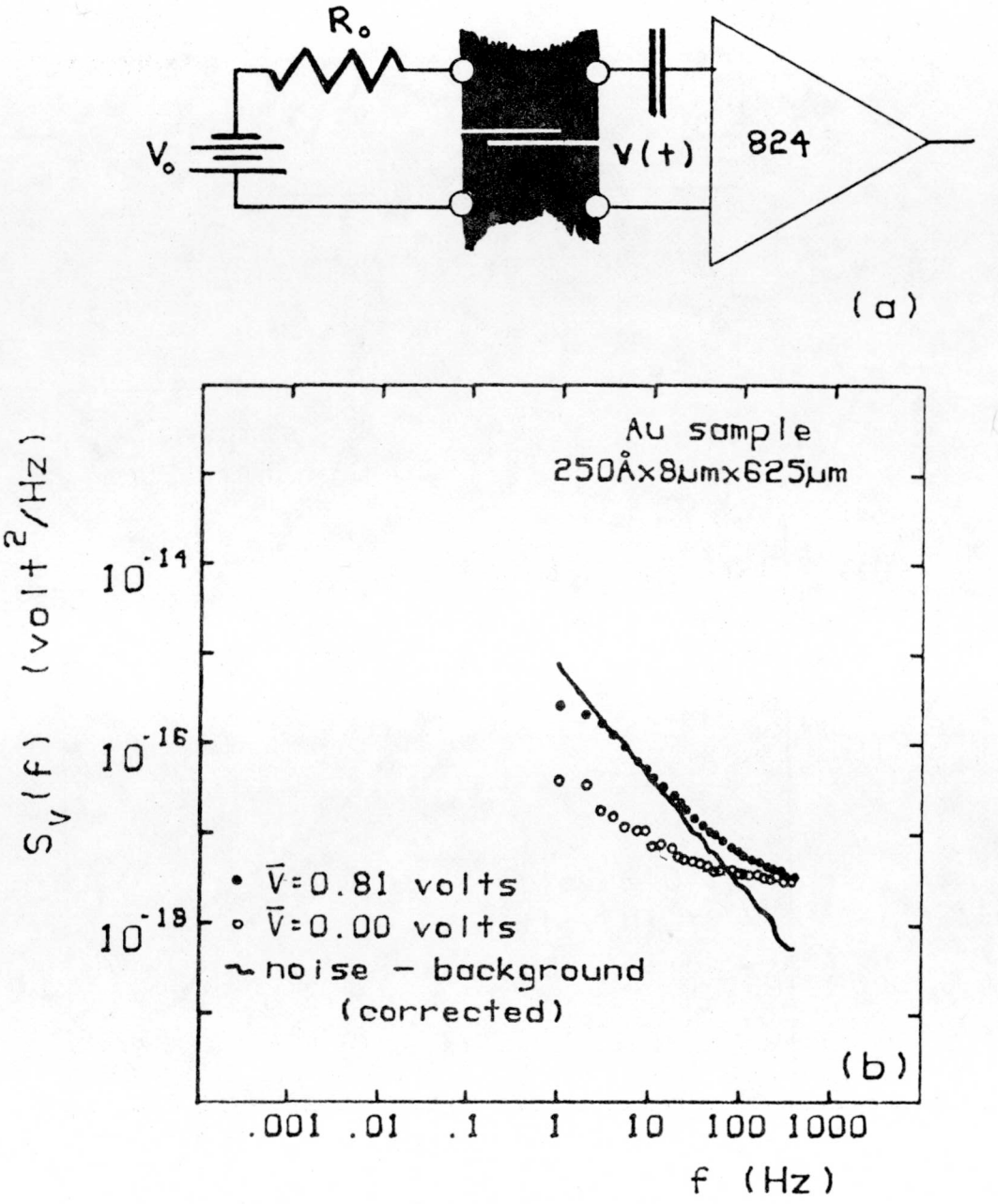

XBL758-6836

Fig. 2

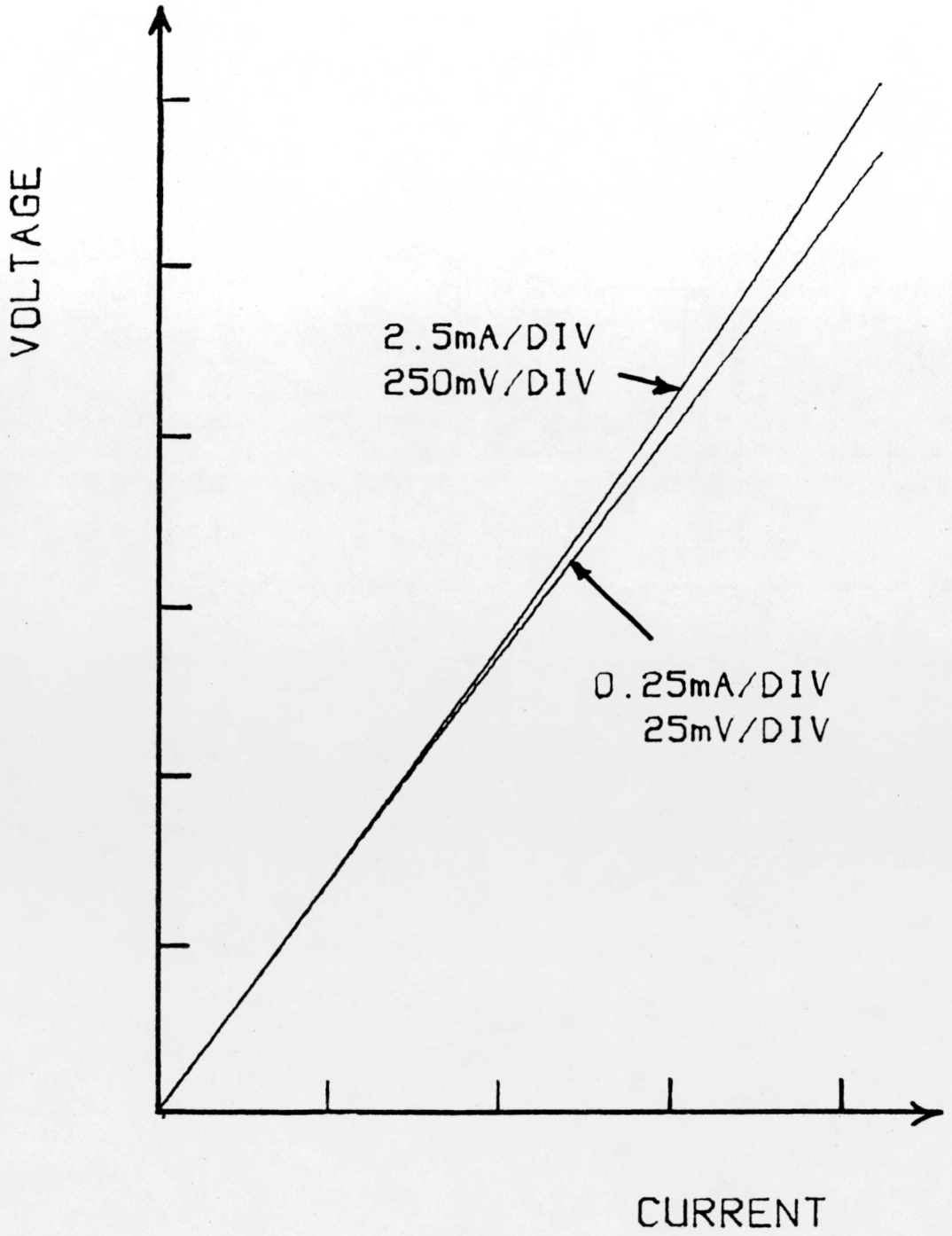

XBL758-6837

Fig. 3

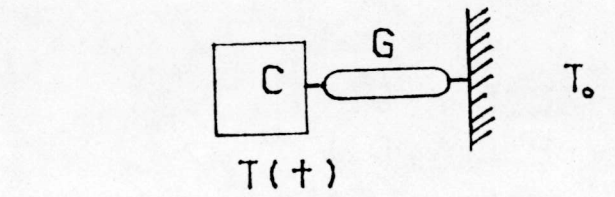

(a)

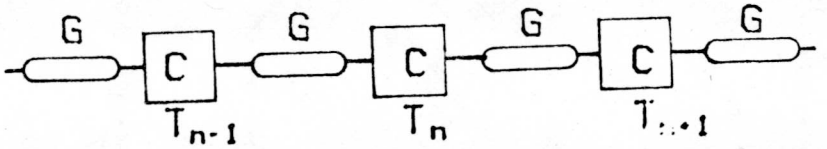

(b)

XBL758-6838

Fig. 4

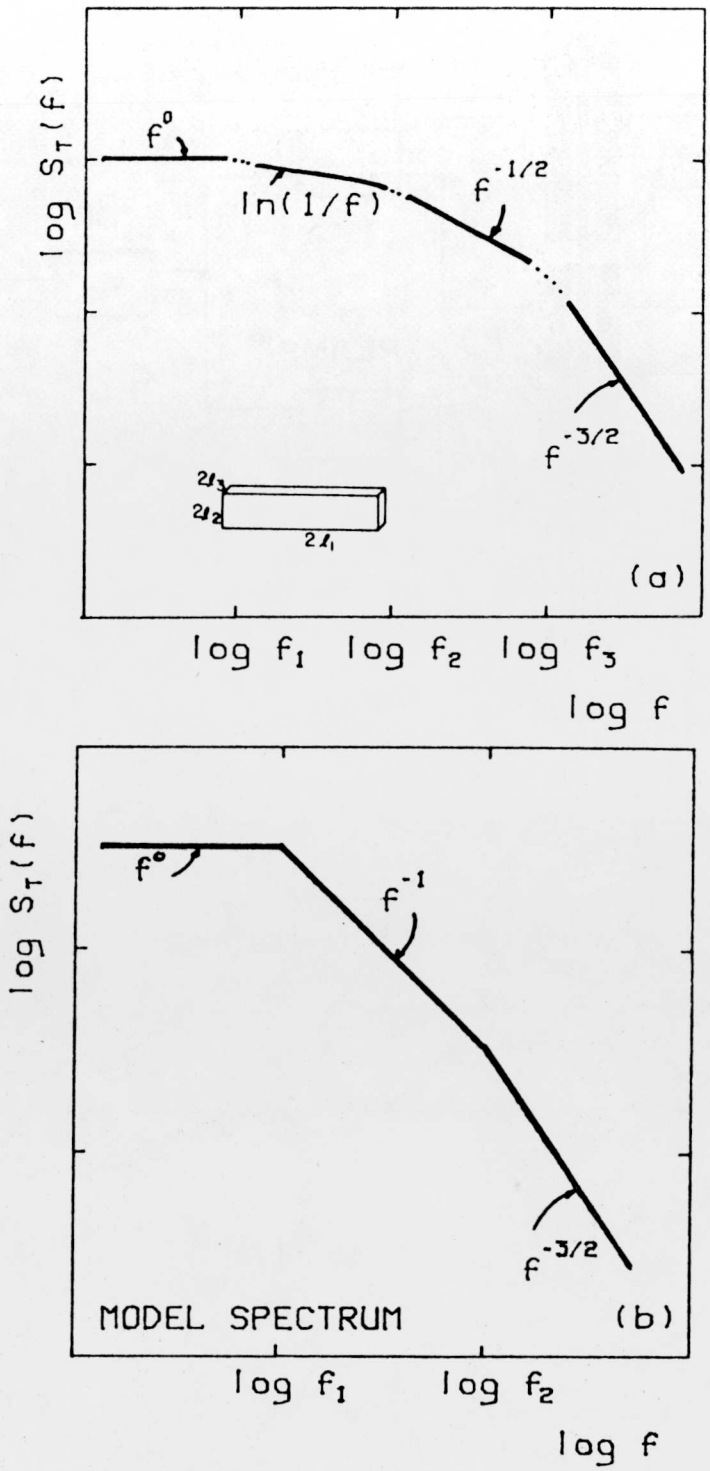

XBL758-6839

Fig. 5

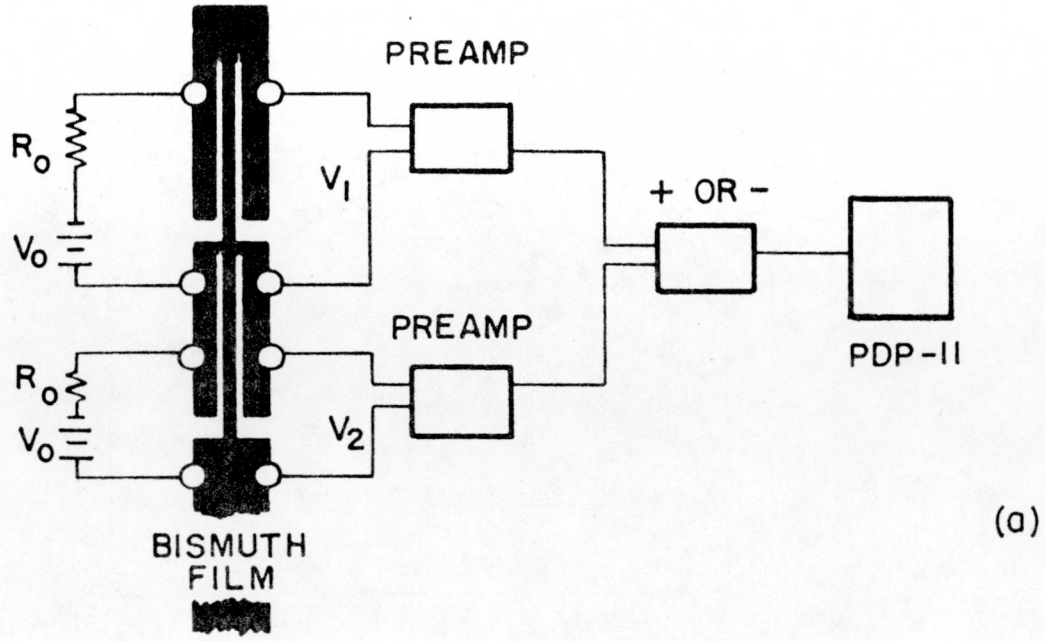

(a)

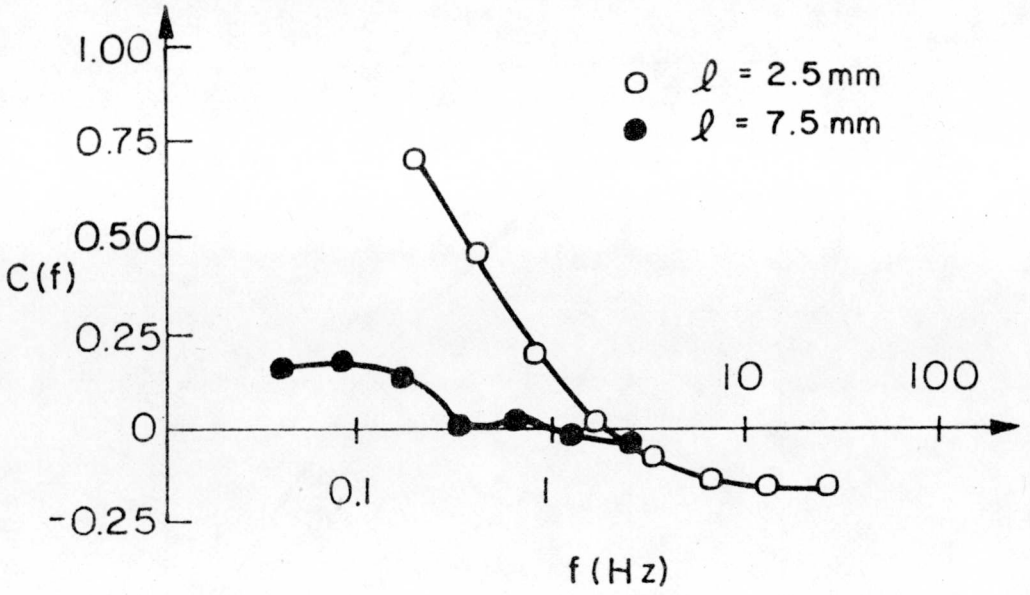

(b)

XBL 7312-6762

Fig. 6

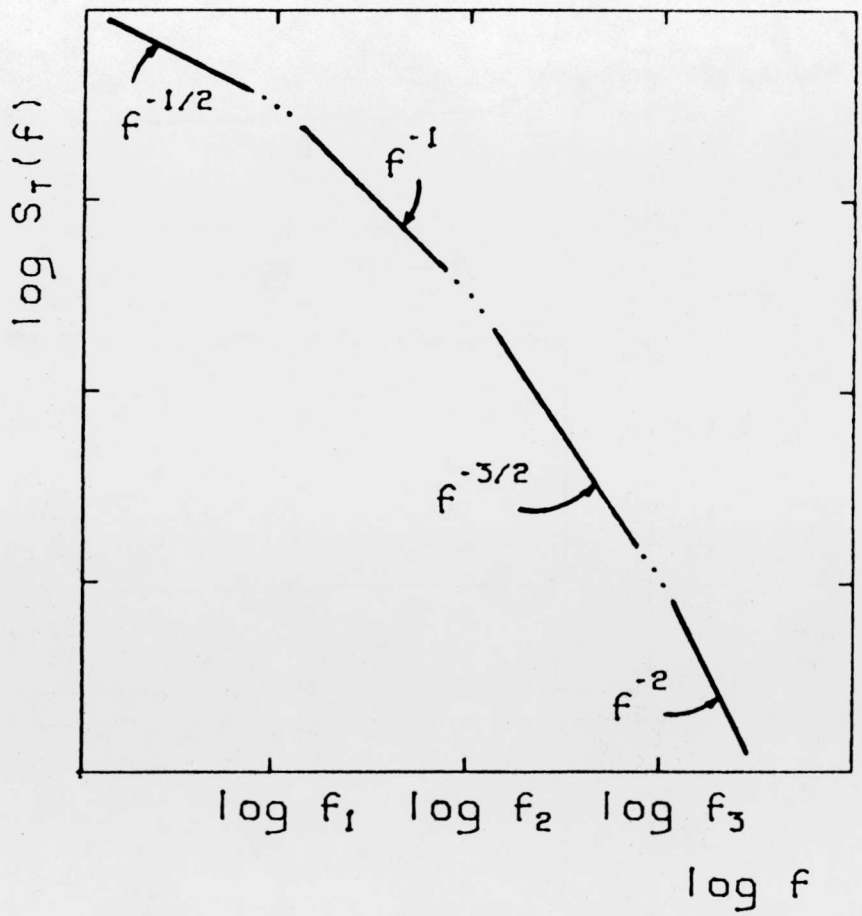

XBL758-6843

Fig. 7

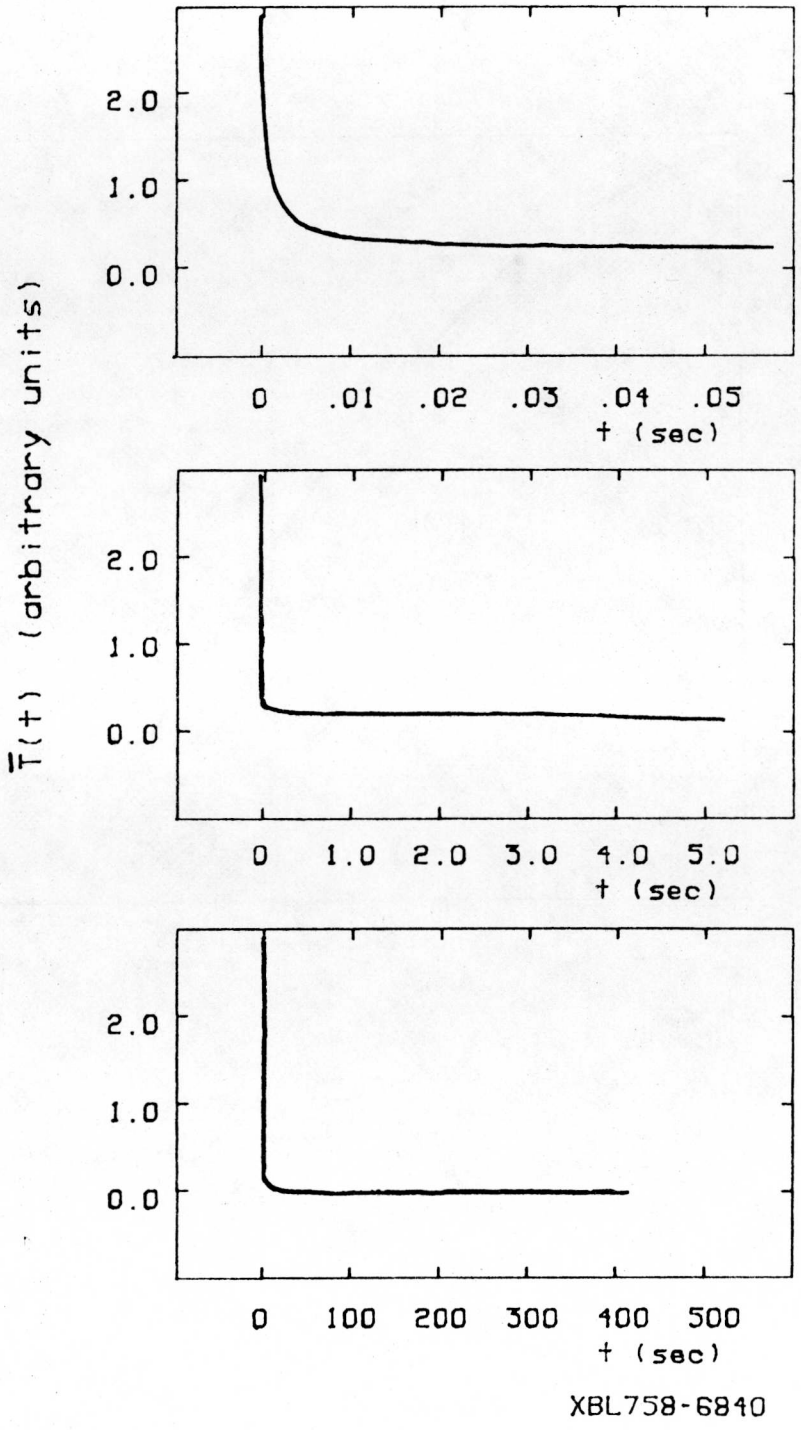
$\bar{T}(t)$ (arbitrary units)
2.0
1.0
0.0
0
.01
.02
.03
.04
.05
t (sec)
2.0
1.0
0.0
0
1.0
2.0
3.0
4.0
5.0
t (sec)
2.0
1.0
0.0
0
100
200
300
400
500
t (sec)
XBL758-6840

Fig. 8

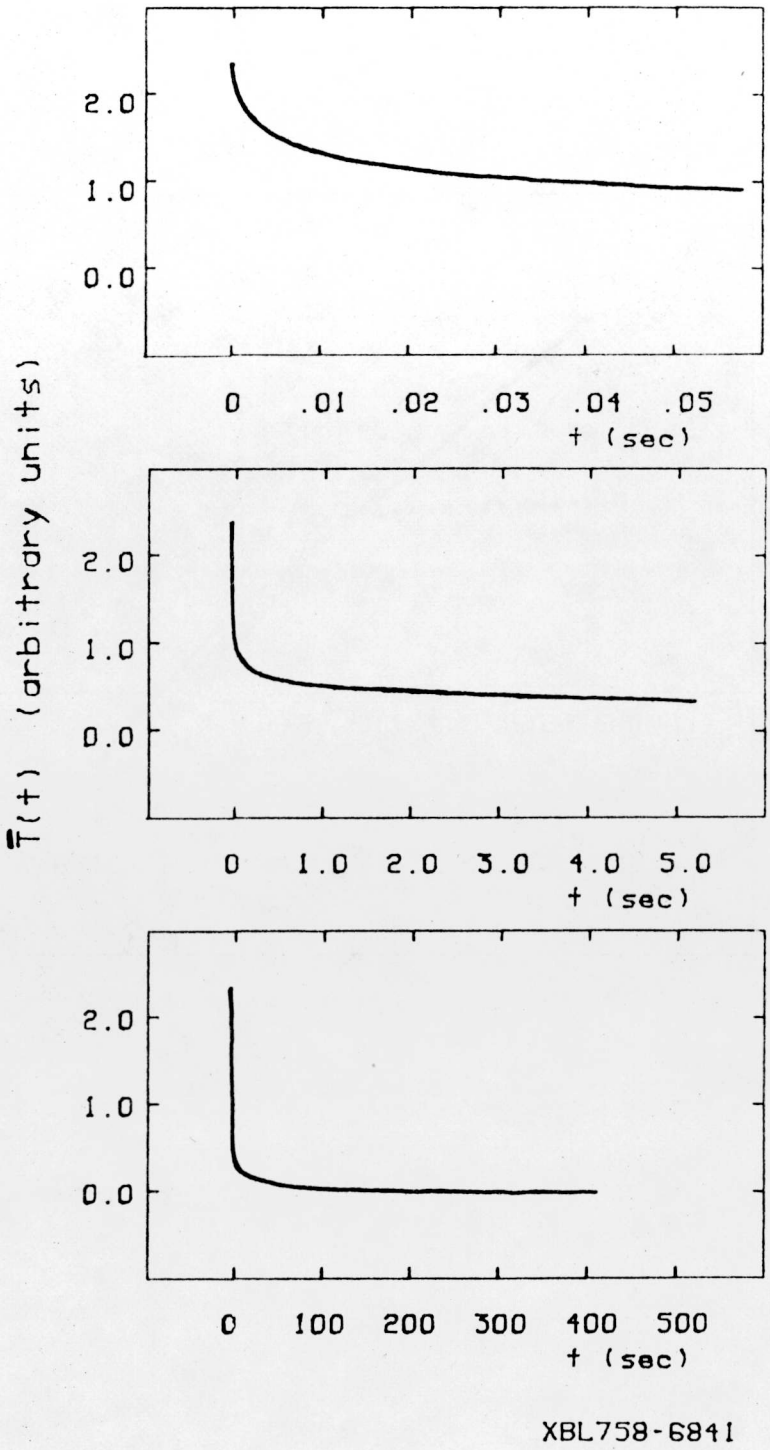
2.0
1.0
0.0
0 .01 .02 .03 .04 .05
t (sec)
2.0
1.0
0.0
0 1.0 2.0 3.0 4.0 5.0
t (sec)
2.0
1.0
0.0
0 100 200 300 400 500
t (sec)
T̄(t) (arbitrary units)
XBL758-6841

Fig. 9

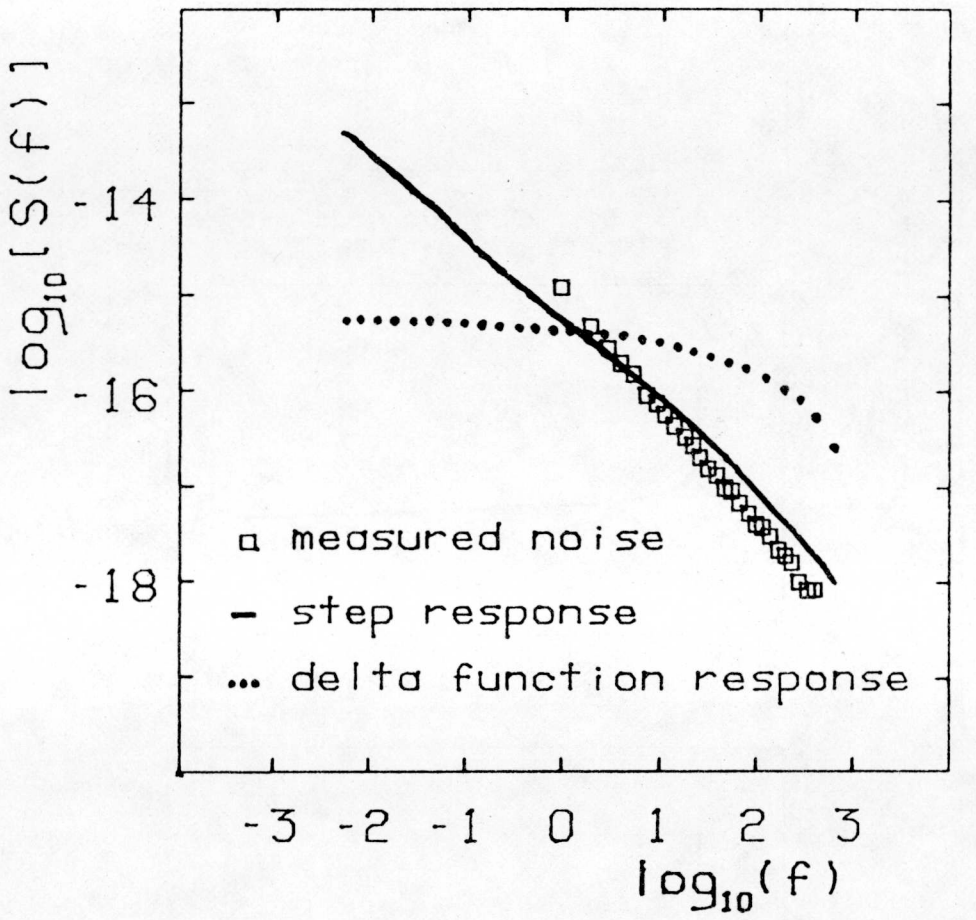

XBL758-6842

Fig. 10

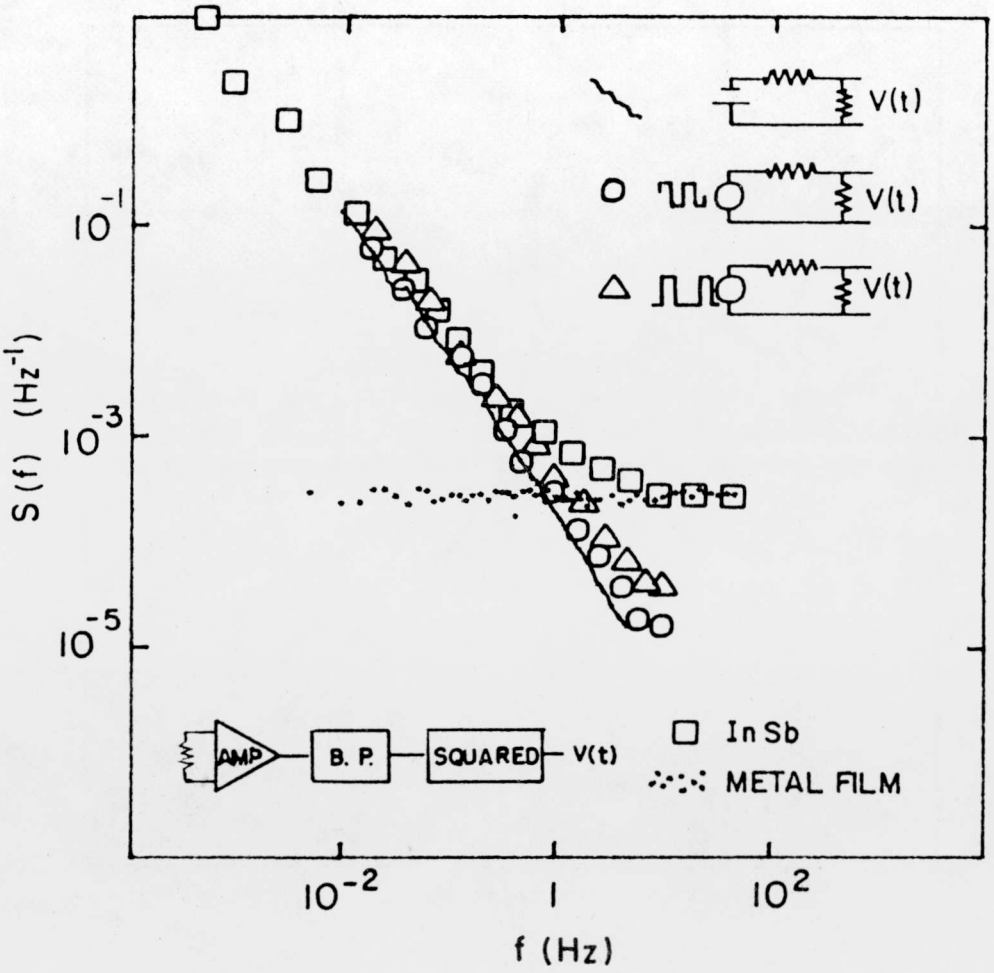

XBL 755-6349

Fig. 11

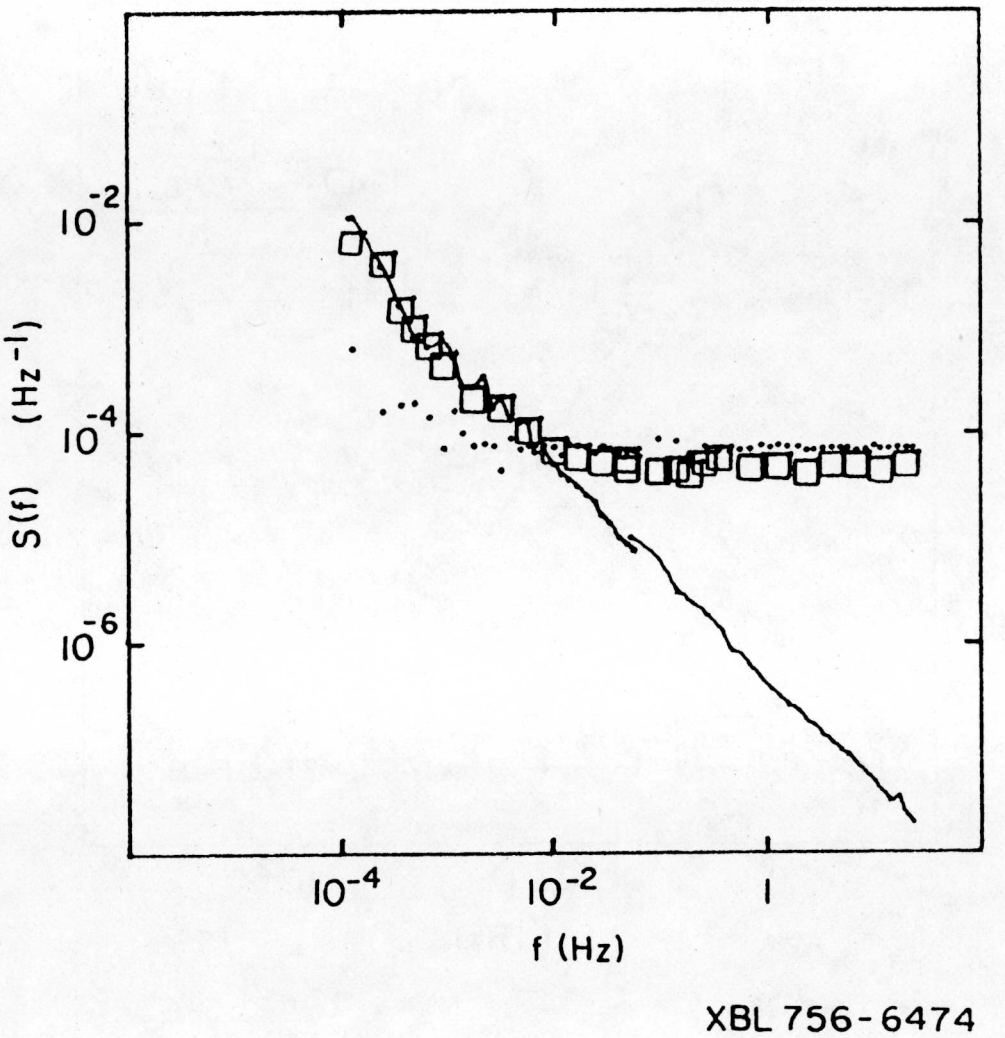

Fig. 12

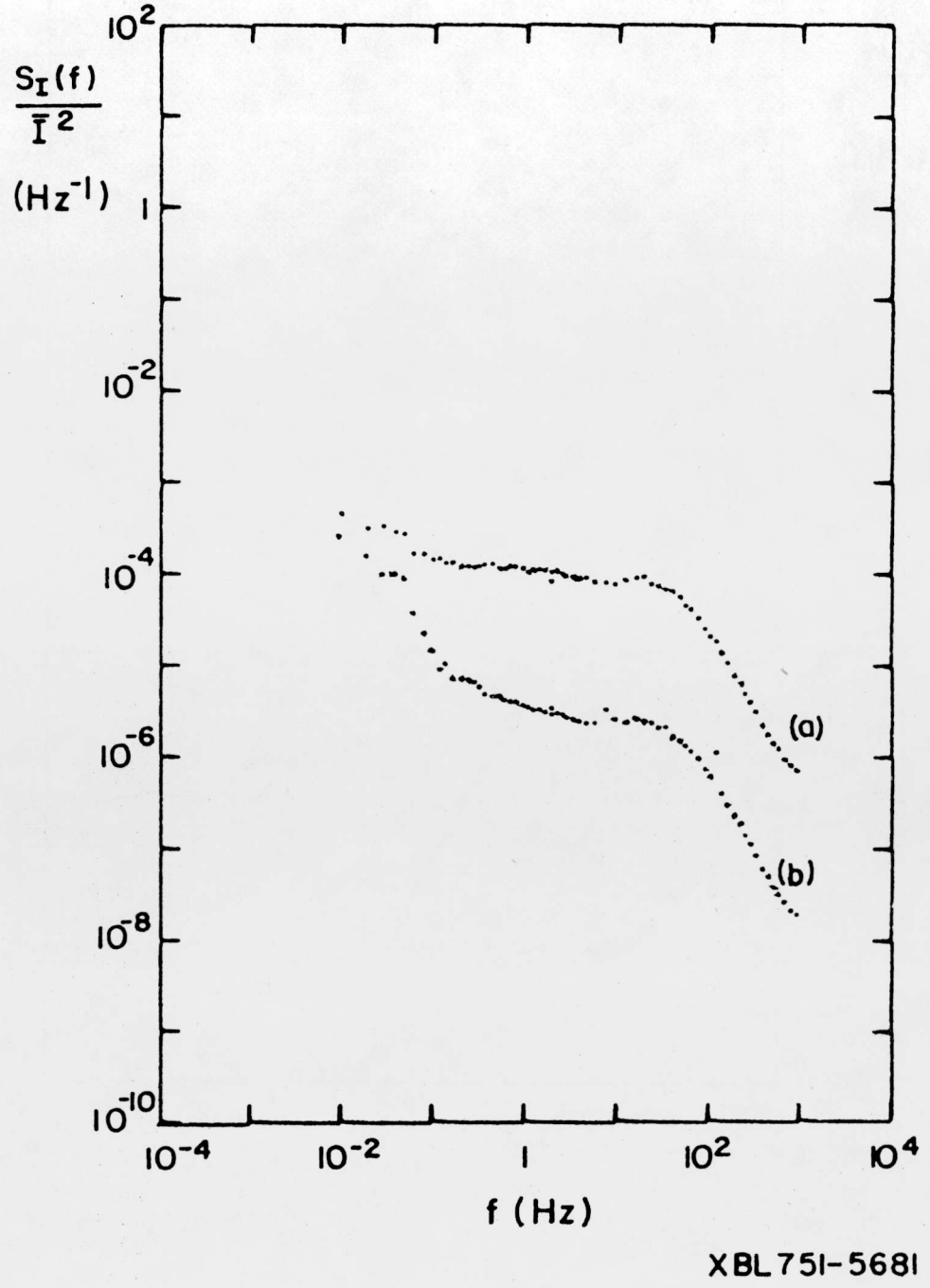
$\frac{S_I(f)}{\bar{I}^2}$
(Hz^{-1})
10^2
1
10^{-2}
10^{-4}
10^{-6}
10^{-8}
10^{-10}
10^{-4}
10^{-2}
1
10^2
10^4
f (Hz)
(a)
(b)
XBL751-5681

Fig. 13

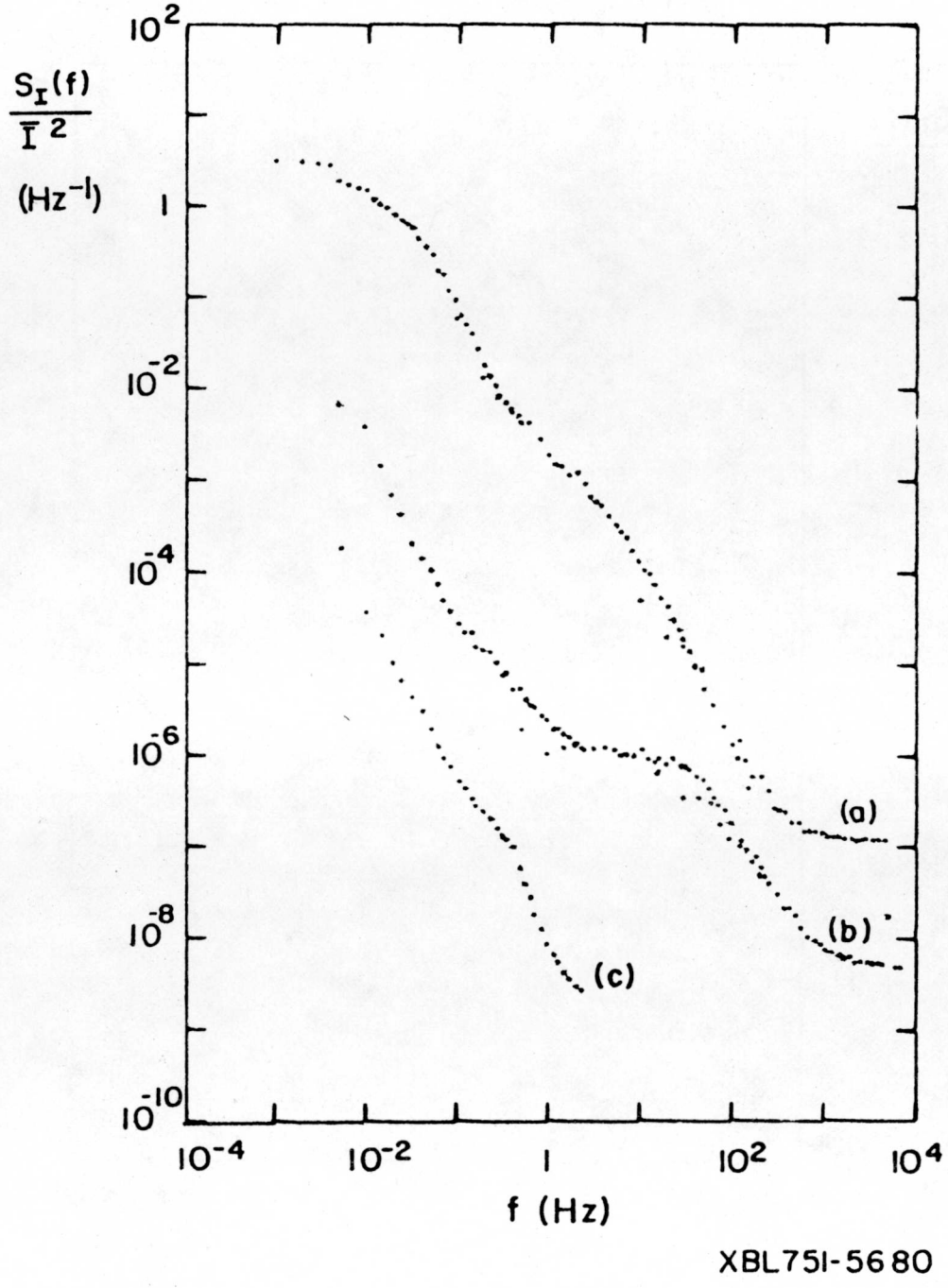
$\frac{S_I(f)}{\bar{I}^2}$
(Hz^{-1})
10^2
1
10^{-2}
10^{-4}
10^{-6}
10^{-8}
10^{-10}
10^{-4}
10^{-2}
1
10^2
10^4
f (Hz)
(a)
(b)
(c)
XBL751-5680

Fig. 14

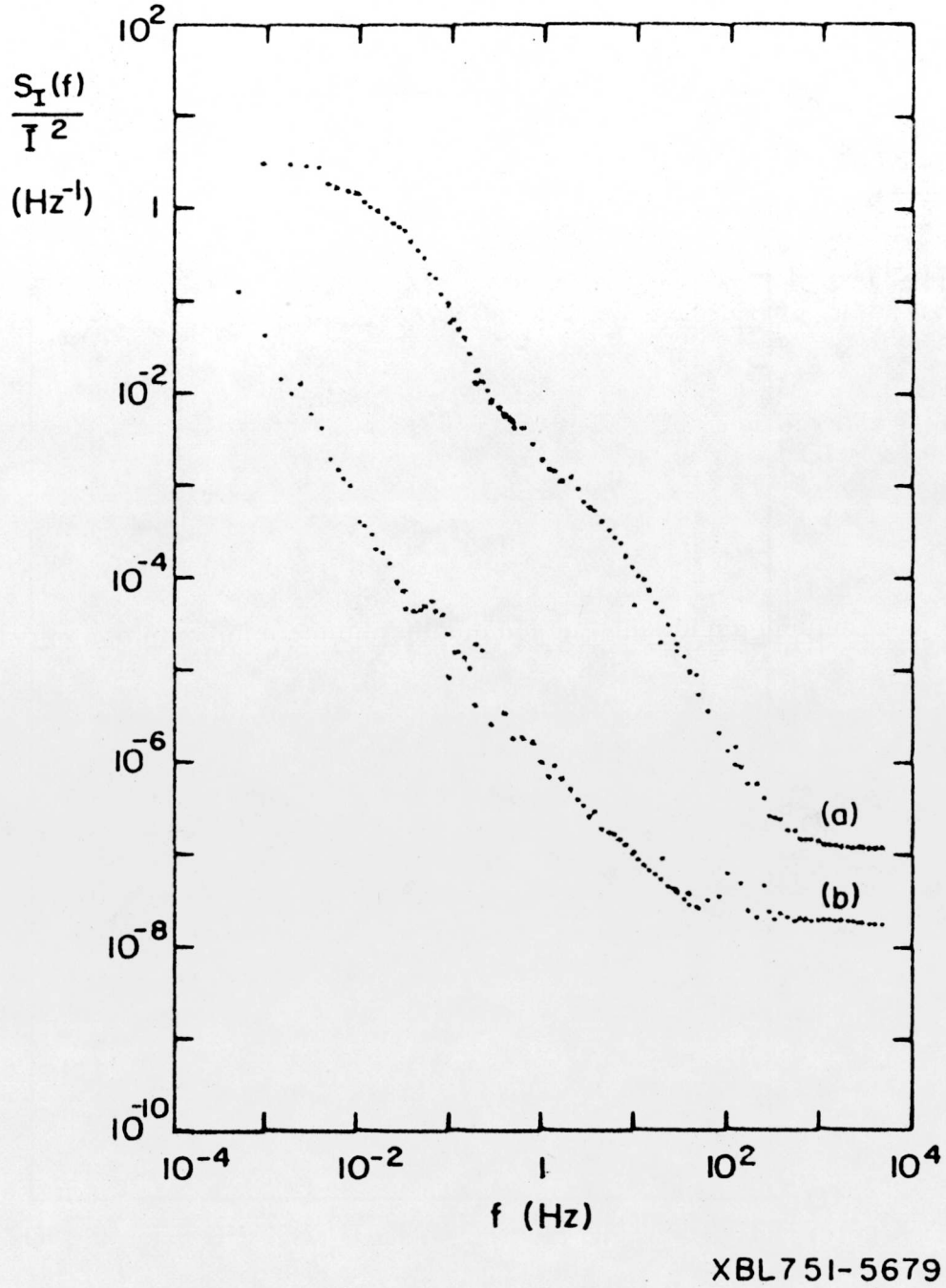
$\frac{S_I(f)}{\bar{I}^2}$
(Hz^{-1})
10^2
1
10^{-2}
10^{-4}
10^{-6}
10^{-8}
10^{-10}
10^{-4}
10^{-2}
1
10^2
10^4
f (Hz)
(a)
(b)
XBL751-5679

Fig. 15

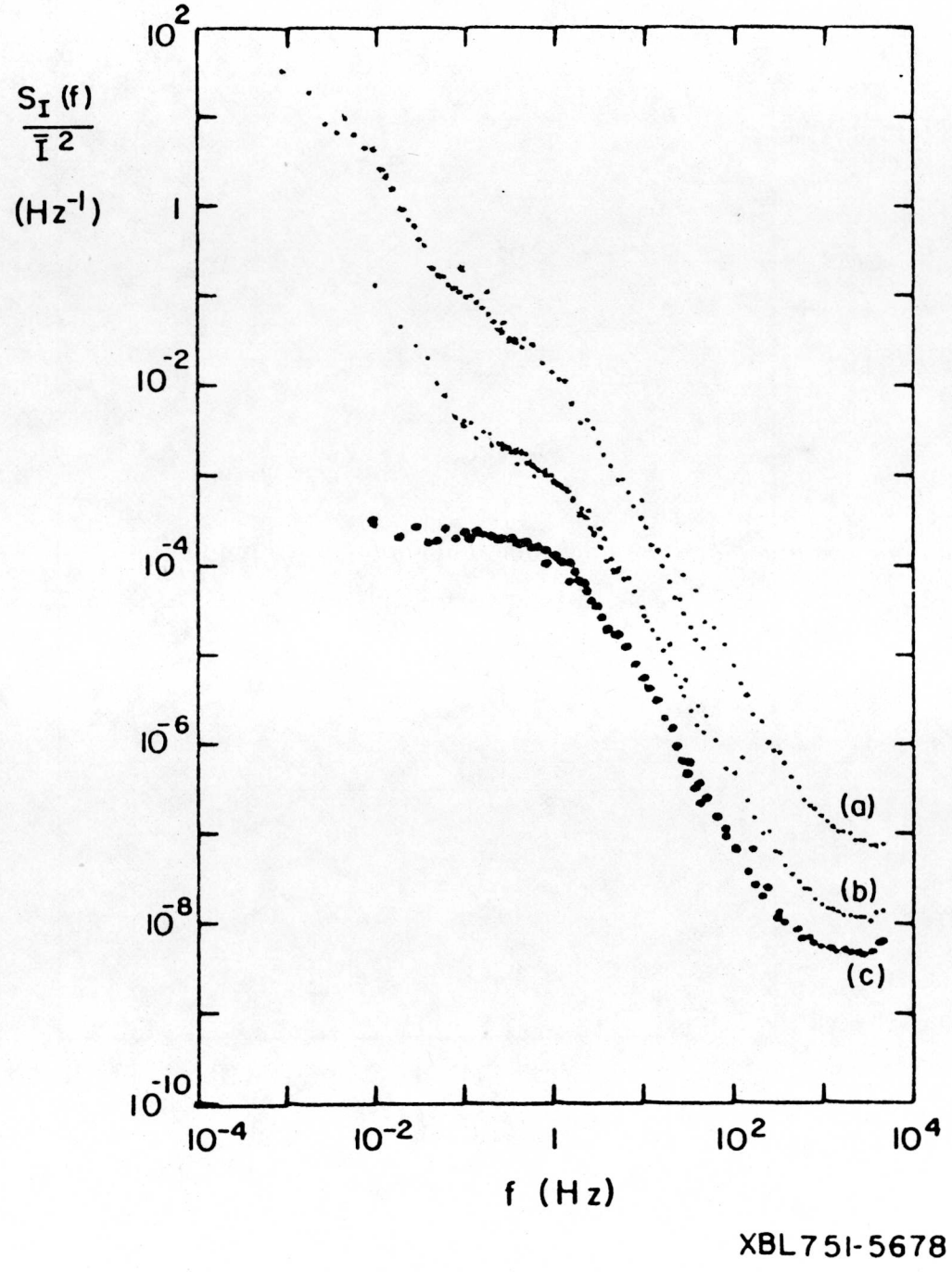
$\frac{S_I(f)}{\bar{I}^2}$
(Hz^{-1})
10^2
1
10^{-2}
10^{-4}
10^{-6}
10^{-8}
10^{-10}
10^{-4}
10^{-2}
1
10^2
10^4
f (Hz)
(a)
(b)
(c)
XBL751-5678

Fig. 16

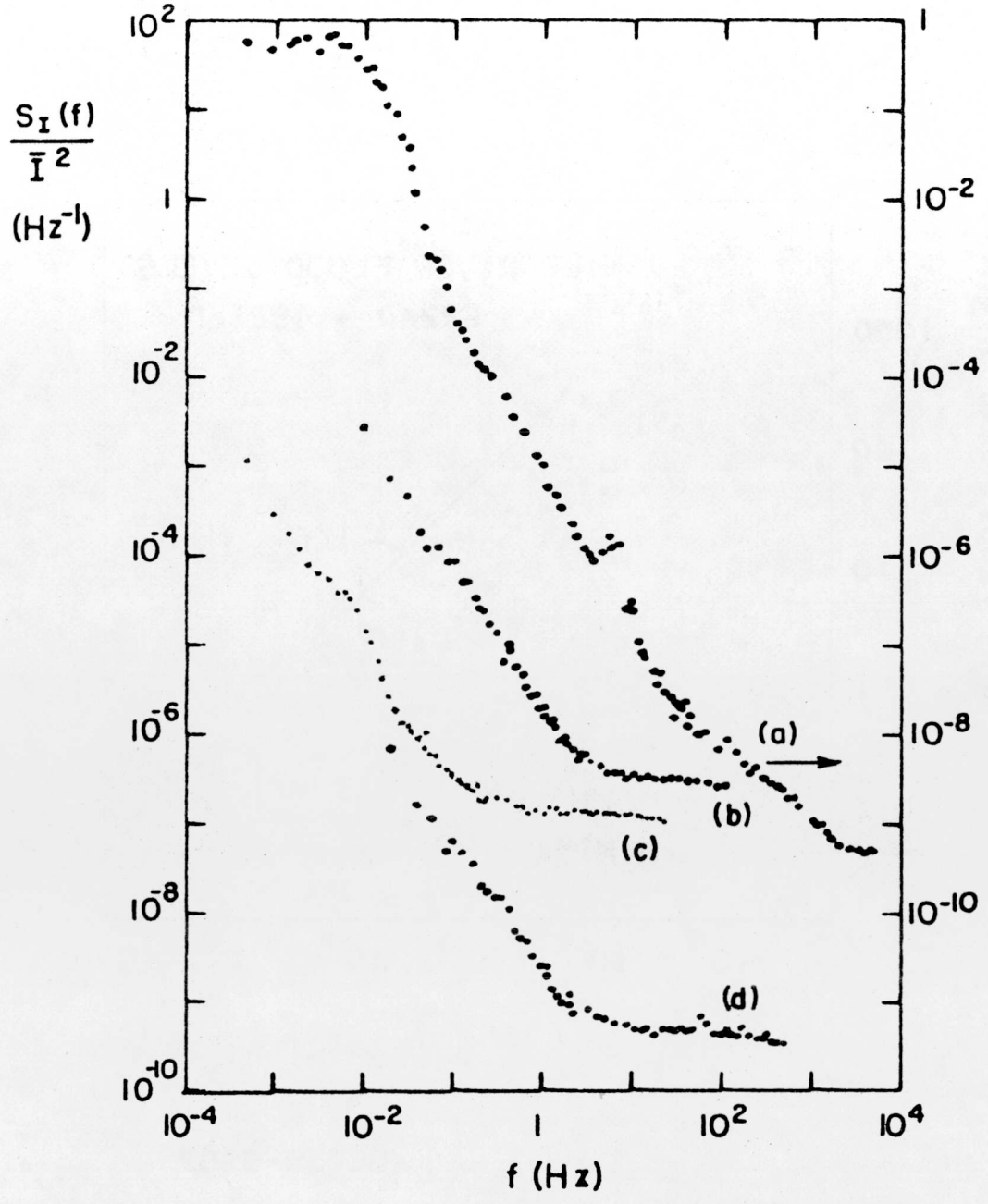
$\frac{S_I(f)}{\bar{I}^2}$
(Hz^{-1})
10^2
1
10^{-2}
10^{-4}
10^{-6}
10^{-8}
10^{-10}
(a)
(b)
(c)
(d)
10^{-4}
10^{-2}
1
10^2
10^4
f (Hz)
XBL 751-5677

Fig. 17

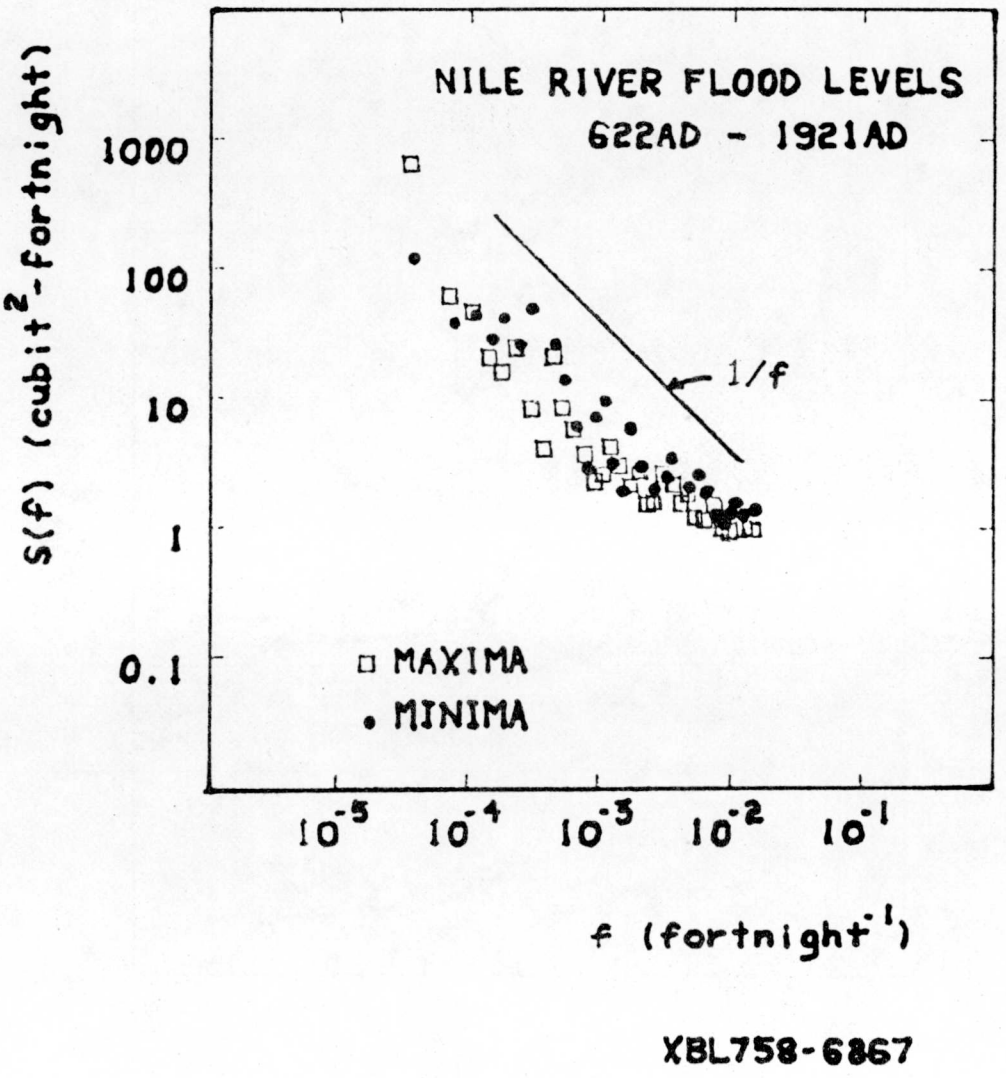
NILE RIVER FLOOD LEVELS
622AD - 1921AD
S(f) (cubit^2-fortnight)
1000
100
10
1
0.1
1/f
□ MAXIMA
• MINIMA
10^{-5}
10^{-4}
10^{-3}
10^{-2}
10^{-1}
f (fortnight^{-1})
XBL758-6867

Fig. 18

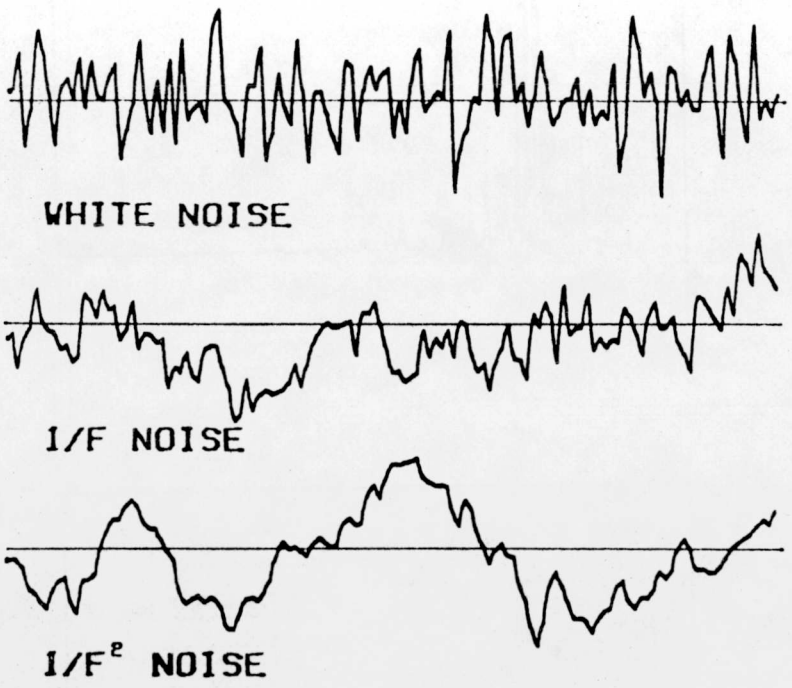

Fig. 19

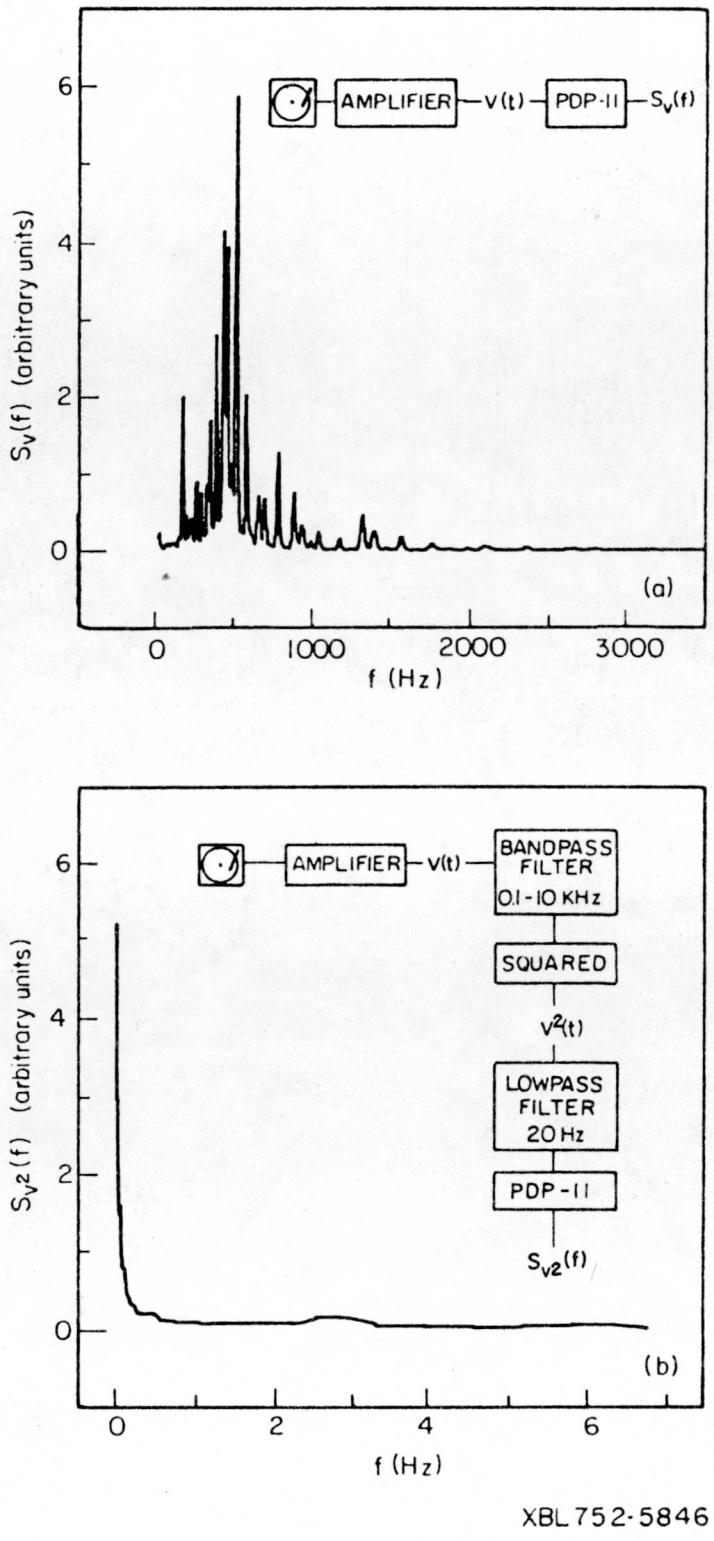
AMPLIFIER
V(t)
PDP-11
$S_v(f)$
$S_v(f)$ (arbitrary units)
6
4
2
0
0
1000
2000
3000
f (Hz)
(a)
AMPLIFIER
V(t)
BANDPASS FILTER 0.1-10 KHz
SQUARED
$V^2(t)$
LOWPASS FILTER 20 Hz
PDP-11
$S_{v2}(f)$
$S_{v2}(f)$ (arbitrary units)
6
4
2
0
0
2
4
6
f (Hz)
(b)
XBL 752-5846

Fig. 20

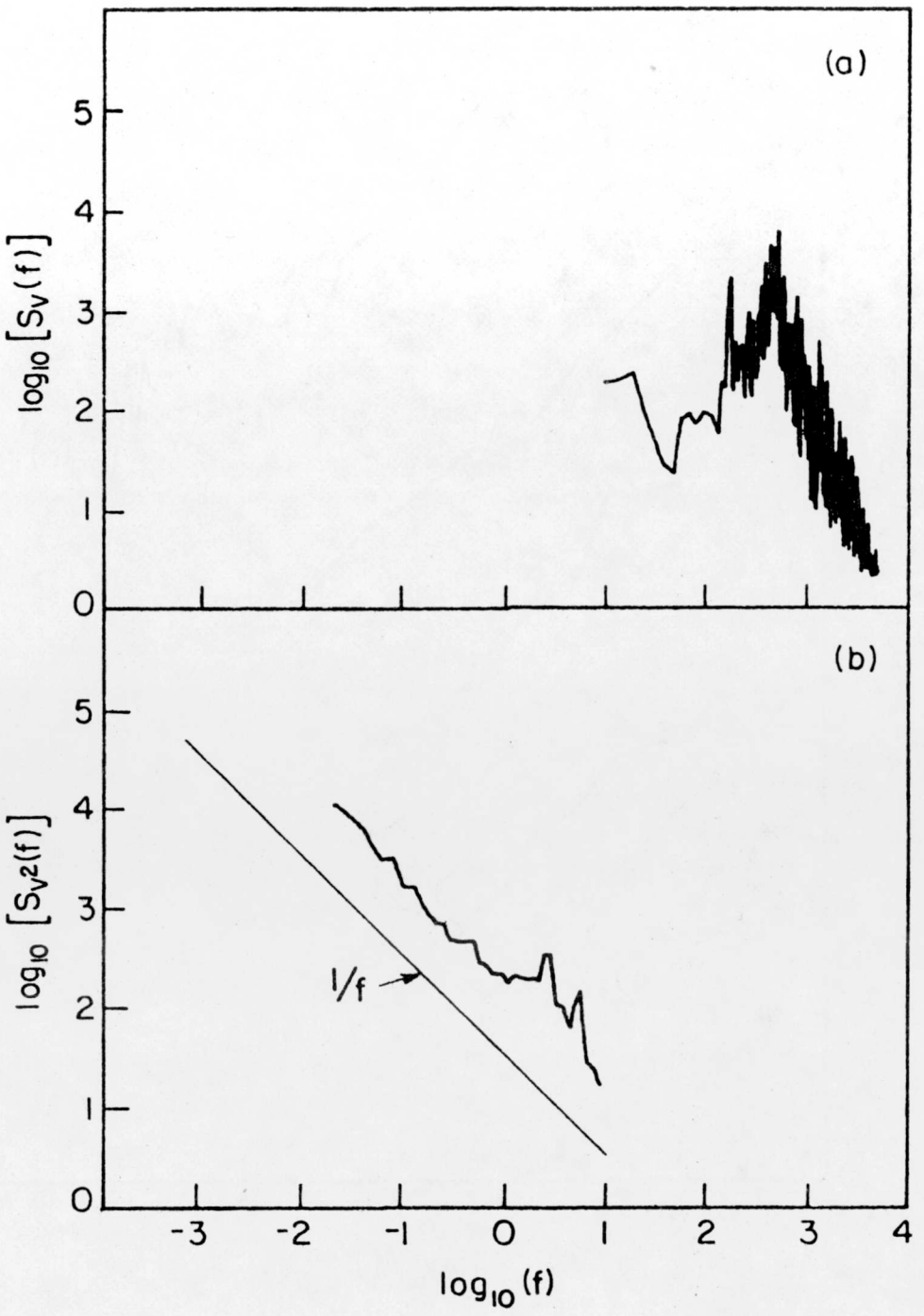

Fig. 21

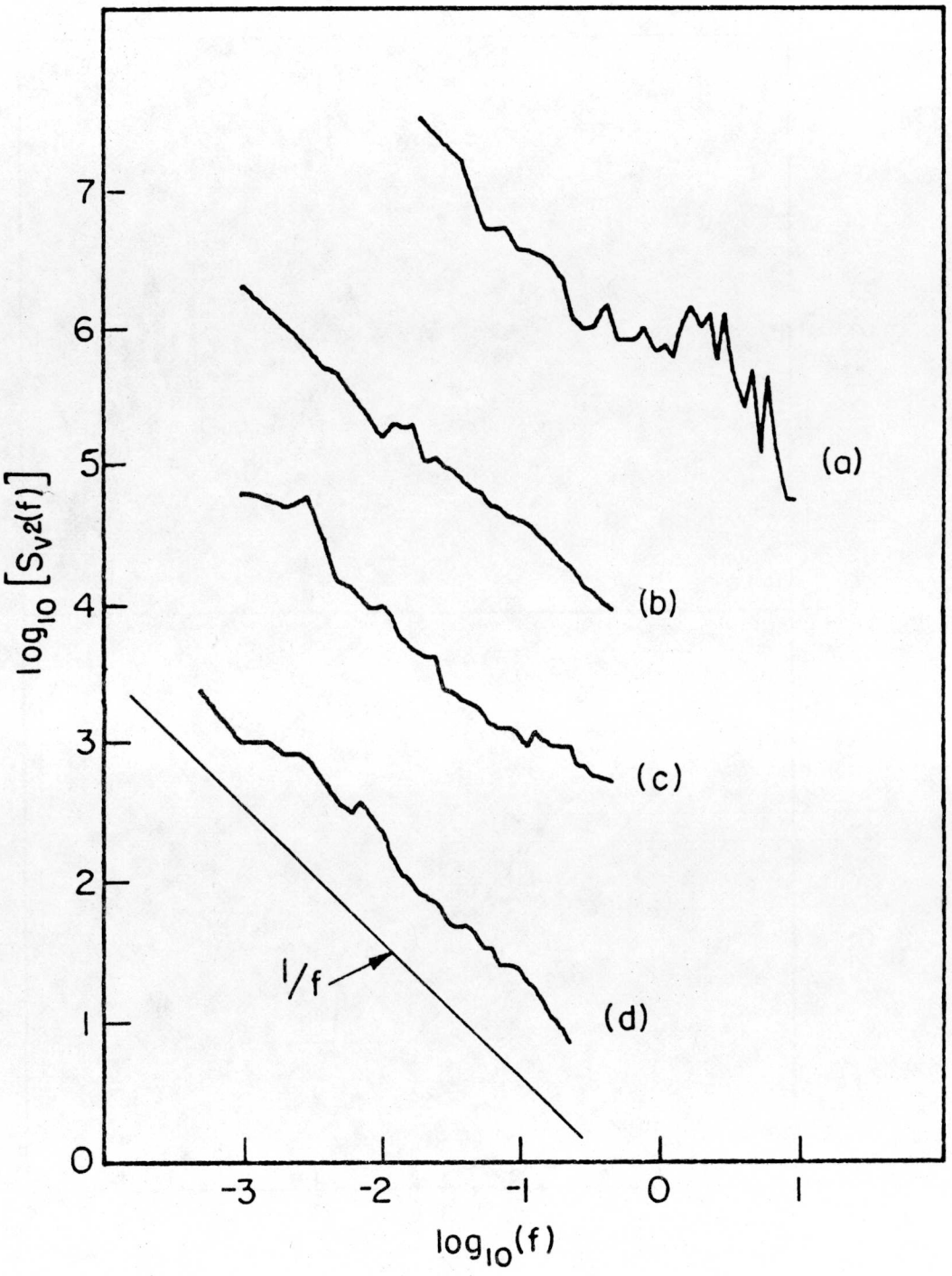

Fig. 22

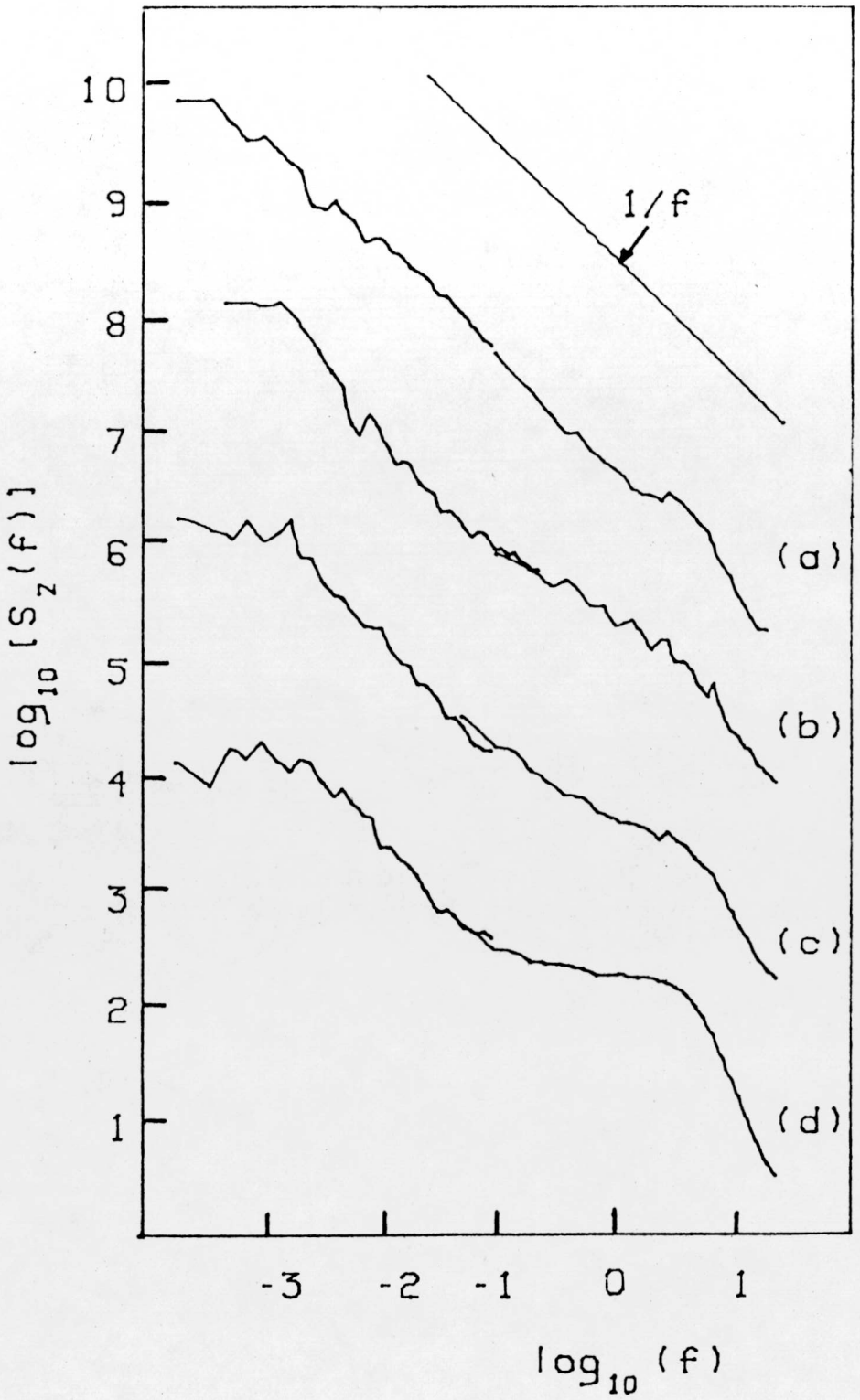

Fig. 23

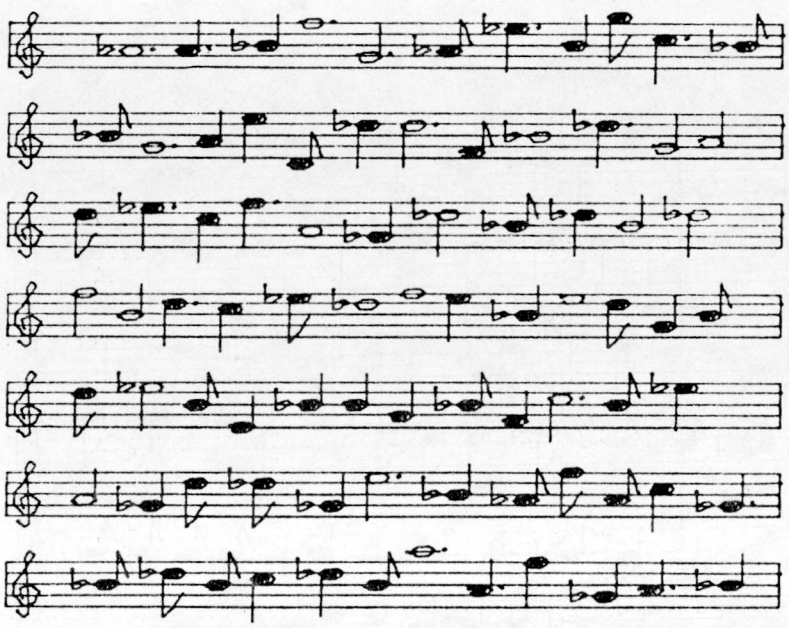

WHITE MUSIC

XBL757-6722

Fig. 24

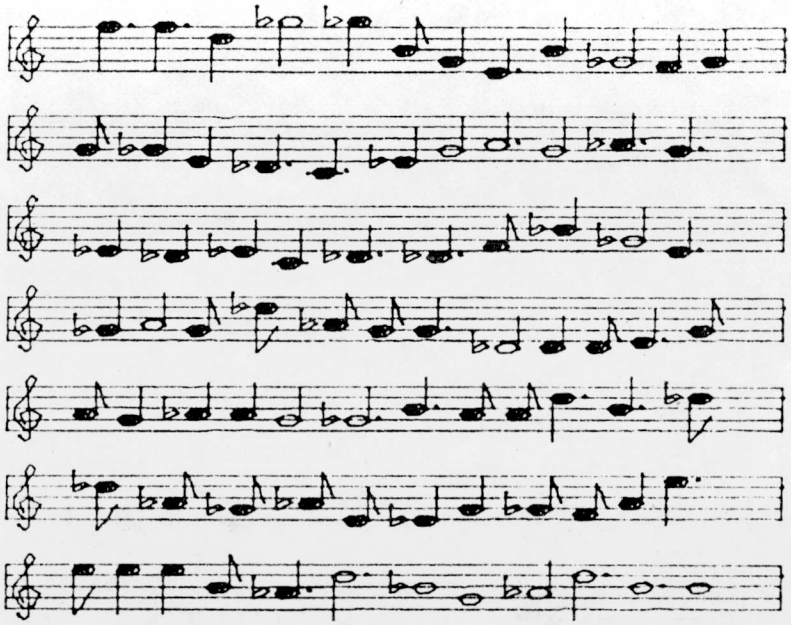

1/F MUSIC

XBL757-6721

Fig. 25

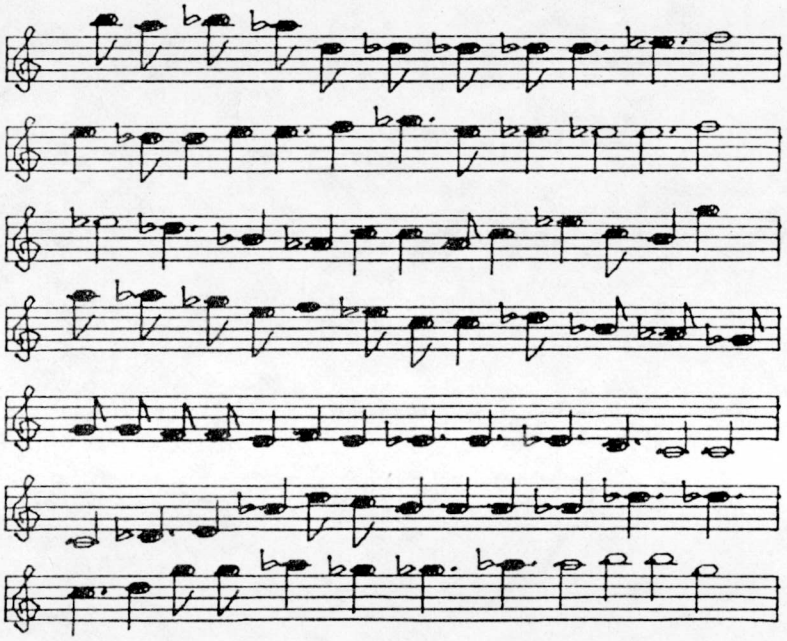

$1/F^2$ MUSIC

XBL757-6727

Fig. 26

TECHNICAL INFORMATION DIVISION
LAWRENCE BERKELEY LABORATORY
UNIVERSITY OF CALIFORNIA
BERKELEY, CALIFORNIA 94720